

DISULFIDE-TRAPPED CXCL12-CXCL4 CHEMOKINE HETERODIMERS PREVENT  
BREAST CANCER MIGRATION

By

Khanh Tran Phuong Nguyen

A dissertation submitted to the faculty of  
The University of North Carolina at Charlotte  
in partial fulfillment of the requirements  
for the degree of Doctor of Philosophy in  
Biology

Charlotte

2021

Approved by:

---

Dr. Irina Nesmelova

---

Dr. Didier Dréau

---

Dr. Ian Marriott

---

Dr. Christine Richardson

---

Dr. Juan Vivero-Escoto



**ABSTRACT**

KHANH TRAN PHUONG NGUYEN. Disulfide-trapped CXCL4-CXCL12 heterodimers prevent breast cancer migration. (Under the direction of Drs. IRINA NESMELOVA and DIDIER DRÉAU)

Triple negative breast cancers (TNBCs), i.e., 10-15% of diagnosed breast cancers, have a triple negative (Her/2<sup>-</sup>, ER<sup>-</sup> and PR<sup>-</sup>) phenotype and are the most aggressive subtype of breast cancer. TNBCs have a worst prognosis because of the high probability of metastasis and limited treatment options. The role of chemokine – chemokine receptor CXCL12-CXCR4 signaling axis in the progression and metastatic spread of breast cancer is well established. Especially, CXCL12 promotes cell migration, an essential step in cancer metastasis. Over the past decades, multiple targeted therapeutic strategies aiming to block the CXCR4 signaling have been assessed. However, their clinical uses remain challenging because of side-effects due to the abundant CXCR4 expression on numerous cell types and its involvement in normal physiological processes. Therefore, new therapeutic approaches without side-effects are required for improving treatments of metastatic breast cancers. The present PhD thesis provides evidence in support of an alternative approach targeting the CXCL12-CXCR4 signaling through heterophilic interactions with chemokine CXCL4 to neutralize CXCL12-CXCR4 driven tumor migration. We first investigated whether CXCL4 heterodimerized with CXCL12 and the biological relevance of CXCL4-CXCL12 heterodimers in breast cancer migration. Our data show that CXCL4 and CXCL12 formed heterodimers via the interactions of the first  $\beta$ -strands from CXCL4 and CXCL12 monomers. Interestingly, treatments with combinations of CXCL12 with increasing concentration of CXCL4 dose-dependently reduced the migration of CXCR4-

expressing triple negative breast cancer cells. The different oligomeric species of chemokines present in equilibria and, in particular, the competition between the homodimers and heterodimers likely hampers assessments of the biological relevance of chemokine heterodimers. Therefore, next, we used a novel disulfide-trapping method to produce a non-dissociating CXCL4-CXCL12 heterodimer designed with inter-molecular disulfide bond that prevents two monomeric units from dissociation. We, then, assessed the biological function of the obligate CXCL4-CXCL12 heterodimers in breast cancer migration. The obligate CXCL4-CXCL12 heterodimers were shown to prevent breast cancer migration. Particularly, through competition with the wildtype CXCL12, the obligate CXCL4-CXCL12 heterodimers reduced CXCL12-driven migration. We also demonstrated that the obligate CXCL4-CXCL12 heterodimers are biologically active and promote the release of intracellular calcium, a key evidence of G-protein activation through the CXCR4 receptor. Taken together, our data indicate that the obligate CXCL4-CXCL12 heterodimer inhibits breast cancer cell migration, at least in part, through the competition for the CXCR4 receptor. Lastly, these data are discussed, and future research outlined to exploit chemokine heterodimerization as a potential target in breast cancer progression. We also highlight the potential of chemokine antagonism by peptides mimicking the heterophilic interactions as a valid therapeutic approach to prevent breast cancer progression.

## ACKNOWLEDGEMENTS

I would like to thank my advisors, Dr. Irina Nesmelova and Dr. Didier Dréau, for providing an opportunity to work in their labs. Their incredible guidance and support have been an invaluable resource for me to complete my dissertation project. I would like to thank other members in my committee, Dr. Christine Richardson, Dr. Ian Marriott, and Dr. Juan Vivero-Escoto for their suggestions and invaluable feedbacks in research and academics. I would like to thank Dr. Peter Thompson at North Carolina State of University (NCSU) for his guidance on NMR technology. I sincerely appreciate your efforts and insightful comments to help me collect data over there. I would like to express my gratitude to Dr. Brian Volkman at Medical College of Wisconsin for his collaboration and invaluable and knowledgeable comments on this chemokine project. I also acknowledge that my doctoral research would not be completed without the help of every past and present lab members of Drs. Nesmelova's and Dréau's lab, including Gage Leighton, Diana Joy, Venkatesh Ranjan, Deepika Suryaprakash, Courtney Samuels, and Katherine Holtzman. I am grateful for their support and friendship that helped me go through the graduate life at UNC Charlotte. It was my pleasure to meet and talk with every person in Woodward and Bioinformatics to share about life and work experiences and to motivate me going through this challenge. I would like to thank UNC Charlotte Graduate School Summer Fellowship Program and Center for Biomedical Engineering and Science for providing me with additional funds for my conference travel and research. Finally, I dedicate this work to my parents, my elder sister, and Paige Vo for their constant support, inspiration, and unconditional love. Thank you very much for always being on my side.

**TABLE OF CONTENTS**

LIST OF TABLES	viii
LIST OF FIGURES	x
LIST OF ABBREVIATIONS	xi
CHAPTER 1: INTRODUCTION	1
1.1 Chemokine classification general structure	1
1.2 Chemokine oligomerization	3
1.3 Chemokine functions	5
1.4 Chemokine signaling	7
1.5 Chemokine heterodimerization	10
1.6 CXCL12-CXCR4 signaling in breast cancer progression	20
1.7 CXCL4 in angiogenesis and cancer	21
1.8 CXCL4-CXCL12 heterodimerization and breast cancer progression	23
1.9 Rationale, Hypothesis and Objectives	23
CHAPTER 2: CXCL12-CXCL4 HETERODIMERIZATION PREVENTS CXCL12-DRIVEN BREAST CANCER CELL MIGRATION	25
2.1 Abstract	25
2.2 Introduction	25
2.3 Materials and methods	27
2.3 Results	30
2.4 Discussion	34
2.5 Figures	37
CHAPTER 3: GENERATION OF THE OBLIGATE CXCL4-CXCL12 HETERODIMER BY DISULFIDE TRAPPING	42

3.1 Abstract	42
3.2 Introduction	43
3.3 Materials and methods	45
3.4 Results	51
3.5 Discussion	54
3.6 Figures	57
CHAPTER 4: EFFECTS OF THE OBLIGATE CXCL4-CXCL12 HETERODIMERS ON BREAST CANCER CELL SIGNALING AND MIGRATION	62
4.1 Abstract	62
4.2 Introduction	64
4.3 Materials and methods	66
4.4 Results	68
4.5 Discussion	71
4.6 Figures	75
CHAPTER 5: SUMMARY, DISCUSSION AND FUTURE DIRECTIONS	79
5.1 Summary	79
5.2 Discussion	82
5.3 Future directions	86
REFERENCES	89
SUPPLEMENTARY DATA APPENDIX	103

**LIST OF TABLES**

TABLE 1.1: Identified chemokine-chemokine heterophilic interactions

11

**LIST OF FIGURES**

FIGURE 1.1: Subfamilies of human chemokines	2
FIGURE 1.2: Chemokine monomeric and multimeric 3D structures	3
FIGURE 1.3: CXCL12-CXCR4 intracellular signaling pathways in cancer	9
FIGURE 2.1: MDA-MB 231 breast cancer cell migration is promoted by CXCL12 through CXCR4 receptor signaling and inhibited by high concentrations of CXCL4 through CXCR3 receptor signaling	37
FIGURE 2.2: CXCL12-driven MDA-MB 231 breast cancer cell migration is dose-dependently inhibited by concurrent increase of CXCL4 concentrations	38
FIGURE 2.3: CXCL12-driven MDA-MB 231 breast cancer cell migration is inhibited by concurrent increase in CXCL4 concentrations through CXCL12-CXCR4 signaling	39
FIGURE 2.4: NMR analyses of CXCL4-CXCL12 heterodimers	40
FIGURE 2.5: The CXCL4-based peptide AHITSLEVIKAG mimics CXCL4 inhibition of CXCL12-driven cell migration	41
FIGURE 3.1: Purification of S26C CXCL4 and L29C CXCL12 chemokine mutants	57
FIGURE 3.2: Purification of the CXCL4-CXCL12 chemokine obligate heterodimers	58
FIGURE 3.3: Obligate CXCL4 <sub>S26C</sub> -CXCL12 <sub>L29C</sub> heterodimers were detected following IP and WB	59
FIGURE 3.4: NMR assessments of the formation and folding of the obligate CXCL4-CXCL12 heterodimer	60
FIGURE 4.1: MDA-MB 231 breast cancer cell migration following chemokine treatments including the obligate CXCL4-CXCL12 heterodimers	75
FIGURE 4.2: Obligate CXCL4-CXCL12 heterodimers competitively inhibit CXCL12-driven migration in MDA-MB 231 cells	77

FIGURE 4.3: Contrasting with wildtype CXCL12 and obligate CXCL12 monomers, obligate CXCL12 homodimer and CXCL4-CXCL12 heterodimer did not promote MDA-MB 231 cell migration	x 78
FIGURE 4.4: Obligate CXCL4-CXCL12 heterodimers induced dose-dependent calcium flux through CXCR4 receptors in MDA-MB 231 breast cancer cells	80
FIGURE S.1: Expression, purification, and NMR characterization of <sup>15</sup> N-labeled CXCL4	107
FIGURE S.2: Expression, purification, and NMR characterization of <sup>15</sup> N-labeled CXCL12	108

**LIST OF ABBREVIATIONS**

AKCRs	atypical chemokine receptors
ANOVA	analysis of variance
Bach-1	BTB domain and CNC homolog 1
bFGF2	basic fibroblast growth factor
BSA	bovine serum albumin
cAMP	adenosine 3',5'-cyclic monophosphate
Co-IP	co-immunoprecipitation
DMEM	Dulbecco's Modified Eagle medium
ECL	enhanced chemiluminescence
ERK1/2	extracellular signal-regulated kinases 1/2
ESI-MS	electrospray ionization mass spectrometry
FBS	fetal bovine serum
FPLC	fast protein liquid chromatography
GAGs	glycosaminoglycans
GCPRs	G-coupled protein receptors
HER2	human epidermal growth factor receptor 2
HO-1	anti-apoptotic heme oxygenase-1
HRP	horseradish-peroxidase
HSQC	heteronuclear single quantum correlation
IPTG	isopropyl $\beta$ -D-1-thiogalactopyranoside
JNK3	c-Jun N terminal kinase-3
LB	Luria broth

NF-kB	nuclear factor-kB
NMR	Nuclear Magnetic Resonance
Nrf2	nuclear factor erythroid 2-related factor 2
ORATH	obligate RANTES-TARC heterodimer
p38 MAPK	p38 mitogen-activated protein kinase
PAK	p21-activated kinase
PBS	phosphate-buffered saline
PI3K	phosphatidylinositol 3-kinase
PKA	protein kinase A
PKB	protein kinase B
PMSF	phenylmethylsulfonyl fluoride
SDS-PAGE	sodium dodecyl-sulfate polyacrylamide gel electrophoresis
SEM	standard error of the mean
TME	tumor microenvironment
VEGF	vascular endothelial growth factor

## CHAPTER 1: INTRODUCTION

This chapter provides the current state of the chemokine field regarding chemokine (1) classification, (2) oligomerization, (3) functions, (4) signaling, and (5) heterodimerization. It also reviews current literature on (6) CXCL12-CXCR4 signaling in breast cancer, (7) CXCL4 signaling and activities in angiogenesis and cancer, and (8) the current knowledge of the functional activities associated with the CXCL4-CXCL12 heterodimerization, because the dissertation focuses on CXCL4-CXCL12 signaling. Finally, this chapter presents (9) the rationale, hypotheses, and objectives of this dissertation.

### 1.1 Chemokine classification and general structure

#### 1.1.1 Classification

Chemokines (MW ~ 8-12kDa) are chemotactic cytokines that mainly regulate cell (in particular, leukocytes) trafficking in both physiological and inflammatory conditions [5]. To date, 48 human chemokines have been identified and structurally categorized based on the number and position of the conserved N-terminal cysteine residues forming disulfide bonds. The CXC- and CC- are the two biggest subfamilies with 17 and 28 chemokine members, respectively. The CXC-chemokine amino acid sequence contains two cysteines separated from each other by one (X) amino acid that varies. In contrast, in CC-chemokines, two cysteines are adjacent (Figure 1.1) [6-8]. Remaining other chemokines belong to two smaller subfamilies XC and CX3C with 1 and 2 members, respectively. XC chemokines lacks both the first and the third conserved cysteine residues [8]. CX3C chemokine contains three amino acids between the first two conserved cysteines [9].

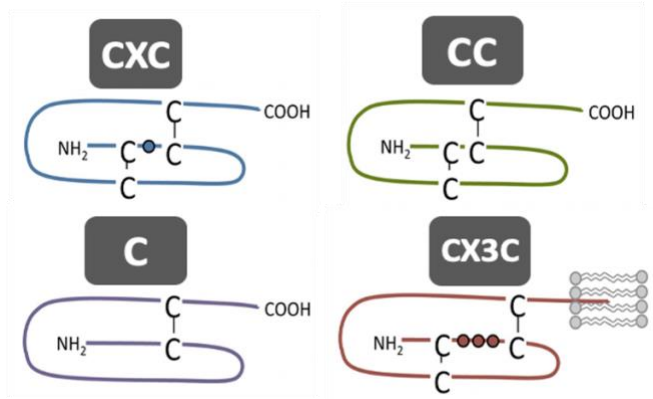


**Figure 1.1: Subfamilies of human chemokines.** Chemokine subfamilies are based on the number and position of the conserved N-terminal cysteine residues. Black line represents for the disulfide bonds. Adapted from [10].

### 1.1.2 Three-dimensional structure of chemokines

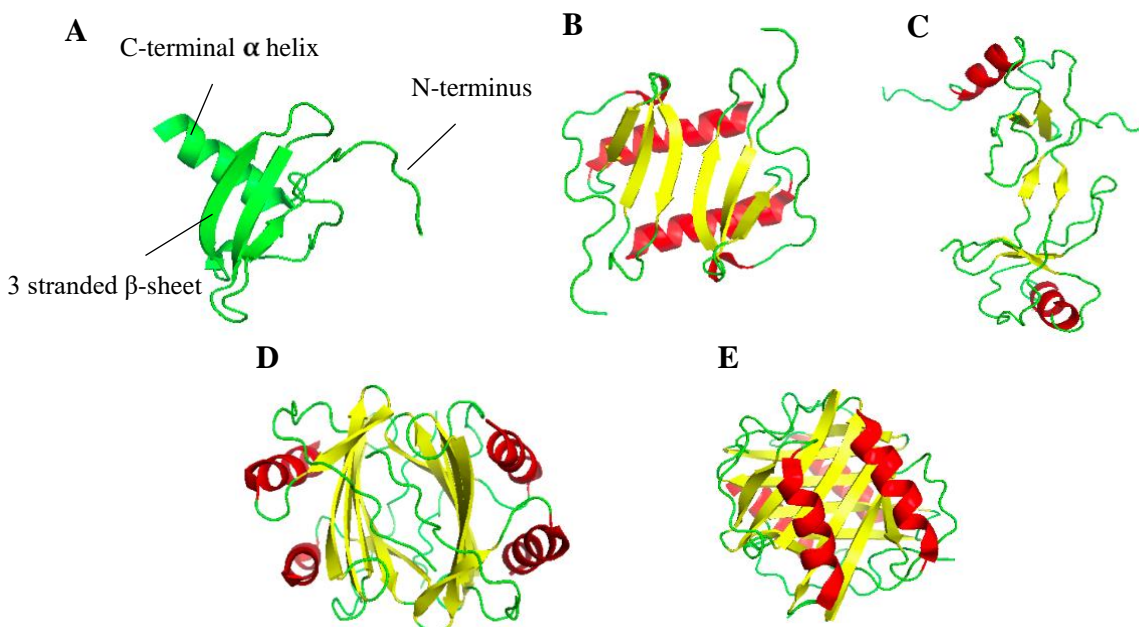


**Figure 1.2: Chemokine monomeric and multimeric 3D structures.** (A) Monomer structure of CXCL12 [1]. 3D structure of the CXC-type CXCL8 homodimer (B) [2], and CC-type CCL2 homodimer (C) [3]. 3D structure of CXCL4 tetramer [4] in two orientations with four monomer CXCL4 subunits, presenting CC-type dimer via N-termini (D) and CXC-type dimer interface via the first  $\beta$ -sheet from each monomer (E).

While the amino acid sequence identity varies from 20 to 70 percent, chemokine tertiary structures are highly conserved [11]. Four conserved cysteine residues form two essential disulfide bonds, Cys1-Cys3 and Cys2-Cys4 [11]. The three-dimensional structure of a chemokine monomer consists of a disordered N-terminal domain, followed by a N-terminal loop ending in a  $3_{10}$  helix,  $\beta$ -sheet consisting of three antiparallel  $\beta$ -strands, and a C-terminal  $\alpha$ -helix folded on top of the  $\beta$ -sheet (Figure 1.2 A) [12].

## 1.2 Chemokine oligomerization

Chemokine monomers can associate with one another to form primarily homodimers, and some form homotetramers [12-14]. More recently, heterodimerization of chemokine has been demonstrated (see section 1.7 below) [15-23].

### 1.2.1 Chemokine homodimerization

Chemokines form different types of homodimers depending on the subfamily they belong to. The homodimer structures of CXC- and CC- chemokines are markedly different from each other since the dimer interfaces are formed by distinct sets of residues. In CXC-type homodimer, the interface is formed by the first  $\beta$ -strand from each monomer resulting in a globular extended six-stranded  $\beta$ -sheet, and of which the two helices folded on top and running antiparallel to each other (Figure 1.2 B-C) [21]. The CC-type dimers are more cylindrical and stabilized through the interactions between the two N-termini from each monomeric unit with the two helices oriented almost perpendicular to each other from the opposite side of the complex (Figure 1.2 B) [21].

### 1.2.2 Chemokine homotetramers and higher-order oligomers

Tetramerization has been observed with CXCL4 [13] and CXCL7 [24]. CXCL4 tetramer consists of both CXC-type and CC-type dimers (Figure 1.2 D-E). The two CXC-type dimers (i.e., A-B and C-D dimers) interact with one another via  $\beta$ -sheets, resulting to the formation of a  $\beta$ -bilayer, stacking both  $\beta$ -sheet on top of one another [4]. Moreover, the tetrameric structure is stabilized by contacts among residues in the N-terminal regions to form A-C and B-D dimers in CC-type dimerization [4]. A few chemokines also form higher-ordered oligomers, such as CCL5 [25] or CCL27 [26].

### 1.2.3 Proportions of the various chemokine oligomers

In solution, the proportions of chemokine monomer, dimer and higher-order oligomers vary. The formation of the oligomeric species is primarily determined by the chemokine concentration, amino acid composition and the conformation of the inter-subunit interfaces, with some chemokines preferentially forming oligomers while the others remain in a monomer-dimer state [21].

In particular, *in vivo* microenvironments including the tumor microenvironment, chemokine equilibria are altered by the solution properties, including pH, composition, ionic strength, or the presence of sequestering molecules such as glycosaminoglycans (GAGs), as reported for CXCL12 [27], CXCL4 [13, 28], and CXCL7 [24, 29, 30].

### **1.3 Chemokine functions**

Chemokines are key mediators regulating cellular migration and cell-cell communications. Chemokines can be functionally grouped as inflammatory and homeostatic chemokines, while some chemokines have these dual functions [31].

#### 1.3.1 Inflammatory and homeostatic chemokines

Inflammatory chemokines (i.e., CCL1-CCL13, CCL23-24, CXCL1-3, CXCL5-11) are produced during immune responses to direct the migration of leukocytes to the site of inflammation [8]. In contrast, homeostatic chemokines (i.e., CCL14-16, CCL25, CCL27, CXCL12-13) are constitutively expressed in non-inflamed tissues and directly guide the trafficking of cells that express certain chemokine receptors to specific organs where their chemokine ligands are expressed during the normal processes of tissue maintenance or development [8]. Some chemokines with dual functions regulate cell migrations during both the immune responses and homeostasis. Examples of dual-function chemokines include CCL11, CCL17, CCL20, CCL22, XCL1-2, CX3CL1 [8].

#### 1.3.2 Angiogenic and angiostatic chemokines

Based on the presence of the Glu-Leu-Arg (ELR) motif prior the first N-terminal cysteine residue, chemokines of the CXC-subfamily were categorized as angiogenic and angiostatic. ELR<sup>+</sup> chemokines (i.e., CXCL1-3, CXCL5-8) are angiogenic, whereas ELR<sup>-</sup> chemokines (i.e., CXCL4, CXCL9-11) are angiostatic [32]. The ELR<sup>+</sup> motif allows binding and activation of

CXCR1 or CXCR2 receptors, widely expressed on normal endothelial cells and various tumor cell types [33]. Indeed, CXCR1 and/or CXCR2 receptors are widely expressed and associated with the aggressiveness in melanoma [34], renal carcinoma [35], pancreatic [36], gastrointestinal [37], and breast cancer [38, 39]. In contrast, the ELR<sup>-</sup> chemokines mediate the angiostatic activity through their putative receptor CXCR3B [40, 41]. CXCL12 is an ELR<sup>-</sup> chemokines with potent angiogenic activity in human invasive breast cancer [42] and many other malignancies [43-45], whereas CXCL4 is an ELR<sup>+</sup> chemokine known as a potent angiostatic agent [41, 46-49].

### 1.3.3 Tumorigenic chemokines

Chemokines actively participate in all phases of tumorigenesis, especially cell migration which is a key step of metastasis. The tumor microenvironment (TME) is complex and comprises tumor cells and multiple stroma cells that communicate with each other via numerous signaling networks [50, 51]. Within the TME, chemokines produced by cancer cells and stroma cells modulate the recruitment of specific subsets of immune cells, and hence, mediate both anti-tumor and pro-tumor responses [52]. Chemokines are also involved in tumor development, including angiogenesis, tumor growth, and organ-specific metastasis [31, 52-55]. In particular, CCL19 and CCL21 mediate metastasis of CCR7<sup>+</sup> carcinoma cells to lymph nodes [56] whereas CCR9<sup>+</sup> melanoma cells preferentially metastasize to the small intestine because of its CCL5 expression [57, 58]. In breast cancer, CXCL12 promotes metastasis to lungs, liver, brain, and bone marrow [31, 59-61].

Altogether, due to their critical roles in orchestrating the variety of functions in pathological conditions, chemokines and chemokine receptors have been intensively studied as therapeutic targets for treatment of multiple inflammatory diseases and cancers.

## 1.4 Chemokine signaling

To mediate cellular responses, chemokines bind to their cognate receptors initiating intracellular signaling cascades. The responses triggered by chemokine receptors rely on the activation of multiple downstream signaling effectors through the G-protein pathways and tightly integrated with the  $\beta$ -arrestin mediated pathway [62, 63]. Chemokine and chemokine receptors are widely expressed on all leukocytes and many non-hematopoietic cells, including cancer cells [32]. In particular, chemokine-chemokine receptor activation critically induces directional migration of these cells [62]. Beside cellular migration, chemokine signaling also regulates numerous intracellular cascades in many cell types, highlighting the pivotal role for chemokine in both normal physiological and pathological conditions.

### 1.4.1 Chemokine receptors

Chemokine receptors consist of 19 G-protein coupled receptors (GPCRs) and 4 atypical chemokine receptors (AKCR1-4) [64]. The GPCRs are further classified into four groups according to the type of chemokine they bind to i.e., CCR, CXCR, XCR, and CX3CR [65]. Most chemokines differentially activate more than one receptor and most receptors can bind multiple chemokines with variable affinities [66]. This critical feature of chemokines and their receptors allows the fine-tuning of specific responses in different tissues, cell types, physiological or pathogenic conditions [65].

### 1.4.2 Chemokine G-protein dependent signaling cascades

Chemokine receptor activation, including CXCL12-CXCR4 axis, regulates cell chemotaxis to the site of inflammation, angiogenesis, and malignant transformation [6]. Key steps of chemokine signaling pathways included in the CXCL12-CXCR4 axis, start with the physical chemokine-receptor interaction leading to downstream signaling transductions (Figure

1.3) [67]. Following the activation of CXCR4, G-coupled proteins ( $G_a$  and  $G_{\beta\gamma}$ ) trigger the generation of secondary messengers such as intra-cytoplasmic calcium spike or cAMP production. In turn, these secondary messengers activate downstream cascades of signals including phospholipase- $C_{\beta}$ , phosphatidylinositol 3-kinase (PI3K), members in the Rho family of GTPases, p21-activated kinase (PAK), p38 mitogen-activated protein kinase (p38 MAPK), extracellular signal-regulated kinases 1 and 2 (ERK1 and ERK2) and/or members of the nuclear factor- $\kappa$ B (NF- $\kappa$ B) family of transcription factors [7, 67-69]. One of the downstream effects of calcium signaling cascade is the activation of cytoplasmic actin polymerization, the formation of pseudopods polarizing cell morphology, and resulting in cell movement [70].

#### 1.4.3 Chemokine G-protein independent signaling cascades

For a long time, GCPRs have been thought to act exclusively on the heterotrimeric G protein and desensitized by  $\beta$ -arrestin. However, chemokines also activate the G-protein-independent  $\beta$ -arrestin mediated pathway, broadening the complexity of chemokine signaling [71, 72]. Indeed, besides terminating the GCPR signaling,  $\beta$ -arrestin also serves as a scaffold protein for key kinases in the MAPK signaling cascade, including ERK1/2, p38, c-Jun N terminal kinase-3 (JNK3) [73, 74]. Moreover, activation of  $\beta$ -arrestin-2 results in the activation of extracellular signal-regulated kinases (ERKs) or protein kinase B (i.e., PKB or Akt) pathway to promote survival and chemotaxis in T cells [75].

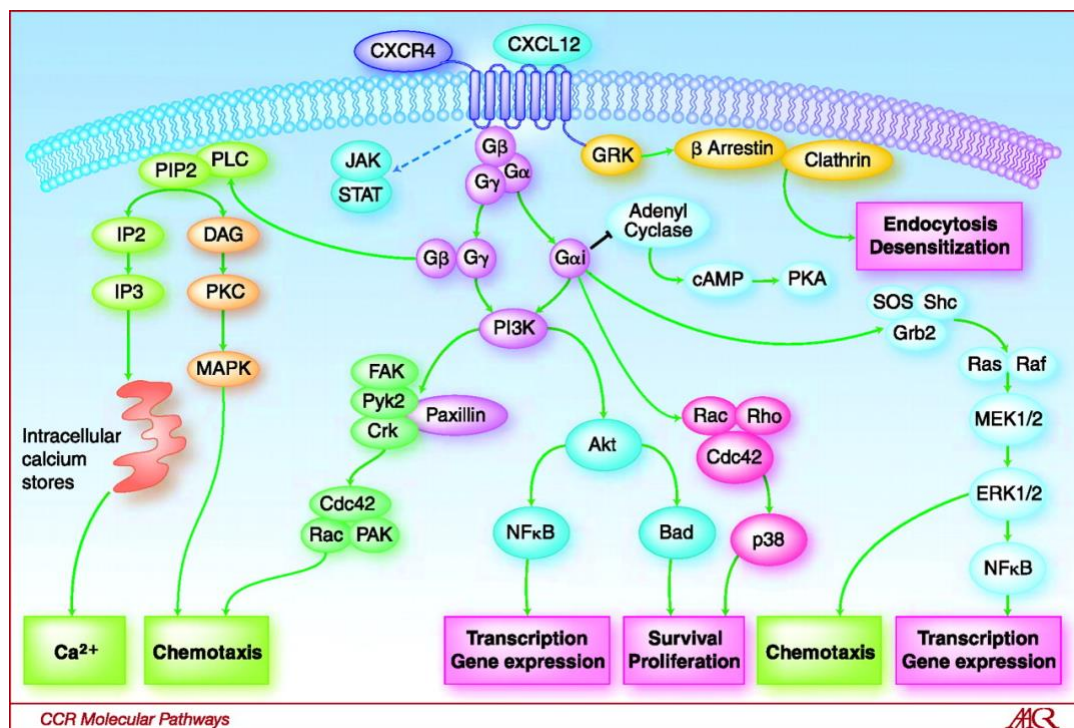


**Figure 1.3: CXCL12-CXCR4 intracellular signaling pathways in cancer.** The precise signaling pathways can vary among cell types and specific tissues [67].

#### 1.4.4 Glycosaminoglycans and chemokine signaling

Chemokines interact with GAGs, which are abundant on cell surfaces and in the extracellular matrix [76]. Chemokine function and the ability to activate GPCR is regulated by binding to GAGs. GAG binding stabilizes chemokine oligomers, protecting chemokines from the proteolytic degradation and generates a chemotactic gradient for GPCR activation [30, 76-79]. In essence, GAG binding is functionally important for CXCL12 activity as CXCL12-GAG complexes increase the local accumulation of CXCL12 near the CXCR4 receptors and provide the chemotactic gradient along cell surfaces [80].

#### 1.4.5 Monomeric and dimeric chemokine signaling

When acting on the same receptor, monomeric and dimeric chemokines can regulate distinct signaling pathways. Thus, CXCL12 dimers induced a transient phosphorylation of ERK1/2, weakly recruited β-arrestin, and minimally promoted polymerization of the cytoskeletal

F-actin in comparison to monomeric CXCL12 [81]. In line with a weak signaling cascade activation, dimeric CXCL12 inhibited chemotaxis in CXCR4<sup>+</sup> monocytic leukemia [59], colorectal carcinoma [81], and *in vivo* metastasis of melanoma [82]. CXCL8 dimer is also less effective than the CXCL8 monomer in mediating calcium flux, phosphoinositide hydrolysis,  $\beta$ -arrestin recruitment and chemotactic activity in CXCR1-expressing basophilic leukemia cells [83]. CXCL10, CCL2, CCL4, and CCL5 oligomerization is not required to activate their respective receptors since the monomeric variants induced chemotactic activity *in vitro* [76, 84]. However, these chemokines need to oligomerize upon GAG binding to retain the *in vivo* function [76, 84]. Likewise, CXCL7 [30] and CXCL8 [85] chemokine dimers, but not monomers, are essential for GAG binding.

### 1.5 Chemokine heterodimerization

Another compelling evidence of chemokine oligomerization to fine-tune biological functions *in vivo* is the heterodimerization between different chemokines. Monomers of different chemokines may swap with each other to form heterodimers if the arrangement of the amino acids at the inter-subunit interface is energetically favorable [86]. To date, about 200 pairwise heterophilic interactions have been identified (Table 1.1) [15-23]. However, our understanding of the molecular mechanism of chemokine heterodimers is limited to a few chemokine heterodimer pairs. The heterophilic interactions can fine-tune chemokine activities by either suppressing or enhancing monomer or homodimer chemokine functions.

There are two different modes of chemokine heterodimerization: CXC- and CC-type dimer (see section 1.2 for structural details) [86]. Structure-function analysis revealed that CC-type heterodimers were synergistic, whereas CXC-typed heterodimers were inhibitory [15]. However, this pattern is not mutually exclusive since some chemokines show opposite effects.

Thus, the heterodimerization function is chemokine-specific and greatly depends on the heterodimer receptor activation. Although the functional effects associated with chemokine heterodimerization have been identified in a few chemokine pairs, the mechanisms related to the observed functions have not been fully investigated.

**Table 1.1: Identified chemokine-chemokine heterophilic interactions.**

<b>Human Chemokine</b>	<b>Interaction?</b>	<b>Binding partner(s)</b>	<b>Known function(s)</b>	<b>Reference</b>
CXCL1	Yes	CXCL7	Interactions with GAGs	[15], [21, 23]
		CCL11; CXCL4, 5-6	N/A	[15]
CXCL2	Yes	CCL5, 8, 11, 21, 28; XCL1-2; CXCL4-6, 9, 11-12, 14	N/A	[15]
CXCL3	Yes	CCL11; XCL2; CXCL5-6	N/A	[15]
CXCL4	Yes	CCL5  CXCL8	Enhanced monocyte arrest, chemotaxis  Inhibited proliferation of endothelial cells; monocyte arrest; and CXCL8-induced	[15], [16]  [15, 17, 19, 86]

		CXCL12  CCL2, 11, 13, 17, 20-21, 23, 25-26, 28; XCL1-2; CXCL1-2, 6, 7, 9- 11, 14, 17	migration in CXCR2- expressing cells Inhibited chemotaxis in T cells  N/A	[15]  [15], [23]
CXCL4L1	Yes	CCL4L1, 11, 19, 21-22, 25-28; XCL1-2; CXCL10-13	N/A	[15]
CXCL5	Yes	CCL11, 20; XCL2; CXCL1-3, 14	N/A	[15]
CXCL6	Yes	CCL5, 7-8, 11; CXCL1-4, 7, 10, 12	N/A	[15]
CXCL7	Yes	CXCL1, 4  CCL2, 5, 8, 13, 17, 21, 23, 26, 28; CXCL6, 9-12, 14	See CXCL1, 4  N/A	[15]

CXCL8	Yes	CXCL4 CCL2, 8	See CXCL4 N/A	[15], [19, 21] [15]
CXCL9	Yes	CXCL12  CCL2, 5, 11, 13, 21, 26, 28; XCL1; CXCL2, 4, 7, 10- 11, 14, 17	Enhanced CXCR4- mediated tumor- infiltrating lymphocytes and malignant B cells  N/A	[15, 87]  [15]
CXCL10	Yes	CCL22  CCL5, 8, 11, 13, 21, 26, 28; XCL1; CXCL4/L1, 6-7, 9, 11-12, 14, 17	Enhanced CCR4- mediated chemotaxis of T cells  N/A	[88]  [15]
CXCL11	Yes	CCL1, 5, 8, 11, 13, 20-21, 24-26; XCL1; CXCL2, 4/L1, 7, 9-12, 14	N/A	[15]
CXCL12	Yes	CCL5	Inhibited T cell	[15]

		CXCL4  CCL11, 13, 20-21, 25-26, 28;  XCL1-2; CXCL2, 4L1, 6, 7, 9-11, 14, 17	chemotaxis  See CXCL4  N/A	[15]
CXCL13	Yes	CCL21  CCL4L1, 28;  CXCL4L1	Enhanced CCL21-mediated chemotaxis  N/A	[15, 20]  [15]
CXCL14	Yes	CCL5, 11, 13, 21, 26, 28  XCL1  CXCL2, 4-5, 7, 9-12, 17	N/A	[15]
CXCL16	No			[15]
CXCL17	Yes	CCL2, 5, 8, 13, 20-21, 25-26, 28  XCL1-2  CXCL2, 4, 9-10, 12, 14	N/A	[15]
CCL1	Yes	CXCL11	N/A	[15]

CCL2	Yes	CCL5  CCL8  CCL4L1, 5, 11, 13, 15, 26 CXCL4 CXCL7 CXCL8-9, 17	Enhanced monocyte arrest; triggered CCR2-CCR5 heterodimerization Enhanced interactions with GAGs N/A	[15, 89]  [15], [90]  [15]
CCL3	Yes	CCL4	May be associated with down-regulation of CCR5 receptor	[91]
CCL3L1	No			[15]
CCL3L3	No			[15]
CCL4	Yes	CCL3	See CCL3	
CCL4L1	Yes	CCL2; CXCL4L1, 13	N/A	[15]
CCL4L2	N/A			
CCL5	Yes	CCL2  CCL17	See CCL2  Enhance monocyte arrest	[15]

		CXCL4 CXCL12 CCL3, 11, 13, 16, 20-21, 24-28; XCL1-2; CXCL2, 6-7, 9-11, 14, 17	See CXCL4 See CXCL12 N/A	[15]
CCL7	Yes	XCL1; CXCL6	N/A	[15]
CCL8	Yes	CCL2 CCL11, 13, 26; CXCL2, 6-8, 10- 11, 17	See CCL2 N/A	[15]
CCL11	Yes	CCL2, 5, 8, 13- 14, 26-28; XCL1; CXCL1-4/L1, 5- 6, 9-12, 14	N/A	[15]
CCL13	Yes	CCL2, 5, 8, 11, 21, 24, 26, 28; XCL1; CXCL4, 7, 9-12, 14, 17	N/A	[15]
CCL14	Yes	CCL11, 22	N/A	[15]
CCL15	Yes	CCL2	N/A	[15]
CCL16	Yes	CCL5	N/A	[15]
CCL17	Yes	CCL5	See CCL5	

		CCL21, 25-26, 28; CXCL4, 7	N/A	[15]
CCL18	No			[15]
CCL19	Yes	CCL22 CXCL4L1	N/A	[15]
CCL20	Yes	CCL5; XCL2; CXCL4-5, 11-12, 17	N/A	[15]
CCL21	Yes	CCL5, 13, 17, 23- 24, 26, 28; XCL1-2; CXCL2, 4/L1, 7, 9-14, 17	N/A	[15]
CCL22	Yes	CCL14, 19; CXCL4L1	N/A	[15]
CCL23	Yes	CCL21; CXCL4, 7		[15]
CCL24	Yes	CCL5, 13, 21; XCL1; CXCL11	N/A	[15]
CCL25	Yes	CCL5, 17; CXCL4/L1, 11- 12, 17	N/A	[15]
CCL26	Yes	CCL2, 5, 8, 11, 13, 17, 21, 28	N/A	[15]

		XCL1-2 CXCL4/L1, 7, 9- 12, 14, 17		
CCL27	Yes	CCL5, 11 CXCL4L1	N/A	[15]
CCL28	Yes	CCL5, 11-13, 17, 21, 26; XCL1-2; CXCL2, 4/L1, 7, 9-10, 12-14, 17	N/A	[15]
XCL1	Yes	CCL5, 11, 13, 21, 24, 26, 28; CXCL2, 4/L1, 9- 12, 14, 17	N/A	[15]
XCL2	Yes	CCL5, 7-8, 20- 21, 26, 28; CXCL2-4/L1, 5, 12, 17	N/A	[15]
CX3CL1	No			[15]

Abbreviation: N/A: not yet determined.

### 1.5.1 Synergy-inducing chemokine heterodimerization

Heterodimerization associated with synergistic effects was mostly found among CC-chemokines or mixed CC-/CXC- chemokine pairs. For example, CCL2-CCL5 enhanced monocyte movement arrest by triggering receptor heterodimerization [15]. CCL2-CCL8

heterodimers significantly increased their interactions with GAGs, which in turn, promoted the chemotactic gradient [90]. Synthesized covalently linked CCL5-CCL17 (named ORATH) heterodimers synergistically triggered monocyte movement arrest on the endothelium and *in vivo* conditions, providing an unambiguous evidence that the heterodimers are functionally active [15, 16]. Likewise, mixed heterodimerization of CXCL4-CCL5 enhanced CCL5-mediated monocyte movement arrest in endothelial cells [16]. CXCL10 forming heterocomplexes with CCL22 synergistically promoted CCR4-mediated chemotaxis in T cells [92].

A few chemokine pairs from CXC-subfamily have shown to form heterodimers with synergistic effects. For example, the administration of both CXCL1 and CXCL2 synergistically enhanced the chemotactic effect of leukocyte recruitment into the central nervous system in rats [92]. Similarly, CXCL9 and CXCL12, co-expressed in the perivascular tumor, formed heterodimers that significantly enhanced CXCR4-mediated migration of the malignant B cells [87]. CXCL7-CXCL1 heterodimers more potently bound to GAGs compared to the CXCL7 alone [23].

### 1.5.2 Inhibitory-inducing chemokine heterodimerization

Chemokines engaged in CXC-type heterodimerization induce inhibition. The CXCL4-CXCL8 hetero-complex prevented the binding of CXCL8 to CXCR2, consequently disrupting the CXCL8/CXCR2 signaling axis associated with endothelial cell survival and proliferation [19, 33]. A CCL5-derived peptide mimicking the inhibitory effect of the CCL5-CXCL12 heterodimers reduced the CXCL12-mediated platelet aggregation in mice, suggesting that the structural information regarding the binding interface between two chemokines can be useful to design inhibitory peptides for therapeutic effect [15].

## **1.6 CXCL12-CXCR4 signaling in breast cancer progression**

### 1.6.1 Breast cancer and CXCL12-CXCR4 expression

Breast cancer is the second common cause of death among women in the US, almost entirely due to metastasis [93]. Breast cancer is primarily characterized by the presence of tumor cells in breast epithelium, mainly of the lobes and duct. Breast tumor cells proliferate and metastasize to lymph nodes, and distant organs, preferentially bones, lungs, and liver [94, 95]. Current treatment options for the advanced stage of breast cancer are limited [96]. Cancer metastasis is governed by many factors within the TME which facilitate tumor cells' escape from the tight control by the normal epithelium, leading to tumor growth at the primary tumor site, migration to distant organs, and establishment of metastases in different tissue niches [94]. CXCR4 is overexpressed by the primary breast tumor cells compared to the normal breast epithelial cells, while its ligand CXCL12 is abundantly produced within the breast cancer metastatic niches, including lymph nodes, bone marrow, lungs, and liver [97]. Breast cancer cell CXCR4 expression is also significantly higher in metastatic lesions than in primary tumors [98].

### 1.6.2 CXCL12-CXCR4 signaling, cancer migration, and protection from apoptosis

Following CXCL12 activation, the G-protein coupled receptor CXCR4 exhibits classic chemokine receptor activities including the initiation of G-protein activation,  $\beta$ -arrestin recruitment and internalization [67]. CXCL12-mediated G-protein activation stimulates the release of intracellular calcium (secondary messenger) that triggers and a cascade of downstream signaling steps, leading to cellular cytoskeleton rearrangement and different protein expression that eventually promote migration [99]. The key role of CXCL12/CXCR4 signaling in breast cancer is demonstrated by the inhibition of breast cancer metastasis in mouse model using neutralizing CXCR4 antibodies [97]. Beyond breast cancer, the CXCL12/CXCR4 axis

contributes to the growth and metastatic potential of at least 22 different types of cancers [97, 100-103].

CXCL12 also promotes protection from apoptosis through CXCL12-CXCR4 signaling and thus enhances the survival of CXCR4+ cancer cells in pancreatic adenocarcinoma [104], glioma [105], leukemia [106], and breast cancer [107]. Targeting CXCR4 using specific antagonists combined with conventional chemotherapies led to tumor regression in the mouse models of glioblastoma multiforme [108] and B16 melanoma [109]. Similarly, treatments by either inhibiting the CXCR4 expression or using CXCR4 antagonist AMD3100 prevented primary tumor growth and lung metastasis in a murine model of 4T1 breast cancer cells [107]. These findings strongly support the key role of CXCL12/CXCR4 axis in the primary cancer development and metastasis.

## **1.7 CXCL4 in angiogenesis and cancer**

### 1.7.1 CXCL4 inhibits angiogenesis

CXCL4 is an angiostatic chemokine [46]. Indeed, CXCL4 inhibits endothelial cell proliferation [110], suppresses *in vivo* growth of murine melanoma and human colon carcinoma in mice [111], and effectively prevents the lung metastasis of melanoma [112].

Three mechanisms of CXCL4 angiostatic activities have been identified. First, CXCL4 inhibits angiogenesis by directly interacting with angiogenic growth factors, including bFGF-2 [113] and VEGF [114]. Interactions of CXCL4 with bFGF2 and VEGF antagonize the signaling through their respective receptors [115]. Second, CXCL4 also inhibits angiogenesis through the formation of a chemokine heterocomplex with CXCL8, thereby inhibiting the CXCL8/CXCR2-mediated angiogenesis [17, 19]. Lastly, CXCL4 signals through the CXCR3B receptor [41]. The CXCR3 receptor has two primary isoforms, CXCR3A and CXCR3B [116-118]. Chemokines

CXCL9-11 bind to both isoforms, whereas CXCL4 is a specific ligand for CXCR3B [119]. Interestingly, CXCR3A and CXCR3B regulate distinct intracellular pathways, leading to inverse biological functions [41, 120, 121]. CXCR3A mediates cell growth and chemotaxis, while CXCR3B induces negative signals that prevent cell proliferation, angiogenesis, and promote programming-cell death [41, 119, 120]. CXCR3A, like other chemokine receptors, is coupled with  $G_{ai}$  to mediate the calcium flux within cells [41, 122], whereas CXCR3B induces signals through  $G_{as}$  protein leading to the activation of PKA and the increased intracellular level of cAMP [41, 123]. CXCL4-mediated activation of  $G_{as}$  signaling led to inhibition of m-calpain – a critical protease that enables cell migration via regulating the rear-end detachment of adherent cells from the focal adhesion complex [123].

#### 1.7.2 Other CXCL4-CXCR3B axis inhibitory activities

CXCL4-mediated activation of CXCR3B is not associated with changes in calcium flux in endothelial cells [41] or the chemotaxis of human type II pneumocytes [124]. Moreover, the anti-angiogenic activities associated with CXCR3B signaling includes inhibition of DNA synthesis and promotion of the programmed-cell death [41]. CXCR3B is expressed by renal [125-127], prostate [123], and breast cancer cells [119, 120]. In prostate cancer, CXCL4/CXCR3B-mediated inhibition of cellular migration is mechanistically resulted from cAMP upregulation and m-calpain inhibition via  $G_{as}$  signaling [123]. CXCR3B can also mediate growth-inhibitory signals via the p38 MAPK pathway, down-regulating the expression of the anti-apoptotic heme oxygenase-1 (HO-1) in human renal cancer cells [126] and breast cancer cells [119]. Furthermore, the downregulation of HO-1 in breast cancer cell lines is associated with changes in the regulation of the negative and positive regulator of HO-1 expression Bach-1 and Nrf2 [119].

## 1.8 CXCL4-CXCL12 heterodimerization in breast cancer progression

CXCL12 is a key mediator in many types of cancer progression, including breast cancer [128-133]; thus, targeting CXCL12 by heterophilic interactions may have a therapeutic benefit for patients suffering from cancers, especially, breast cancer. CXCL12 directs the migration of CXCR4<sup>+</sup> tumor cells to organs with its high expression resulting in breast cancer metastasis [103, 107, 134-136]. Furthermore, CXCR4 expression in cancer biopsies is associated with poor clinical outcomes in patients with a triple negative breast cancer [137]. CXCL12 physically forms hetero-complexes with CXCL4 in human platelets [22], and CXCL4-CXCL12 heterodimers were further characterized using biophysical methods [15, 138]. Functionally, the mixture of CXCL4 and CXCL12 attenuates the CXCL12-mediated chemotaxis in T cells [15], suggesting the possibility of similar effects in other cells as well. Whether CXCL12-CXCL4 heterodimerization inhibits breast cancer migration and the role of CXCL4-CXCL12 heterodimers in CXCL12-CXCR4 signaling remains unknown. Our research of the role of CXCL4-CXCL12 heterodimerization in the migration of triple negative breast cancer cells provides new insight into the structural and regulatory mechanisms associated with CXCL4-CXCL12 chemokine heterodimerization.

## 1.9 Rationale, Hypothesis and Objectives

Our understanding of the biology of chemokines mainly results from observations of individual chemokines assumed to act independently. Indeed, most *in vitro* studies were conducted based on a single chemokine activity [139-141]. Those experiments were conducted in conditions that marginally mimic *in vivo* biological conditions, where multiple chemokines co-localize and the hetero-dimerization may be one of the mechanisms to fine-tune the biological activities of an individual chemokine [142]. Although the formation of CXCL4-CXCL12

heterodimers has been described [15, 22], whether CXCL12-CXCL4 heterodimers significantly alter breast cancer activities remains unknown. Our research seeks to fill this gap.

This dissertation investigates the role of chemokine CXCL4-CXCL12 heterodimerization in breast cancer migration. We hypothesized that CXCL4-CXCL12 heterodimers will fine-tune the CXCL12 and CXCL12-CXCR4 signaling during breast cancer migration. Chapter 2 presents data (a) using CXCL4-CXCL12 chemokine mixtures to elucidate the biological relevance of chemokine heterodimerization *in vitro* breast cancer migration, and (b) using the CXCL4-derived peptide mimicking the binding interface of CXCL4 with CXCL12 to investigate the inhibitory activity on CXCL12-induced MDA-MB-231 cell migration. The data presented in Chapter 2 have been published [138]. Chapter 3 presents a novel methodology to overcome the challenge associated with the co-presence of multiple chemokine species and describes the production and characterization of a non-dissociating CXCL4-CXCL12 heterodimer by using the disulfide trapping strategy [23, 59]. (Note: Methods and data to produce and characterize recombinant human wildtype CXCL4 and CXCL12 are provided in the appendix). The generation of the CXCL4-CXCL12 heterodimer has been applied for patent (“Obligate CXCL4-CXCL12 Heterodimers”, U.S. Provisional patent, application number 63161108, USPTO received submission on March 15<sup>th</sup>, 2021). Chapter 4 presents data on the biological relevance of the new disulfide-trapped CXCL4-CXCL12 heterodimer by assessing its effects on the migration of breast cancer cells. These data are in the preparation for publication. Chapter 5 discusses the findings of this research.

Overall, this thesis provides a new insight into the biological role of CXCL4-CXCL12 heterodimers in breast cancer.

## CHAPTER 2: CXCL12-CXCL4 HETERODIMERIZATION PREVENTS CXCL12-DRIVEN BREAST CANCER CELL MIGRATION

This chapter is published: Nguyen *et al.*, 2020.

### 2.1 Abstract

Despite improvements in cancer early detection and treatment, metastatic breast cancer remains deadly. Current therapeutic approaches have very limited efficacy in patients with triple negative breast cancer. Among the many mechanisms associated that contribute to cancer progression, signaling through the CXCL12-CXCR4 is an essential step in cancer cell migration. We previously demonstrated the formation of CXCL12-CXCL4 heterodimers [22]. Here, we investigated whether CXCL12-CXCL4 heterodimers alter tumor cell migration. CXCL12 alone dose-dependently promoted the MDA-MB 231 cell migration ( $p < 0.05$ ), which could be prevented by blocking the CXCR4 receptor. The addition of CXCL4 inhibited the CXCL12-induced cell migration ( $p < 0.05$ ). Using NMR spectroscopy, we identified the CXCL4-CXCL12 binding interface. Moreover, we generated a CXCL4-derived peptide homolog of the binding interface that mimicked the activity of native CXCL4 protein. These results confirm the formation of CXCL12-CXCL4 heterodimers and their inhibitory effects on the migration of breast tumors cells. These findings suggest that specific peptides mimicking heterodimerization of CXCL12 might prevent breast cancer cell migration.

### 2.2 Introduction

Breast cancer progression, especially metastasis, relies on breast cancer cell migration orchestrated mainly through CXCL12-CXCR4 chemokine-receptor signaling [143-146]. The role of CXCL12-CXCR4 signaling in cell migration has been clearly demonstrated in breast

cancer cell models including in the triple negative breast cancer MDA- MB 231 cells [128, 147, 148]. CXCR4 tumor cell expression associated with high constitutive secretion of CXCL12 in organs, including lungs, bone marrow, and liver generates a gradient that promotes cell migration and targeted metastasis [128]. Moreover, clinically, the overexpression of CXCR4 on tumor cells is associated with the most aggressive form of breast cancer, i.e., triple negative breast cancer [143, 149]. The migration of breast cancer cells has been targeted to prevent cancer progression using CXCR4 chemokine receptor antagonists [150, 151], nanoparticles [152], and oncolytic virotherapy [153]. However, the results of clinical trials using CXCR4 antagonist-based approaches have been mixed [154, 155], possibly because of the multiple forms of CXCL12 signaling through the CXCR4 receptor [155], and of the key role of CXCL12-CXCR4 signaling in normal immune cell trafficking [156-158]. Thus, new targeted approach is needed to prevent breast cancer progression.

Chemokines exist as monomers and can form homodimers, which either enhance or inhibit their respective monomer signaling [29, 81, 159]. Using immune-ligand blotting, von Hundelshausen *et al.* recently screened 45 human chemokines and identified over 200 distinct binary heterophilic chemokine interactions [15]. The response from cells treated with chemokine mixtures differs from the cellular responses by individual chemokines or chemokines in various combinations and can lead to synergistic enhancement or reduction [15, 16, 18]. For example, cell chemotaxis enhanced by monomeric CXCL12 was inhibited by a mixture of CXCL4 and CXCL12 chemokines [15], suggesting that chemokine heterodimers may be responsible for the observed altered activity. This finding suggests that the CXCL4 chemokine may interfere with CXCL12-CXCR4 signaling, or, alternatively, CXCL12 chemokine may interfere with CXCL4-mediated signaling. It has been shown that CXCL4 binds with greater affinity to the CXCR3B

receptor isoform than to CXCR3A [49, 160] and promotes anti-tumorigenesis and apoptosis in tumor cells [49]. This signaling contrasts with signaling induced by the activation of the CXCR3 receptor isoform CXCR3A by the chemokines CXCL9, CXCL10, and CXCL11 that promotes tumor growth, chemotactic migration, invasion, and metastasis [49, 161]. Whether CXCL12 affects CXCL4-CXCR3 signaling is unclear.

To unambiguously identify the activity of a chemokine heterodimer in the mixture of chemokines where competing homophilic and heterophilic interactions lead to an equilibrium of coexisting of species (monomers, homodimers, and heterodimers), non-dissociating CXCL4-CCL5, CCL5-CCL17, and CXCL7-CXCL1 heterodimers have been generated and functionally assessed [15, 23, 162]. Previously, we have shown that CXCL12 and CXCL4 form heterodimers using electrospray ionization mass spectrometry (ESI-MS) experiments and co-immunoprecipitation of CXCL12-CXCL4 heterodimers from human platelets [22]. While the regulation of breast cancer cell migration through monomeric CXCL12 and CXCR4 is well established in patients, animal, and *in vitro* cell models, whether CXCL12-CXCL4 heterodimers influence breast cancer cell migration is unknown. Here we determined the effects of CXCL12-CXCL4 heterodimers on breast cancer cell migration in the well-established triple negative MDA-MB 231 breast cancer cell *in vitro* model [163].

## **2.3 Materials and methods**

### **2.3.1 MDA-MB 231 cells and CXCL12-driven migration using wound-healing assays**

MDA-MB 231 (ATCC, Manassas, VA) were cultured in DMEM/F12 media (Corning) supplemented with 10% FBS (Atlanta Biologics), L-glutamine, Amphotericin B and Gentamycin (Corning). Briefly, following an overnight coating with Collagen type I (12  $\mu\text{g}/\text{cm}^2$ , BD Biosciences) at 37 °C with 5% CO<sub>2</sub> and > 85% humidity and washes of the

unbound Collagen I with sterile PBS, 96-well tissue culture plates (Greiner) were seeded (40,000 cells/well) with MDA-MB 231 cell suspension in culture media. Cells were grown to confluency and then incubated overnight with fresh media without FBS (0%). Cells were identified through the addition of the vital nuclear dye Hoechst (Promega). The confluent MDA-MB 231 cell monolayers were then scratched using a sterile pipet tip and the wells washed to remove non-adherent cells. Thereafter, cells were incubated with concentrations of CXCL12 (0–100nM; Shenandoah Biotechnology Inc), CXCL4 (0–200nM; Shenandoah Biotechnology Inc.) chemokines and/or peptides diluted with 0% FBS media as described. Overlapping microphotographs encompassing the entire area of each scratch/wound were taken at the start of the treatment (0 h) and following a 24-hour incubation (24 h) using an IX71 Olympus microscope equipped with a DP70 camera and the associated software (Olympus). Overlapping microphotographs were stitched together, and the area of the wound was determined using ImageJ software (NIH). After normalization to the area measured at time 0, results were expressed as percentage of wound healing.

### **2.3.2 CXCR4 and CXCR3 receptor inhibition**

To investigate whether migration was critically dependent of either the ligand-receptor CXCL12-CXCR4 or the ligand-receptor CXCL4-CXCR3 signaling pathways, wound healing assays were conducted in the presence of 20nM of CXCR4 inhibitor AMD3100 or 5nM of the CXCR3 inhibitor AMG487. The optimal concentrations of AMD3100 and AMG487 were defined in preliminary experiments and derived from previous work [128, 150, 164]. Wound healing assays with CXCL12 and/or CXCL4 following pre-treatment with either AMD3100 and/or AMG487 were conducted and evaluated as detailed above.

### **2.3.3 NMR spectroscopy**

Uniformly  $^{15}\text{N}$ -enriched CXCL4 was expressed and purified as described previously [165]. Briefly, wild-type (WT) human PF4 (CXCL4) in the pT7-7 was expressed in BL21 DE3 pLysS.  $^{15}\text{N}$ -CXCL4 was isolated from the supernatant of the bacterial lysate grown in M9 media (3%  $\text{KH}_2\text{PO}_4$ , 12.8%  $\text{Na}_2\text{HPO}_4 \cdot 7\text{H}_2\text{O}$ , 0.5%  $\text{NaCl}$ , 1%  $^{15}\text{NH}_4\text{Cl}$ ) by affinity chromatography using a HiTrap Heparin high-performance (HP) affinity column. Eluted proteins were purified further by fast protein liquid chromatography (FPLC) using a Resource RPC FPLC column. Protein purity was assessed by 12% NuPAGE Bis-Tris gel electrophoresis (ThermoFisher). Protein concentrations were determined according to the manufacturer's instructions using the bicinchoninic acid assay (Pierce) with BSA as standard.

CXCL12 was purchased from Shenandoah Biotechnology Inc. (Warwick, PA) and used without further purification.  $^{15}\text{N}$ -CXCL4 was dissolved in a  $\text{H}_2\text{O}/\text{D}_2\text{O}$  (95%/5%) mixture containing 20 mM  $\text{NaCl}$  at the concentration of 1 mg/ml. pH was adjusted to 5.0 by adding microliter increments of 0.1 M  $\text{HCl}$ . A series of two-dimensional  $^1\text{H}$ - $^{15}\text{N}$  HSQC (heteronuclear single quantum coherence) spectra were collected by titrating unlabeled CXCL12 to  $^{15}\text{N}$ -CXCL4 solution at 1:1 and 2:1 molar ratio and chemical shift changes of  $^{15}\text{N}$ -CXCL4 caused by the interactions with CXCL12 were monitored. Carrier frequencies for  $^{15}\text{N}$  and  $^1\text{H}$  were positioned at 116.5 and 5.2 ppm, respectively. All NMR experiments were carried out at 313 K on a Bruker Advance-III 950 MHz spectrometer at David H. Murdock Research Institute (Kannapolis, NC). Raw data were converted and processed using NMRPipe [166] and analyzed using NMRview [167] software. CXCL4 resonance assignments have been reported previously [13, 19]. The spectra collected in this work were identical to those published previously [19] allowing NMR chemical shift assignments.

### 2.3.3 CXCL4-derived peptide

A CXCL4-derived peptide matching the putative binding interface with CXCL12 was derived from our NMR studies and synthesized AHITSLEVIKAG (Pepmic Co, Suzhou, China). The peptide at increasing concentrations (0-500nM) was used in combination with 50nM CXCL12 to investigate the effects of peptide/CXCL12 on MDA-MB 231 cell migration. These experiments were repeated in the presence of AMG487 (5nM).

### 2.3.4 Statistical analyses

All data are presented as mean  $\pm$  SEM. Differences between chemokine conditions were assessed using one-way ANOVA and Dunnet's post-hoc tests. Correlation between increasing CXCL4 concentrations and CXCL12-activated MDA-MB-231 cell migration was assessed using linear regression. Statistical significance was set at  $p < 0.05$ .

## 2.4 Results

### 2.4.1 CXCL12 promotes and CXCL4 inhibits MDA-MB 231 breast cancer cell migration

CXCL12 stimulates the migration of MDA-MB 231 breast cancer cells uniquely through CXCL12-CXCR4 signaling [168, 169]. Therefore, we first confirmed that CXCL12 stimulates the migration of MDA-MB 231 breast cancer cells using wound-healing assays. As expected, the CXCL12-driven migration of MDA-MB 231 cells was dose-dependent and increased as the concentration of CXCL12 increased in the *in vitro* migration assays ( $p < 0.05$ ; Figure 2.1 A). In particular, when the tumor cells were treated with 100nM of CXCL12, a two-fold migration increase was observed as reported previously [170]. The activation of the CXCL12-CXCR4 signaling pathway leading to MDA-MB 231 cell migration was verified by inhibition of cell migration in the presence of the CXCR4 antagonist AMD3100 (20nM, ns;

Figure 2.1 B).

Next, in similar assays, we assessed the effect of CXCL4 on MDA-MB 231 cell migration. No effect was observed in the presence of 50nM of CXCL4 (Figure 2.1 D). However, the addition of CXCL4 at a higher concentration (100nM) led to ~2-fold decrease of MDA-MB 231 cells migration ( $p < 0.05$ ; Figure 2.1 C). Inhibition using the CXCR3 inhibitor AMG487 (5nM) prevented CXCL4-CXCR3B activation and the associated inhibition (Figure 2.1 D).

#### **2.4.2 The CXCL12 and CXCL4 chemokine mixture inhibits MDA-MB 231 breast cancer cell migration**

CXCL12 and CXCL4 readily form heterodimers *in vitro* [15, 22]. To assess the biological activity of the CXCL12-CXCL4 chemokine mixture, combinations of CXCL12 and CXCL4 at different ratios were tested on MDA-MB 231 cell migration in wound-healing assays (Figure 2.2 A). In these experiments, the concentration of CXCL12 was kept constant at 100nM, whereas the concentration of CXCL4 varied (0 to 200nM, Figure 2.2 B-C). Unlike CXCL12 alone, the incubation with CXCL12 and CXCL4 mixtures significantly and dose-dependently reduced the MDA-MB 231 cell migration (Figure 1 B-C,  $p < 0.001$ ). The effect observed with CXCL12-CXCL4 mixtures is enhanced resulting in a  $> 2.5$  times reduction compared to CXCL4 alone, suggesting that the response is synergistic rather than additive. These data show that CXCL4 effectively inhibits the CXCL12-induced MDA-MB 231 cell migration, and the effect is more potent than when it is added alone, suggesting that the CXCL12-CXCL4 interaction could be, at least in part, responsible for the observed alteration in migration.

### **2.4.3 The CXCL12-CXCL4 chemokine mixture prevents MDA-MB 231 breast cancer cell migration through CXCR4 receptor signaling and does not affect the CXCR3 signaling**

We tested whether the synergistic effect of the CXCL12-CXCL4 mixture on MDA-MB 231 cell migration is CXCR4 receptor mediated. The addition of the CXCR4 inhibitor AMD3100 (20nM) blocked the migration of MDA-MB 231 cells following incubation with 100nM CXCL12 ( $p < 0.001$ ; Figure 2.3 A) as well as with the mixture of CXCL12 (100nM) and CXCL4 (50 or 100nM) (Figure 2.3 A) confirming that CXCL12-driven migration of MDA-MB 231 cells occurs via the activation of the CXCR4 receptor. As CXCL4-CXCR3 signaling can inhibit cell migration [123], we tested whether the CXCR3 receptor inhibitor AMG487 could reverse the effect of CXCL4 on MDA-MB 231 cells migration induced by CXCL12 (Figure 2.1 A & Figure 2.2 B). At the concentration used, AMG487 had no effect on the 2-fold increase in MDA-MB 231 cell migration induced by CXCL12 (100nM;  $p < 0.001$ ; Figure 2.2 B). Moreover, regardless of the presence of AMG487, the CXCL12-CXCL4 mixture significantly prevented MDA-MB 231 cell migration ( $p < 0.001$ ; Figure 2.3 B).

### **2.4.4 Binding interface between CXCL4 and CXCL12 chemokines defined by NMR spectroscopy**

To define the binding interface between CXCL12 and CXCL4, NMR titration experiments were performed where unlabeled CXCL12 was added into solution of uniformly  $^{15}\text{N}$ -labeled CXCL4 at two molar ratios 1:1 and 1:2 (Suppl. Fig. 1S). The interactions between CXCL12 and  $^{15}\text{N}$ -labeled CXCL4 were assessed through evaluation of chemical shift changes in  $^{15}\text{N}$ -CXCL4 monitored by recording [ $^1\text{H}$ - $^{15}\text{N}$ ]-HSQC spectra upon addition of CXCL12 (Figure 2.4 A). The [ $^1\text{H}$ - $^{15}\text{N}$ ]-HSQC spectrum of CXCL4 alone shows multiple

peaks of varying intensities for multiple amino acid residues suggesting (1) the co-existence of monomer, dimer, and tetramer states in a slow exchange on the NMR experimental time scale [28, 171], and (2) the asymmetry of the tetramer [172]. Consequently, some amino acid residues could not be unambiguously assigned. Nevertheless, the residues that could be definitively assigned were well distributed throughout the protein, enabling the mapping of the CXCL4-CXCL12 interaction interface.

Overall, addition of CXCL12 to the  $^{15}\text{N}$ -labeled CXCL4 solution caused major chemical shift changes of many amino acid peaks in the  $[\text{}^1\text{H}^{15}\text{N}]$ -HSQC spectrum of CXCL4, while some of amino acids remained minimally chemically altered (Suppl. Fig. 1S-A). Some cross-peaks merely shifted such as residues A32, E28, and T25. For other residues, the number of cross-peaks representing these residues was reduced as observed for G33 and G48, for which only two peaks remained following the CXCL12 addition to the CXCL4 solution. The latter findings indicate a significant shift in the monomer-dimer-tetramer states CXCL4 equilibrium. Several new peaks were observed in the  $[\text{}^1\text{H}-^{15}\text{N}]$ -HSQC spectrum of CXCL4 in the presence of CXCL12, possibly representing a new CXCL12-CXCL4 heterodimer state. While many CXCL4 resonances were affected by the addition of CXCL12, some resonances remained minimally affected, i.e., K66, T44, or I63, supporting the specificity of the interactions between CXCL4 and CXCL12. The amino acid residues in CXCL4 demonstrating chemical shift changes above (red) and below (blue) averages are highlighted on the CXCL4 monomer three-dimensional structure (Suppl. Fig. 1S-A- B), and on the amino acid sequence (Figure 2.4 C). Notably, the amino acid residues with large chemical shift changes are clustered on the first  $\beta$ -strand suggesting that these residues may form the contact interface with CXCL12 (Figure 2.4 B-C). This contact interface concurs with our previously proposed computational CXC chemokine

model of CXCL12- CXCL4 heterodimers [22].

#### **2.4.5 The CXCL4-CXCL12 binding interface derived peptide AHITSLEVIKAG inhibits the CXCL12-stimulated MDA-MB 231 breast cancer cell migration**

To further confirm that CXCL4-CXCL12 interactions inhibit CXCL12-driven migration, we synthesized the CXCL4-derived peptide AHITSLEVIKAG mimicking the CXCL12 binding site of the CXCL4 chemokine (Figure 2.4 C). This peptide dose-dependently decreased the CXCL12-induced migration of MDA-MB 231 cells (Figure 2.5 A;  $p < 0.05$ ). At a concentration of 500 nM, addition of the peptide fully prevented the stimulatory effect of CXCL12. Additionally, activity of the peptide on CXCL12-CXCR4 driven MDA-MB 231 migration was not significantly altered by the presence of the CXCR3 inhibitor AMG 487 (Figure 2.5 B).

### **2.5 Discussion**

Chemokine signaling is attracting increasing interest in cancer biology as chemokines critically regulate cellular functions, including cell migration, and are highly expressed within the tumor microenvironment [55]. Most chemokines exist in a monomer-dimer equilibrium under physiological conditions and structural analyses demonstrated that chemokines could form homodimers [27, 29, 171, 173]. Moreover, monomers and homodimers can significantly modulate signaling through their cognate receptors [81]. For some chemokines such as CXCL8, the dimerization is essential for receptor binding [174]. More recently, the formation of heterodimers has been demonstrated [16, 19, 22]. Here we assessed the biological relevance of CXCL12-CXCL4 heterodimers in the CXCL12-CXCR4 driven migration, an essential step in breast cancer progression [147, 157]. Our observations in the MDA-MB 231 breast cancer cell migration in vitro model indicate that a mixture of CXCL12 and CXCL4, likely through the formation of CXCL12-CXCL4 heterodimers,

inhibits of the CXCL12-CXCR4 signaling independently of the CXCL4-CXCR3 signaling. Moreover, signaling through CXCL12-CXCR4 was associated with changes in multiple transcripts encoding proteins associated with cytoskeleton and membrane reshaping, which were abrogated in the presence of the CXCL12-CXCL4 mixture. Using NMR spectroscopy, we identified a putative region of CXCL4 interacting with CXCL12 to form CXCL12-CXCL4 heterodimers and demonstrated that a CXCL4 peptide mimicking the putative CXCL4-CXCL12 binding sequence led to inhibition of MDA-MB 231 cell migration, similar to that observed with the CXCL12-CXCL4 mixture.

Our data also demonstrate that incubation with CXCL4 at a concentration of 100nM reduced the migration of MDA-MB 231 cells by 30%, possibly through CXCR3B activation. Although activation of the CXCR3A receptor activation leads to pro-migratory responses and tumor metastasis, activation of the CXCR3B receptor isoform mediates tumor growth inhibition and induces apoptosis [175, 176]. Importantly, the inhibitory effects of the CXCL12-CXCL4 mixture were observed with CXCR3 signaling inhibition, supporting the inhibition of CXCL12-CXCR4 signaling by the CXCL12-CXCL4 mixture, possibly through CXCL12-CXCL4 heterodimers. Additionally, the mixture of a CXCL4-derived peptide mimicking the CXCL12-CXCL4 binding interface also suppressed CXCL12-driven tumor cell migration, further supporting the hypothesis that CXCL12-CXCL4 heterophilic interactions prevent tumor migration. Our data also highlight the therapeutic potential of CXCL4-mimicking peptides in preventing CXCL12-CXCR4 signaling and thus limiting breast tumor cell migrations. Although limited as suggested by our data, the effects of CXCL4-mimicking peptide(s) on the CXCR3B signaling pathway should be clarified. Furthermore, as the CXCL12-CXCR4 and the CXCL4-CXCR3A/CXCR3B signaling

mechanisms are essential for normal physiological functions including immune responses, further investigations are needed to validate the benefits the treatment with CXCL4-mimicking peptide(s) in *in vivo* immuno-competent models of breast cancer progression.

Collectively, our data indicate that CXCL12-CXCL4 heterophilic interactions alter the CXCL12-CXCR4 signaling associated with breast tumor cell migration. These results warrant further studies of the molecular mechanisms by which chemokine heterodimers modulate specific signaling events, in particular those associated with tumor cell migration. Inhibition of the CXCL12-driven tumor cell migration induced by a peptide mimicking the binding sequence of the CXCL12- CXCL4 chemokine heterodimers opens new avenues for chemokine targeted approaches to prevent cancer progression.

## 2.6 Figures

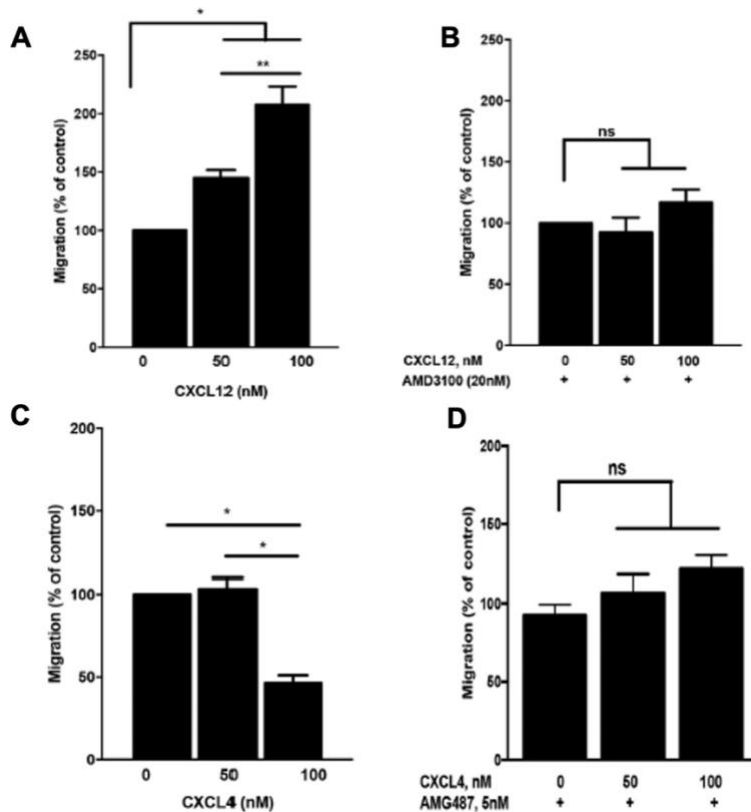


**Figure 2.1:** MDA-MB 231 breast cancer cell migration is promoted by CXCL12 through CXCR4 receptor signaling and inhibited by high concentrations of CXCL4 through CXCR3 receptor signaling. **(A)** CXCL12 (50 or 100nM) significantly increased MDA-MB 231 cell migration ( $p < 0.01$ ) compared to control conditions. **(B)** The CXCR4 receptor antagonist AMD3100 (20nM) prevented the CXCL12-driven MDA-MB 231 cell migration ( $p = n.s.$ ). **(C)** 100nM but not 50nM of CXCL4 significantly decreased MDA-MB-231 cell migration ( $p < 0.05$ ). **(D)** AMG487 (5nM) prevented CXCL4 (100nM) associated cell migration inhibition. Data presented as mean  $\pm$  SEM,  $N > 3$  independent repeats; n.s = not significant;  $*p < 0.05$ ;  $**p < 0.01$ .

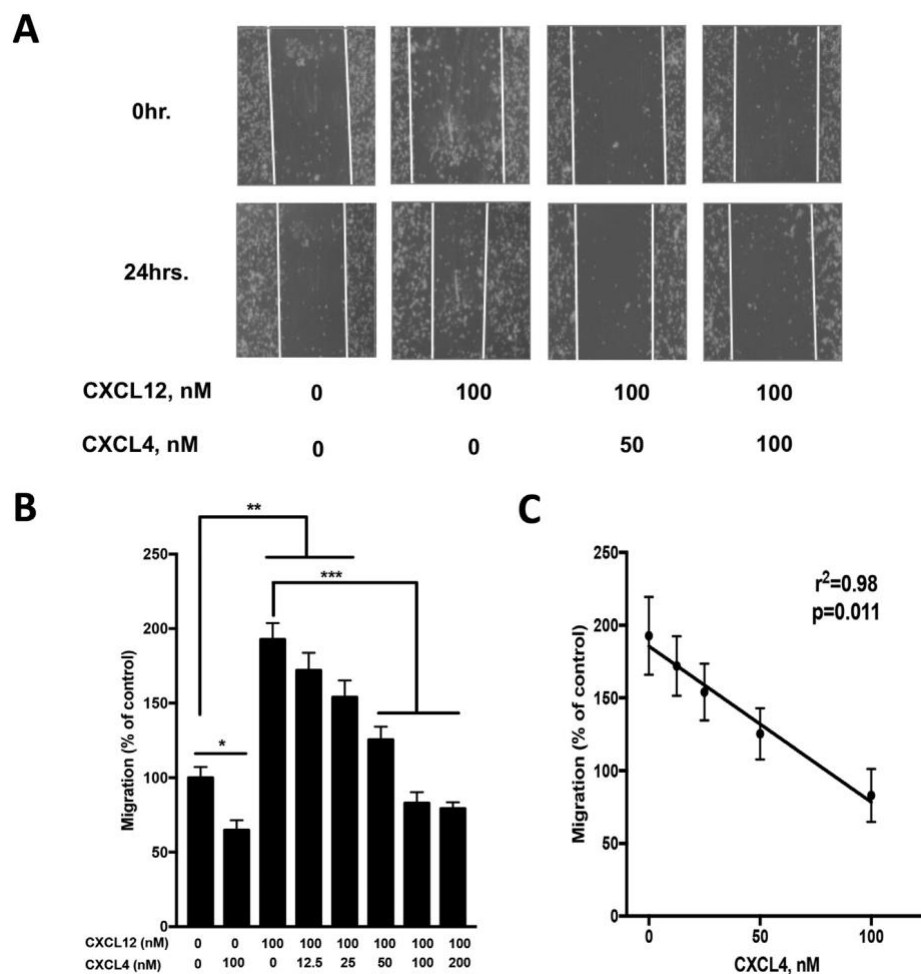


**Figure 2.2:** CXCL12-driven MDA-MB 231 breast cancer cell migration is dose-dependently inhibited by concurrent increase of CXCL4 concentrations. **(A)** Representative microphotographs of the MDA-MB-231 cell monolayer wound at 0 and 24 h following the different chemokine treatments. **(B)** Quantification of the MDA-MB 231 cell migration following treatment with CXCL12 (100nM) or the combination of CXCL12 (100nM) with increasing concentrations (0–100nM) of CXCL4. **(C)** Correlation between increased concentration of CXCL4 (0-100nM) added to 100nM of CXCL12 and MDA-MB 231 cell migration. Data presented as mean  $\pm$  SEM,  $N > 4$  independent repeats. \* $p < 0.05$ , \*\* $p < .01$ , \*\*\* $p < .001$ , and \*\*\*\* $p < .0001$ .

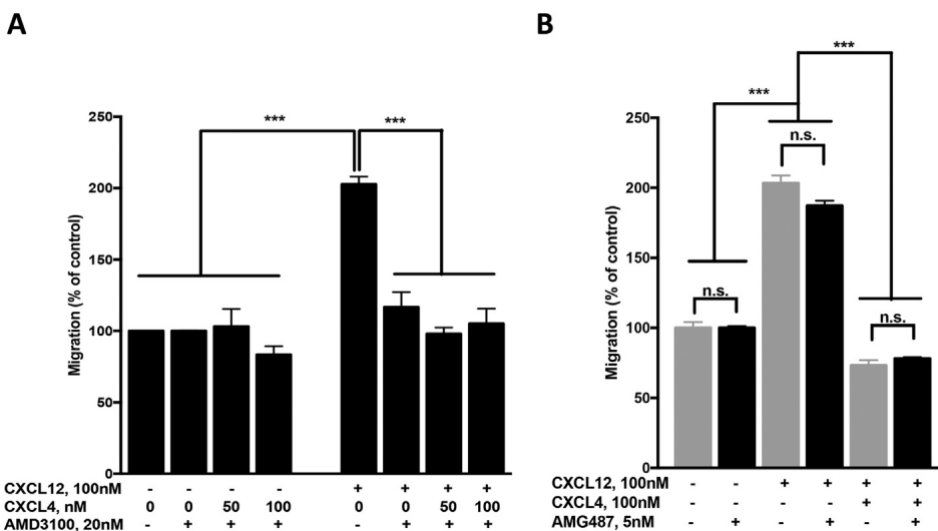


**Figure 2.3:** CXCL12-driven MDA-MB 231 breast cancer cell migration is inhibited by concurrent increase in CXCL4 concentrations through CXCL12-CXCR4 signaling. Quantification of the MDA-MB-231 cell migration following treatment with CXCL12 (100nM) or the combination CXCL12 (100nM) with increasing concentrations (0–100nM) of CXCL4 in the presence of the CXCR4 inhibitor AMD3100 (20nM) (**A**) or of the CXCR3 inhibitor AMG487 (5nM) (**B**). Data presented as mean  $\pm$  SEM,  $N > 4$  independent repeats. n.s = not significant, \*\* $p < .01$ , \*\*\* $p < .001$ , and \*\*\*\* $p < .0001$ .

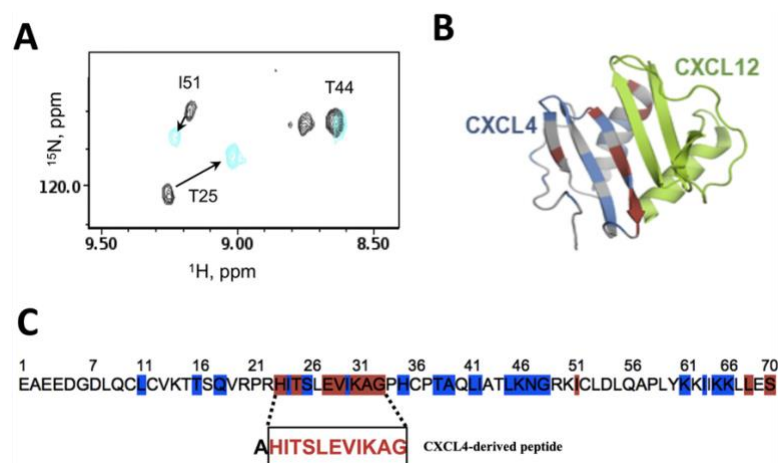


**Figure 2.4:** NMR analyses of CXCL12-CXCL4 heterodimers. **(A)** Chemical shift changes of I51, T25 and T44 of  $^{15}\text{N}$ -CXCL4 following the addition of unlabeled CXCL12 as determined by NMR. **(B)** The CXCL4-CXCL12 heterodimer structure as determined by NMR. Residues experiencing chemical shift changes above average are shown in red, whereas those experiencing chemical shift changes below average are shown in blue on the CXCL4 monomer and the CXCL12 monomer is shown in green. **(C)** The amino acid sequence of the first  $\beta$ -sheet of CXCL4 highlighting (in red) the amino acids with chemical shift in the interface sequence and the CXCL4-derived peptide sequence.

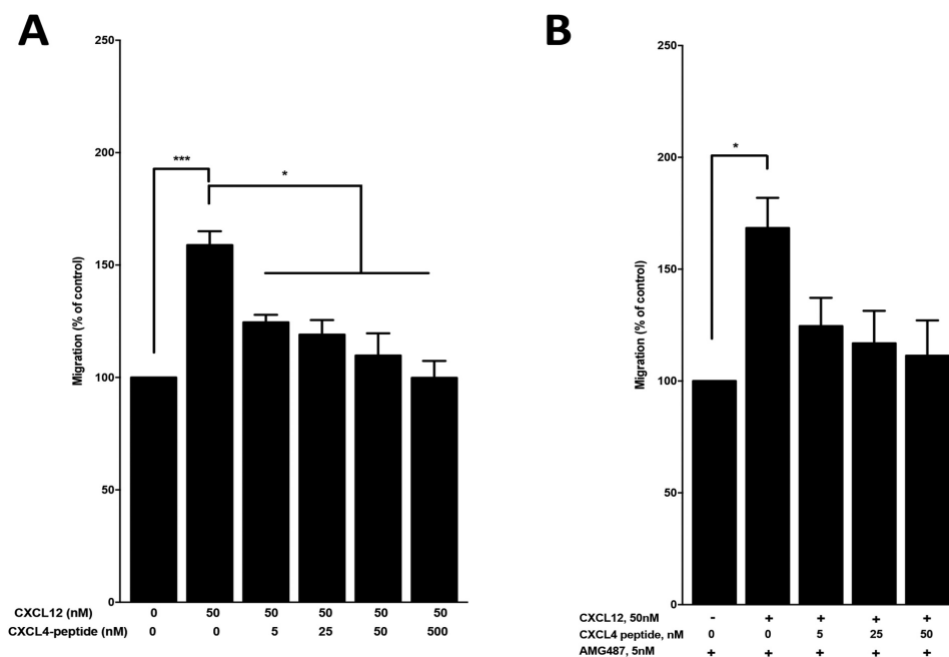


**Figure 2.5:** The CXCL4-based peptide AHITSLEVIKAG mimics CXCL4 inhibition of CXCL12-driven cell migration. **(A)** CXCL4-derived peptide dose-dependently reduced the CXCL12-driven migration of MDA-MB 231 breast cancer cells. **(B)** In the presence of the 5nM of the CXCR3 inhibitor AMG487, CXCL12-driven migration of MDA-MB-231 cell was not significantly decreased. Data presented as mean  $\pm$  SEM,  $N \geq 3$  independent repeats.

## CHAPTER 3: GENERATION OF THE OBLIGATE CXCL4-CXCL12 HETERODIMER BY DISULFIDE TRAPPING

### 3.1 Abstract

CXCL12 and CXCL4 chemokines are concomitantly produced *in vivo* with CXCL12 abundantly produced by stromal cells, whereas CXCL4 is released in high concentration by platelets rendering the formation of heterodimers. Chemokine heterodimers likely play a role in fine-tuning the chemokine activity. However, the presence of chemokine monomers and homodimers in chemokine mixtures hinders the assessment of chemokine heterodimer functions. Thus, in this chapter, we present a disulfide-trapping method to generate an obligate CXCL4-CXCL12 heterodimers by mutating serine amino acid at the position (S26) in CXCL4 and leucine amino acid at the position 29 (L29) in CXCL12 to cysteines. The disulfide-trapping method serves as a novel strategy to stabilize the heterodimers from dissociation; and thus, provides a valuable tool for further functional and structural studies of heterodimers. We validated the formation of the obligate heterodimers by Co-IPs and NMR analyses of purified obligate CXCL4-CXCL12 heterodimers.

### 3.2 Introduction

Biophysical and biological evidence highlight the formation and potential role of chemokine heterodimers in cell signaling in both physiological and pathological conditions [15, 16, 18, 21-23, 87, 90]. In particular, our previous observations in platelets and breast tumor cells suggest that CXCL4 and CXCL12 chemokines likely form heterodimers [22, 138]. However, the presence of many chemokine species, i.e., monomers, homodimers, heterodimers, and tetramers in wildtype chemokine mixture hinders the direct assessment of CXCL4-CXCL12 heterodimer activities [30].

To overcome this challenge, we generated an obligate, non-dissociating CXCL4-CXCL12 chemokine heterodimer to unambiguously demonstrate the biological activity of CXCL4-CXCL12 heterodimers in breast cancer progression. Here, we describe a disulfide trapping method for generating a covalently bonded protein complex from two dissociable binding partners through the introduction of a single non-native cysteine into each protein partner: S26 on CXCL4 and L29 on CXCL12. The design of the disulfide crosslink between CXCL4 and CXCL12 was guided by our NMR HSQC data of CXCL4 in complex with CXCL12 (see Chapter 2). We selected the mutation to (1) minimally affect the protein natural folding and (2) to favor the formation of disulfide-linked heterodimers but not disulfide-linked homodimers. Mutation sites in CXCL4 and CXCL12 were selected based on putative and biophysically favorable interface and away from the two-fold symmetry axis (Figure 3.2 A) [23].

The mutated proteins were expressed and purified separately. When the two engineered cysteine residues are in close proximity, a disulfide bond spontaneously forms upon mixing the proteins; and therefore, preventing the complex from dissociation [177]. The resulting non-dissociated CXCL4-CXCL12 complexes were detected using nonreducing SDS-PAGE and

Western blotting. The formation of the complex was further validated by Co-IP, and the correct folding was characterized by NMR spectroscopy.

The purification protocol for the chemokines or their mutants included several common steps. The chemokines were expressed in inclusion bodies that were solubilized in 8M urea. Under these conditions, the chemokines were unfolded. Therefore, the purification protocol included a refolding step to ensure the generation of correctly paired disulfide bonds. The first purification step was accomplished through cation exchange chromatography. This technique is especially useful for chemokine purification since most chemokines are highly positively charged proteins, due to the abundant presence of basic residues (i.e., arginine, lysine, and histidine) in their primary amino acid sequence [178]. Under a slight basic buffer condition (pH 7-8), positively charged chemokines will bind to the cation exchange resin, while the negatively charged proteins present in the cell lysate will not [179]; and thus, allowing the initial purification of chemokines from the crude lysate. The second purification step was performed using heparin affinity chromatography. All chemokines interact with heparan sulfate which is an ubiquitous class of GAGs on cell surface or extracellular matrix [180]. Particularly, CXCL4 has an exceptionally strong affinity to heparin sulfate [181]. Thus, following the cation exchange column, a heparin affinity chromatography with an increasing salt gradient was selected to purify CXCL4 chemokine mutant. Finally, the purity of the protein fractions was further improved through size-exclusion chromatography to remove misfolded chemokines and other impurities from the purified chemokines. Purification procedures were further optimized for each chemokine separately.

### 3.3 Materials and methods

#### 3.3.1 Bacterial expressions of mutated CXCL12, CXCL4 chemokines

*E. coli* BL21 DE3 competent bacteria were transformed with pET24d+ plasmids (2.5ng/uL) containing mutant sequence of either S26C CXCL4 or L29C CXCL12. For the transformation, the mixture of chemically competent *E. coli* bacteria and a plasmid coding for the studied mutant was incubated on ice for 30 min, heat-shocked at 42°C for 10s, and placed on ice for 5 min before the addition of 100uL of the Super Optimal Broth media (Sigma-Aldrich). The bacteria were incubated at 37°C for 1 hour with shaking at 225rpm. Successful transformation was assessed by the growth of bacteria colonies on kanamycin (60µg/mL) LB agar plates. Kanamycin-resistant bacteria were then cultured in 10mL of the LB medium at 37°C, with shaking (250rpm) for 6 hours. Bacteria were pelleted by centrifugation at 3000rpm for 10 minutes, resuspended in 100mL of the M9 medium supplemented with 60µg/mL kanamycin, and incubated overnight in the same conditions. Overnight bacterial cultures were then transferred to 1L of the M9 medium (1:10 dilution) and grown to an optical density of 0.6, measured at 600nm (OD<sub>600</sub>). Protein production was induced by the addition of 0.5mM IPTG. After an additional 4-hour incubation at 37°C with shaking (250rpm), bacteria were collected by centrifugation for 30min at 3000rpm.

#### 3.2.2 Bacteria lysis and mutant chemokine protein collection

Bacteria pellets were resuspended in the lysis buffer (50mM Tris, 1% Triton, pH 8; 3 ml per gram of bacteria), freshly supplemented with the protease inhibitor PMSF (100mM) and beta-mercapto-ethanol (0.1%) and sonicated (40% power, 2 seconds ON and 0.5 second OFF, Branson Digital Sonifier). After sonication, bacteria lysates were centrifuged 20,000rpm for 1 hour at 4°C forming pellets of the inclusion bodies containing the produced chemokines [182].

Inclusion bodies were resuspended in the extraction buffer (50mM Tris, 8M Urea, 0.1% beta-mercaptoethanol, pH 8.0; 12ml per gram of pellet), and incubated overnight at 4°C with stirring. After homogenization of the inclusion bodies, cell debris were removed by ultracentrifugation (20,000rpm, 4°C, 1 hour) and the supernatant containing unfolded soluble proteins was used in purification steps.

### **3.2.3 S26C CXCL4 and L29C CXCL12 mutant purification**

#### **3.2.3.1 Purification of S26C CXCL4 mutant**

The cell lysate containing unfolded S26C CXCL4 mutant was initially purified by cation exchange chromatography and refolded by extreme dilution in an indicated cysteine/cystine refolding buffer (see the below section of protein refolding). Successfully refolded protein was finally purified by heparin affinity chromatography.

#### **Cation exchange chromatography**

The supernatant was primarily purified using a cation exchange column (20-mL SP/FF Sepharose, GE Healthcare) and the AKTA-FPLC system (GE Healthcare) driven by the Unicorn software 7.3 (GE Healthcare). Elution fractions were monitored by UV-L9 flow cell, and automatically fractionated by the PF-9 fractionator. The column was initially equilibrated with the cation exchange binding buffer A (100mM Tris, 8M Urea, pH 8.0; 4 x column volume (CV)). Samples were injected at 3 ml/min, followed by a wash with 5 CV with buffer A and 2.5% of the cation exchange elution buffer B (100mM Tris, 6M Urea, 2M Sodium Chloride, pH 8.0). Protein elution was completed using a gradient of buffer B for 20 CV.

#### **Protein refolding**

The eluate fraction from cation exchange chromatography was refolded in the buffer containing 100mM Tris, 10mM Cysteine, 1mM Cystine, pH 8.0 to gradually remove urea and re-

fold the protein [179]. The protein sample was drop-wise added into a pool of the refolding buffer with the dilution factor 1:50 (v/v) and allowed to stir overnight at room temperature. After refolding, precipitates were removed by centrifuging at 4000rpm for 1 hour at 4°C.

### **Heparin affinity chromatography**

The heparin column (20-mL SF/FF heparin, GE Healthcare) was initially equilibrated by 3 CV of the heparin column buffer A (50mM Tris, pH 7.3). The refolded fraction was injected into the column at 3mL/min, followed by 5 CV wash by buffer A containing 2.5% buffer B (50mM Tris, 2M Sodium Chloride, pH 7.3). Proteins were eluted from the column using a NaCl gradient (from 0 to 100% B) and monitored by UV280 nm. Heparin eluate fractions containing CXCL4 were pooled together and concentrated by centrifugation using a 3kDa MW Amicon filter (Millipore Sigma, MA, USA), and stored at -20°C for future use. The protein concentration of the purified mutant CXCL4 was determined using the BCA assay kit (Thermo Scientific, MA, USA).

#### **3.2.3.2 Purification of mutant L29C CXCL12**

Purification of the L29C CXCL12 mutant was completed by cation exchange and size exclusion chromatography. Similar to the purification of mutant CXCL4 described in 3.2.3.1, mutant L29C CXCL12 was initially purified by cation exchange chromatography due to its basic nature [183]. Our preliminary trials suggested that the mutant L29C CXCL12 has low affinity to heparin column; thus, we selected size exclusion as a second step to purify this mutant. Briefly, cell lysate containing unfolded L29C CXCL12 mutant was initially purified, and on-column refolded in cation exchange chromatography. Then, the purity of the refolded mutant was further polished by size exclusion chromatography.

### **Cation exchange chromatography and on-column refolding**

The mutant L29C CXCL12 was purified and refolded in the cation exchange column. Inclusion bodies were extracted as described above (see section 3.2.2). The cation exchange column was first equilibrated with wash buffer 1 (100mM Tris, 8M Urea, pH 8.0). The protein sample was loaded onto the column to allow the binding to the resin, followed by the second wash. The refolding process was completed by gradually decreasing urea concentration from 8M to 4M, and then 1M. Denatured proteins were refolded by running through 10 CV of the refolding buffer 1 (50mM Tris, 4M Urea, 10mM reduced Glutathione, 1mM oxidized Glutathione, pH 7.0) and overnight incubation in the same buffer. The refolding process was continued by washing the column with another 10 CV of the refolding buffer 2 (50mM Tris, 1M Urea, 10mM reduced Glutathione, 1mM oxidized Glutathione, pH 7.0) and overnight incubation. After completing the refolding process, the CXCL12 mutant chemokine bound to the resin was extensively washed with the binding buffer A (50mM Tris, pH 7.3) containing 50mM NaCl. Finally, the refolded CXCL12 mutant chemokines were eluted from the column by gradually increasing NaCl gradient using the elution buffer B (50mM Tris, 2M NaCl, pH 7.3). The protein elution was monitored by a UV280 nm flow cell. The elution fractions were pooled together and concentrated by centrifugation using the 3kDa filters and injected to the size exclusion chromatography.

### **Size exclusion chromatography**

The CXCL4 and CXCL12 chemokine protein mutants were further purified through Sephacryl size exclusion chromatography (GE Healthcare). Briefly after column equilibration according to the manufacturer using 50mM sodium phosphate buffer containing 150mM sodium chloride, pH 7.0, CXCL12 chemokine protein mutant was eluted in the same equilibration

buffer, concentrated by centrifugation using 3kDa exclusion filters, and stored at -20°C for future use. Protein concentrations were determined using BCA assays.

### **3.2.4 Generation of the disulfide trapped CXCL4-CXCL12 heterodimers**

CXCL4-CXCL12 disulfide-trapped, obligate chemokine heterodimer was generated as previously described [184]. Briefly, the purified fractions of S26C CXCL4 and L29C CXCL12 were combined, and the mixture was dialyzed for 18-24 hours at 4°C in a 50mM sodium phosphate, 150mM NaCl, 10uM CuCl<sub>2</sub>, pH 7.0 buffer (4L). The mixture was then centrifuged to remove precipitates and the supernatant loaded into the heparin column. The heparin column was initially equilibrated and washed after sample injection as described (see section 3.2.3.1 above). The purification of the disulfide trapped CXCL4-CXCL12 heterodimers was optimized by extending the elution process to 80 CV. The disulfide trapped CXCL4-CXCL12 heterodimers collected in the 500-600mM NaCl fractions were further purified through Superdex increase 75 (GE Healthcare) size exclusion. Disulfide trapped CXCL4-CXCL12 heterodimer concentration was determined by BCA (Thermo sciences).

### **3.2.5 Assessment of CXCL4-CXCL12 chemokine obligate heterodimers**

#### **3.2.5.1 Protein electrophoresis**

CXCL4-CXCL12 chemokine obligate heterodimer protein size and purity was verified through tricine SDS-PAGE using 16.5% acrylamide gel as previously described [185] with non-reduced samples. Non-reduced samples of CXCL4-CXCL12 chemokine obligate heterodimers were prepared as following. Sample aliquots (15uL) were mixed with Laemmli loading buffer (2x) without reducing agents, boiled for 5 minutes at 100°C, centrifugated (13,200rpm, 5 min) and 15uL loaded onto the gel. The electrophoresis was run at 100V for 10 min and 200V when protein entered the separating gel for a total run of 2 hours (BioRad gel apparatus) on ice. The

presence of protein was detected following overnight Coomassie blue staining (2.5g brilliant blue R, 10mL acetic acid, 45mL methanol, and 45mL water) and de-staining in a water/methanol/acetic acid (50:40:10 v/v) solution.

### **3.2.5.2 Western blots**

Briefly, CXCL4-CXCL12 chemokine obligate heterodimers were denatured, loaded onto the 16.5% polyacrylamide gels, and separated with the SDS-PAGE electrophoresis (as in 3.2.5.1 above). The proteins were then transferred to 0.2 $\mu$ m nitrocellulose membrane using a semi-transfer apparatus (Biorad, CA). Membranes were blocked in Tris-buffered saline containing 0.1% tween-20 and 5% non-fat milk overnight at 4°C, then incubated with the primary antibody including anti-CXCL4 and anti-CXCL12 (R&D systems). Following wash, the membranes were incubated with the appropriate horseradish-peroxidase (HRP)-conjugated secondary antibody. After additional washes, the presence of specific proteins was determined based on chemiluminescence following addition of an ECL substrate detected using a ChemiDoc Imaging System (BioRad).

### **3.2.5.3 CXCL4<sub>S26C</sub>-CXCL12<sub>L29C</sub> co-immunoprecipitation (Co-IP)**

Mutant CXCL4 and CXCL12 were mixed at the molar ratio 1:1 and allowed to heterodimerize through Cu<sup>2+</sup> oxidation as described previously (see section 3.2.4). Following the Cu<sup>2+</sup> oxidation step, samples were centrifugated (4000rpm, 4°C, 5 min) to remove precipitates and incubated with magnetic microbeads pre-coated with mouse anti-CXCL4 (R&D System) at 4°C for 2 hours. After incubation, microbeads were magnetically bound and washed to remove the unbound fractions. After elution, the CXCL4<sup>+</sup> protein solution was incubated with anti-CXCL12 coated magnetic beads and the proteins CXCL4<sup>+</sup>CXCL12<sup>+</sup> eluted. Similarly, IPs using the anti-CXCL12 coated magnetic microbeads first and followed by anti-CXCL4 coated

magnetic beads second were also prepared. Western blot analysis of the immune-precipitated samples was performed using mouse-anti CXCL4 and goat-anti CXCL12 monoclonal antibodies (R&D System).

#### **3.2.5.4 Nuclear Magnetic Resonance spectroscopy**

NMR experiments were performed on the Bruker Avance-III 750 MHz spectrometer equipped with the CryoProbe at NCSU. The  $N^{15}$ -labeled CXCL4<sub>S26C</sub>-CXCL12<sub>L29C</sub> (~68 $\mu$ M) sample was prepared in 10mM NaCl, pH 6.9 at 40°C containing 10% D<sub>2</sub>O. All NMR raw data was processed by NMRPipe software and analyzed by using NMRview [186].

### **3.4 Results**

#### **3.4.1 Production of the mutants S26C CXCL4 and L29C CXCL12**

Mutant S26C CXCL4 was initially purified by cation exchange and followed by heparin affinity chromatography (Figure 3.1 A). The mutant was eluted from the heparin column using NaCl gradient and the peak detection ranges from 1.2 to 1.4M of NaCl. S26C CXCL4 eluted from the heparin column led to a single ~8kDa band in SDS-PAGE gel stained with Coomassie blue (Figure 3.1 B). Furthermore, NMR analysis overlaying two spectra demonstrated similar folding of the mutant (cyan) with the wildtype CXCL4 (black) (see supplementary data appendix).

The L29C CXCL12 mutant was successfully expressed in inclusion bodies similarly to the wildtype CXCL12 (see supplementary data appendix). For purification, we used a novel on-column refolding in cation exchange protocol to improve the yield [187]. This refolding strategy allows a gradual removal of the denaturing agent urea and exposes the mutant to the refolding condition. Following the elution from the cation exchange column, the refolded L29C mutant was further purified using size exclusion chromatography. Peak was detected by the UV280 flow

cell monitor compatible with the AKTA pure 25 FPLC (Figure 3.1 C). A highly enriched CXCL12 L29C mutant protein fraction was isolated as determined by SDS-PAGE gel stained with Coomassie blue (Figure 3.1 D).

### **3.4.2 Generation of the obligate heterodimer CXCL4-CXCL12 via the disulfide bridge**

We generated the obligate heterodimer CXCL4-CXCL12 using the disulfide-trapping strategy combining CXCL12 L29C and CXCL4 S26C mutant monomers (Figure 3.2 A).

Following the incubation and passage through a size exclusion column, the complex detected in the eluate (Figure 3.2 B) has a sharp symmetric peak suggesting that the complex is not aggregated in solution. Moreover, the protein complex peak eluted at the same time as myoglobin (~16.7kDa), indicative of the formation of a ~16kDa complex. Immunoblotting detected the presence of both CXCL4 and CXCL12 (Figure 3.2 C).

To further assess the formation of CXCL4-CXCL12 heterodimers, co-immunoprecipitation experiments were performed first isolating CXCL12<sup>+</sup> fraction and detecting CXCL12-CXCL4<sup>+</sup> protein complex (see Figure 3.3 A). In parallel, isolation with anti-CXCL4 first and then detection with anti-CXCL12 to confirm the presence of the CXCL12<sup>+</sup>CXCL4<sup>+</sup> heterodimer complex was also conducted. Following a non-reducing SDS-PAGE, co-IP fractions were analyzed by Western blots and demonstrated the presence of a CXCL12<sup>+</sup>CXCL4<sup>+</sup> heterodimer band at 16kDa (Figure 3.3B).

### **3.4.3 The obligate heterodimers have a specific NMR spectroscopy profile**

The NMR spectrum of <sup>15</sup>N-enriched CXCL4-CXCL12 heterodimer displayed well-dispersed cross-peaks, evidencing the presence of a folded structure (Figure 3.4 A, blue spectrum). Moreover, the number of observed cross-peaks (~130) corresponds to the number of amino acids in CXCL4-CXCL12 heterodimer without prolines (132 residues).

Figure 3.4 B show a portion of the overlaid  $^{15}\text{N}$ - $^1\text{H}$  HSQC spectra of the obligate CXCL4-CXCL12 heterodimer with CXCL12 wildtype. Resonances of peaks originating from the residues away from the heterodimerization interface such as C11, S16, L29, L42, N46, V49, D52, K54 L60, L66 are minimally perturbed. In contrast, residues K24, H25 in the interface are strongly affected by the heterodimerization. Furthermore, the spectrum of the obligate CXCL4-CXCL12 heterodimers exhibits a significantly simplified cross-peak pattern as compared to the CXCL4 wildtype (Figure 3.4 C-D). Whereas each amino acid A43, G33, G48 in the CXCL4 wildtype (green) are presented by multiple cross-peaks due to the intermediate exchange equilibrium of CXCL4 monomers, dimers, and tetramers [13], the obligate CXCL4-CXCL12 heterodimer alone presents as a single species (i.e., A43, G33) or has a simplified peak pattern (i.e., G48). Collectively, these data demonstrate that chemokine monomers in the obligate CXCL4-CXCL12 heterodimer have similar, but not identical three-dimensional structures and some structural rearrangements likely occur. One such rearrangement could be the re-orientation of alpha helix in the CXCL12 monomer as previously observed in the molecular dynamic simulation [22].

### 3.5. Discussion

Investigating the biology of chemokine heterodimers is challenging given the contribution of many chemokine species present at equilibrium, i.e., monomers, dimers, heterodimers, and tetramers. To bypass this issue and directly assess the biological activity of the chemokine heterodimers, we generated an obligate disulfide-trapped CXCL12-CXCL4 heterodimer by introducing an intermolecular disulfide bridge. To avoid the formation of disulfide-linked homodimers, we selected residues L29 and S26 on the first  $\beta$ -sheet of CXCL12 and CXCL4, respectively, which are away from the two-fold symmetry axis. The obligate heterodimers were formed via  $\text{Cu}^{2+}$  oxidation and further purified by size exclusion. The formation of CXCL4-CXCL12 chemokine heterodimers was verified by Coomassie staining of SDS-PAGE gel, and by using specific anti-CXCL12 or anti-CXCL4 antibodies in Western blots and co-IPs. Furthermore, NMR  $^{15}\text{N}$ - $^1\text{H}$  HSQC spectroscopy showed a spectrum with well-dispersed distribution of cross peaks, confirming the correct folding of the obligate CXCL12-CXCL4 heterodimers.

This study presents a disulfide trapping strategy to generate the heterodimers for further structural and biological assessments of the heterodimeric chemokines. Indeed, this strategy has been successfully applied to generate other disulfide-trapped chemokine heterodimers CXCL7-CXCL1 [23], CXCL12 and CXCL8 homodimers [59, 83, 85], and other protein hetero-complexes [184]. Recently, this strategy was also used to generate a disulfide-trapped chemokine-chemokine receptor complex for further structural evaluations of ligand-receptor interactions [188]. A major advantage of this strategy over other types of crosslinking is that the substituted cysteine does not cause the artificial conformational change in the complex as the cysteine side chain is small [188].

Combined evidence from biological and biophysical analyses shows for a successful formation of the disulfide-trapped CXCL4-CXCL12 heterodimers. Our size exclusion chromatogram (SEC) shows a tall sharp peak with its retention time similar to the standard pure myoglobin protein (16.7kDa), indicating a formation of obligate CXCL4-CXCL12 heterodimers with high degree of purity and conformational homogeneity [189, 190]. Of note, a small shoulder on the left of the HD peak could be due to aggregated proteins [189]; thus, separated from the main peak by fractionation. Non-reducing SDS-PAGE and Western blot are indispensable techniques routinely used to characterize protein presence based on size (molecular weight) and unique antigenic site recognized by antibodies [191]. Although non-reducing SDS-PAGE and Western blot analyses demonstrated a formation of the heterodimers, the results are still ambiguous due to similar molecular weight of CXCL4 (7.9kDa) and CXCL12 (8kDa); and thus, required further verification. The heterodimer formation was strongly confirmed by our Co-IP analyses by which the target protein was selected using specific antibodies and further precipitated along with its binding partner [192].

From the biophysical perspective, we further characterized that the correct folding of the heterodimer. The two-dimensional  $^1\text{H}$ - $^{15}\text{N}$  NMR HSQC is a robust technique that has been used to determine folding state of many chemokines [13, 25, 27, 29, 81, 171]. The NMR spectrum with well-dispersed chemical shift indicates a folded obligate CXCL4-CXCL12 heterodimer, unlike other unfolded proteins presented by clusters of peaks in the middle of the spectra. The pattern of cross-peaks in the heterodimer NMR spectrum is similar to individual chemokines, and many peaks in the heterodimer spectrum can be mapped to CXCL4 or CXCL12 monomers. Furthermore, overlays of NMR spectra show a significant simplification of peak pattern as compared to CXCL4, indicating the presence of a single heterodimer species. We also observed

chemical shift changes corresponding to the heterodimerization when comparing with the CXCL12 wildtype that are likely due to mutations and/or a structural change such as the re-orientation of alpha-helix in the CXCL12 monomer [22].

We demonstrated the formation the disulfide-trapped CXCL4-CXCL12 by using a series of stringent validation steps. As noted, the yield on heterodimer production was quietly low (~180ug/mL of the heterodimers obtained from 4L of the L29C CXCL4 and 2L of the S26C CXCL12 cell growth). Thus, further optimization, starting with the production of mutant L29C, could increase the yield. Overall, the generation of obligate CXCL12-CXCL4 heterodimers provides a tool to directly study the mechanism of action of the CXCL12-CXCL4 heterodimers on breast cancer progression.

## 3.6 Figures

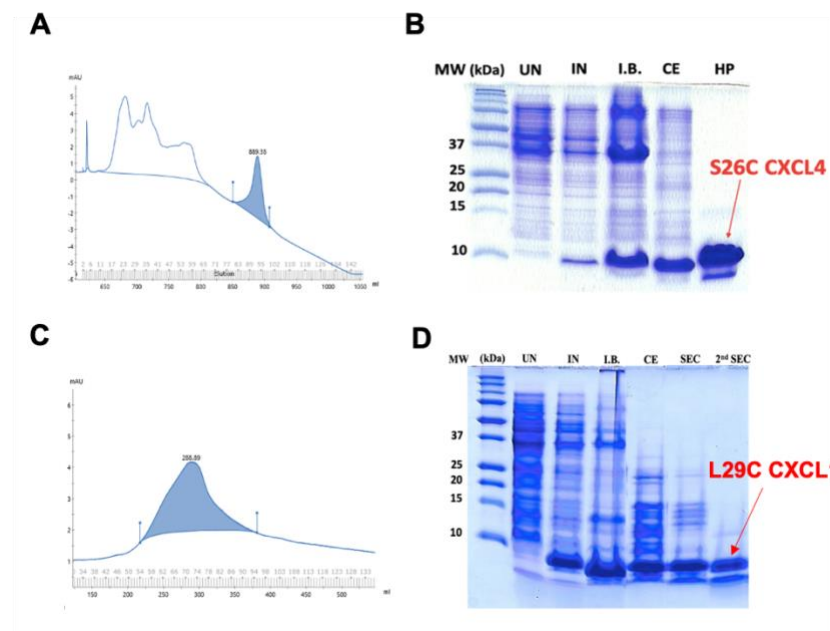


**Figure 3.1: Purification of S26C CXCL4 and L29C CXCL12 chemokine mutants.** (A) Heparin chromatogram of the last purification step for S26C CXCL4. The shaded peak eluted with a 1.2 to 1.4M NaCl gradient corresponds to S26C CXCL4. (B) SDS-PAGE of the different S26C CXCL4 fractions through the purification process stained with Coomassie blue (MW: molecular weight in kDa - protein ladder. UN – uninduced cells, IN – induced cells, IB – inclusion bodies, CE – cation exchange chromatography, HP – heparin affinity chromatography, SEC – size exclusion chromatography). (C) Size exclusion chromatogram of the last purification step for L29C CXCL12. The shaded peak eluted with a 1 CV of the equilibration buffer corresponds to L29C CXCL12. (D) SDS-PAGE of the different L29C CXCL12 fractions through the purification process (2<sup>nd</sup> SEC – eluate from the second size exclusion chromatography purification). Prior to SDS-PAGE, all samples were treated with 5% beta-mercapto-ethanol and boiled (100°C, 15 min).

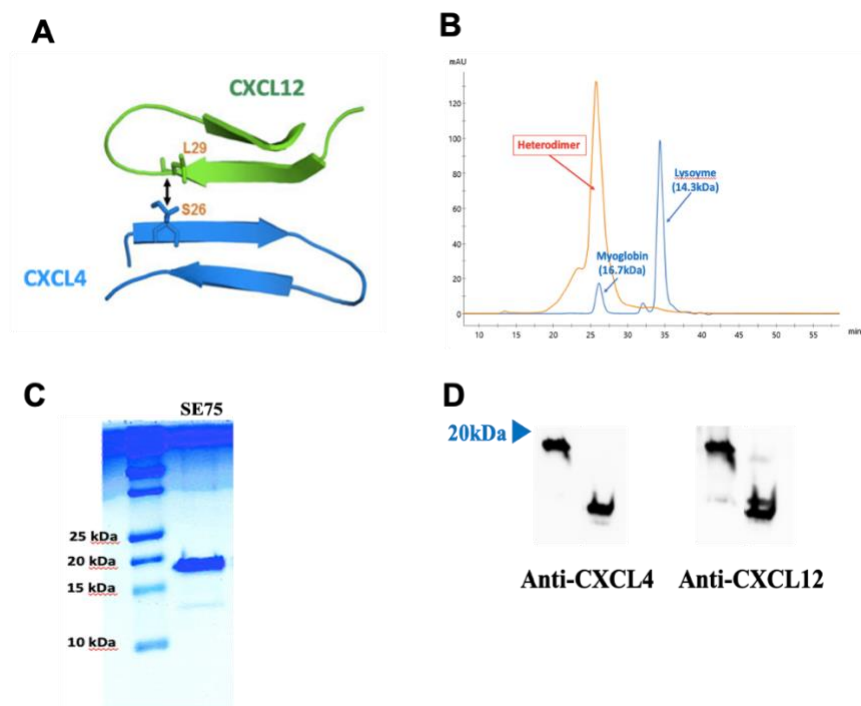


**Figure 3.2: Purification of the CXCL4-CXCL12 chemokine obligate heterodimers.** (A) 3D model of the obligate CXCL4<sub>S26C</sub>-CXCL12<sub>L29C</sub> heterodimers via the disulfide crosslink between L29C and S26C on CXCL12 and CXCL4 mutants, respectively (only two beta-strands from chemokine structure are shown for clarity). (B) The elution from size exclusion column of the CXCL4-CXCL12 chemokine obligate heterodimers (16kDa, orange peak) is compared to standard proteins myoglobin (16.7kDa) and lysozyme (14.3kDa). (C) Coomassie blue stained SDS-PAGE in non-reducing conditions demonstrates the presence of the ~16kDa CXCL4<sub>S26C</sub>-CXCL12<sub>L29C</sub> heterodimers. (D) Western blot analysis of the obligate CXCL4-CXCL12 chemokine heterodimers. Briefly, samples mixed with Laemmli buffer (2x) in the (-/+ reducing agents) were electrophorized and transferred onto a nitrocellulose membrane. The presence of the obligate CXCL4<sub>S26C</sub>-CXCL12<sub>L29C</sub> heterodimers (~16kDa) was detected by Western Blots in reduced and non-reduced conditions with anti-CXCL4 and anti-CXCL12 antibodies.

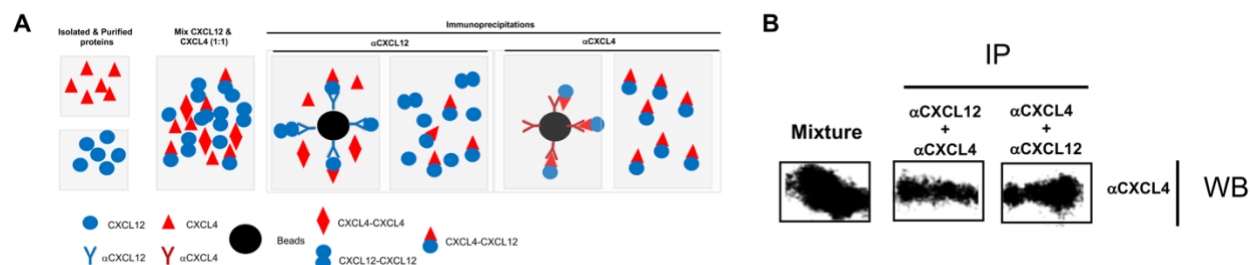


**Figure 3.3: Obligate CXCL4<sub>S26C</sub>-CXCL12<sub>L29C</sub> heterodimers were detected following IP and WB.** (A) Briefly, CXCL4<sub>S26C</sub> and CXCL12<sub>L29C</sub> proteins were expressed following transformation of *E. coli* with pET24d+ expression plasmids (GenScript) and purified as described (see materials and methods section). Next, the two purified protein fractions were mixed (1:1 molar ratio) and dialyzed against Cu<sup>2+</sup> to generate disulfide-trapped heterodimers [184, 193]. The obtained protein mixture was first immuno-precipitated with anti-CXCL4 antibody coated magnetic microbeads and then the CXCL4+ protein mixture was further selected by immuno-precipitation using anti-CXCL12 antibody coated magnetic microbeads. IPs using first the anti-CXCL12 antibody coated magnetic microbeads followed by anti-CXCL4 antibody coated magnetic microbeads were also prepared. (B) The original protein mixture (1/2000 dilution, Left) and the IP products (anti-CXCL12 ( $\alpha$ CXCL12) then  $\alpha$ CXCL4 (Middle) and  $\alpha$ CXCL4 then  $\alpha$ CXCL12 (Right)) were separated using 16.5% non-reducing SDS-PAGE gels, transferred onto 0.22 $\mu$ m PVDF nitrocellulose membrane and the presence of obligate CXCL4<sub>S26C</sub>-CXCL12<sub>L29C</sub> heterodimers (~16kDa) detected by Western blot with chemo-luminescence using antibodies against CXCL4 (R&D System).



**Figure 3.4: NMR assessments of the formation and folding of the obligate CXCL4-CXCL12 heterodimer.** (A) An overlay of full  $^{15}\text{N}$ - $^1\text{H}$  HSQC spectra of uniformly  $^{15}\text{N}$ -labeled CXCL4-CXCL12 obligate heterodimer (blue peaks) with  $^{15}\text{N}$ -labeled CXCL4 wildtype (green peaks) and  $^{15}\text{N}$ -labeled CXCL12 wildtype (red peaks). Cross-peaks of the CXCL4 and CXCL12 wildtype were respectively assigned based on the previous publications [19, 27]. Cross-peaks of the backbone amides are labeled by the one-letter amino acid code and position number (red code – CXCL12 wildtype, green code – CXCL4 wildtype). (B) Selected region taken from figure A (red rectangle) shows the chemical shift changes in the selected amino acids of CXCL12 wildtype (red peaks) and the appearance of new peaks corresponding to the formation of the obligate CXCL4-CXCL12 heterodimer (blue peaks). (C-D) Selected regions taken from figure A (green rectangles) show an overlay of cross-peaks of A43, G33 and G48 in CXCL4 wildtype (green peaks) with those in the obligate CXCL4-CXCL12 heterodimer (blue peaks). All HSQC spectra were collected at 40°C on the 750MHz spectrometer at NCSU. Labeled obligate CXCL4-CXCL12 heterodimer (68uM), wildtype CXCL4 (150uM), and wildtype CXCL12 (129uM) were separately prepared in 90% H<sub>2</sub>O/10% D<sub>2</sub>O in water, 20mM NaCl, pH 6.9.

## CHAPTER 4: EFFECTS OF THE OBLIGATE CXCL4-CXCL12 HETERODIMERS ON BREAST CANCER CELL SIGNALING AND MIGRATION

### 4.1 Abstract

Triple negative breast cancer is associated with high morbidity due to the high probability of metastasis and lack of effective therapies. The breast cancer microenvironment including extracellular matrix, tumor cells, non-tumor cells, and signaling molecules such as chemokines critically modulate cancer progression and metastasis. Chemokine CXCL12 and its receptor CXCR4 are actively involved every step of cancer progression, including the migration of tumor cells to surround local tissues and distant organs. Thus, targeting CXCL12-CXCR4 signaling axis is a potential approach for anti-cancer treatments. Many chemokines co-localize *in vivo*; heightening the likelihood of the formation of chemokine heterodimers that may synergistically enhance or inhibit chemokine activity. We previously demonstrated that CXCL12 forms heterodimers with the CXCL4 chemokine (Chapter 2). We also generated a non-dissociating CXCL4-CXCL12 heterodimer by using the disulfide trapping strategy (Chapter 3). Here, we investigated whether the CXCL4-CXCL12 heterodimers are functional, i.e., could prevent cancer cell migration mediated by CXCL12-CXCR4 chemokine-receptor activation. The results indicate that the obligate CXCL4-CXCL12 heterodimers at 100nM and 200nM significantly inhibited MDA-MB 231 cell migration ( $p < 0.05$ ). While both wildtype CXCL12 (100nM) and obligate monomer CXCL12 (100nM) stimulated cell migration ( $p < 0.05$ ), the obligate CXCL4-CXCL12 heterodimers similarly to obligate CXCL12 homodimers, did not induce cell migration regardless of concentration tested. Furthermore, the cancer cell migration induced by CXCL12 was decreased when cells were incubated with wildtype CXCL12 and increasing concentrations of the obligate CXCL4-CXCL12 heterodimers. In particular, incubation with 50nM of the

obligate CXCL4-CXCL12 heterodimers was associated with CXCL12-induced migration suppression ( $p < 0.05$ ). Mechanistically, obligate heterodimers induced calcium mobilization via CXCR4. Altogether, these findings suggest that the CXCL4-CXCL12 obligate heterodimers inhibited cell migration by competing with CXCL12 in CXCR4 activation. Further investigations are needed to determine the molecular mechanism by which obligate heterodimers exerts differential cellular behavior, possibly via distinct interactions with CXCR4 and signaling pathways.

## 4.2 Introduction

Chemokines are chemotactic cytokines that regulate trafficking of cells both in the normal and pathological conditions [8, 194-200]. To date, at least 48 different chemokines have been identified in humans and further classified into CXC, CC, XC, and CX3C subfamilies [8]. Chemokines induce signaling via interactions with the seven transmembrane G-coupled protein receptors (GPCRs) [7, 201]. The chemokine activities *in vivo* are also governed by their interactions with glycosaminoglycans (GAGs) on the cell surfaces or extracellular matrix [202, 203]. Additionally, chemokine activities are also mediated by chemokine oligomerization [16, 59, 76, 84, 204-206]. Chemokines exist in multiple states of oligomerization, from the primary monomers-dimers equilibrium to tetramers in some chemokines (i.e., CXCL4, CXCL7) or even higher-ordered oligomers (i.e., CCL5) [25-27, 29, 171].

Considering that chemokines are expressed concomitantly *in vivo*, chemokines can form heterodimers. Chemokine heterodimerization has been intensively investigated over the past decade, resulted in the discovery of many pairs of chemokine heterodimers. Molecular dynamics simulations on some selected chemokine pairs from CC- and/or CXC- subfamily show that monomers of different chemokines can exchange with one another when the residues at the interface is sterically and energetically favorable for the formation of heterodimers [21]. In 2017, Von Hundelshausen and colleagues reported a complete map of chemokine interactome with more than 200 heterophilic interactions identified by using immunoblotting [15]. Likewise, several pairs of chemokine heterodimerization have been reported by the other groups [16, 18, 19, 22, 23]. Altogether, these findings suggest that the formation of chemokine heterodimers may be a common mechanism to fine-tune the chemokine activity *in vivo*. However, our knowledge on the biological relevance associated with chemokine heterodimerization is limited

in only a few pairs. i.e., CXCL4-CXCL8 [19], CXCL4-CCL5 [16], or CCL5-CCL17 [15]. So far, CXCL4-CCL5 heterodimer was intensively studied *in vivo* and that the peptide inhibiting this heterophilic interaction yielded therapeutic benefits in preventing atherosclerosis disease [18].

Investigation of chemokine heterodimerization is relevant to the *in vivo* tumor microenvironment as it co-localizes various chemokines, and thus allowing the formation of chemokine heterodimers that may act synergistically to modify chemokine activity [5]. However, the coexistence of many species in the mixture hampers the direct assessment of chemokine heterodimer. To overcome this issue, we produced an obligate CXCL4-CXCL12 chemokine heterodimer (see Chapter 3). Here, we investigate the receptor activation and the biologically relevant breast cancer migration induced by the obligate CXCL4-CXCL12 heterodimers produced. Furthermore, we also compared biological relevance of the obligate CXCL4-CXCL12 heterodimers with the other variants of CXCL12, i.e., obligate CXCL12 monomers and homodimers provided by Dr. Brian Volkman at Medical College of Wisconsin. To our knowledge, this is the first report that unambiguously compares the biological relevance of the heterodimers with other CXCL12 species.

Our data indicate that the CXCL4-CXCL12 obligate chemokine heterodimer inhibited the migration of breast cancer cells. The migration was decreased compared to that generated by the wildtype CXCL12 and the CXCL12 obligate monomers. Moreover, our analyses confirm that CXCL4-CXCL12 obligate heterodimers bind to and activate CXCR4 leading to a spike in intracellular free  $\text{Ca}^{2+}$ .

## 4.3 Materials and methods

### 4.3.1 Wound healing assays

Briefly, MDA-MB 231 cells were grown to confluency in media supplemented with 10% FBS (see section 2.3.1 for cell culture). After a 6-hour starvation in media with 0% FBS, the cell monolayer was wounded and cells were treated with various concentrations of obligate heterodimers, mutants of CXCL4 and CXCL12, obligate monomer and homodimer of CXCL12, or CXCL4-derived peptide. After an additional 9-hour incubation, cell migration was determined. After the addition of the vital nuclear dye Hoechst, microphotographs of the entire wound area were taken at both 0 and 9-hour post-treatment. Cell migration (%) over 9 hours was determined using image J software.

Wound healing assays were also conducted (as above) in the presence of either the CXCR4 antagonist (20nM AMD 3100) or the CXCR3 antagonist (5-50nM AMG 487) to determine whether the migration was associated with either the CXCL12-CXCR4 or CXCL4-CXCR3 signaling. When using those inhibitors, MDA-MB 231 cells were pre-incubated with the receptor antagonist at indicated concentrations for 1 hour at 37°C and then treated with chemokines as described above.

### 4.3.2 Calcium mobilization assays

CXCR4 receptor activity of the obligate heterodimers was determined using calcium ( $\text{Ca}^{2+}$ ) flux assay as previously [99]. Briefly, MDA-MB 231 breast cancer cells were seeded at 50,000 cells/well (100uL per well, 96-well tissue culture plates, Greiner) and grown to confluence. After 48 hours, cells were starved in serum-free media for 6 hours. Cells were then incubated (45 min, 37°C) with the  $\text{Ca}^{2+}$  intracellular indicator Fura-2 (2 $\mu\text{M}$ ). After a PBS wash, changes in  $\text{Ca}^{2+}$  flux were measured using a Molecular Device ID5 plate fluorescence reader in

which cells were administered increasing concentrations (0-250nM) of the CXCL4-CXCL12 chemokine obligate heterodimers and the change in fluorescence measured for every 1.5s for up to 1 min at two different wavelength 340/510nm and 380/510nm according to the Fura-2AM manufacturer's recommendations. Background fluorescence was measured for 30s prior to the addition of the obligate heterodimers. Fluorescent signals were subsequently normalized to the average background reading.

To investigate whether the release of intracellular calcium results from the receptor activation, calcium mobilization was measured in the presence of CXCR4 inhibitor (20nM of AMD3100) and CXCR3 inhibitor (5-50nM of AMG487). Briefly, MDA-MB 231 cells were pre-treated with the receptor antagonists for an hour at 37°C. After removing old media, cells were loaded with Fura-2 AM and followed by steps as described above.

#### **4.3.3 Statistical analysis**

Wound healing data are represented as mean  $\pm$  SEM. Differences between conditions were assessed using one-way ANOVA and post-hoc tests. Significance was set at  $p < 0.05$ . Values in the dose-dependent curve of calcium mobilization was averaged from at least 3 independent experiments and presented as mean  $\pm$  SEM.

## 4.4 Results

### 4.4.1 Obligate CXCL12-CXCL4 chemokine heterodimer inhibits breast cancer migration

The functional effects of the CXCL12-CXCL4 chemokine obligate heterodimers (HD) were tested using a wound healing assays assessing the migration in the MDA-MB 231 triple negative breast cancer cells (Figure 4.1 A). The MDA-MB 231 cells express both chemokine receptor CXCR4 and CXCR3 [138]. Obligate CXCL4-CXCL12 heterodimers (1-200nM) dose-dependently inhibited the migration of breast cancer cells ( $p < 0.05$ , Figure 4.1 B). Obligate CXCL4-CXCL12 heterodimers (100 and 200nM) exhibited a significant reduction compared to wild-type CXCL12 chemokine ( $p < 0.05$ ). Addition of obligate CXCL4-CXCL12 heterodimers (100 and 200nM) led to 25% and 35% decrease in cell migration compared to 0-10nM concentration of the obligate CXCL4-CXCL12 heterodimers.

To assess whether the obligate CXCL4-CXCL12 heterodimers triggered cell migration via CXCL12-CXCR4 signaling axis, MDA-MB-2321 cells were treated with the CXCR4 antagonist AMD3100 (20nM). In the presence of AMD3100, no change in wound healing was observed regardless of the obligate CXCL4-CXCL12 heterodimers concentrations used, suggesting that obligate CXCL4-CXCL12 heterodimers likely mediate the migration inhibition through CXCR4 signaling ( $p = ns$ , Figure 4.1. B).

To determine whether the introduced mutations contribute to the observed migration that may hamper our assessment on the heterodimers function, we assessed the activities of mutants CXCL4<sub>S26C</sub> and CXCL12<sub>L29C</sub>. The mutant CXCL12<sub>L29C</sub> was as potent as CXCL12 wildtype in inducing MDA-MB 231 breast cancer cell migration ( $p < 0.05$ , compared to control and  $p = ns$  to wildtype CXCL12, respectively, Figure 4.1 A). CXCL12<sub>L29C</sub>-mediated migration was also inhibited in the presence of the CXCR4 antagonist (Figure 4.1 C) and was not associated with

CXCL4-CXCR3 signaling (Figure 4.1 D). The mutant CXCL4<sub>S26C</sub> did not mediate MDA-MB 231 breast cancer cell migration regardless of the presence of CXCR3 antagonist, suggesting that CXCL4-CXCR3 signaling was not associated with cell migration (Figure 4.1 B and D).

#### **4.4.2 Obligate CXCL4-CXCL12 heterodimer competes with CXCL12 to prevent cancer migration**

Next, we assessed whether the obligate CXCL4-CXCL12 heterodimers competed with CXCL12 leading to cancer cell migration inhibition (Figure 4.2 A). As expected, CXCL12 (100nM) alone effectively stimulated MDA-MB 231 cell migration ( $p < 0.05$ , Figure 4.2 A). However, when combining CXCL12 (100nM) with increasing obligate CXCL4-CXCL12 heterodimer concentrations (0-200nM), the CXCL12-CXCR4 driven cell migration was significantly reduced. Notably, the obligate CXCL4-CXCL12 heterodimers ( $\geq 50$ nM) fully reduced (Figure 4.2 A) wound healing promoted by 100nM of CXCL12 (Figure 4.2 A).

This finding suggests that the obligate CXCL4-CXCL12 heterodimers can compete with the wildtype CXCL12 when concomitantly present. Particularly, a molar ratio 1:2 of the obligate CXCL4-CXCL12 heterodimer and CXCL12 wildtype would effectively prevent CXCL12-induced migration. In similar assays, the effects of the obligate CXCL4-CXCL12 heterodimers were compared to that of the CXCL4-derived peptide, previously demonstrated to prevent the CXCL12-driven migration (see Chapter 2 and Figure 4.2 B). As expected, addition of either obligate CXCL4-CXCL12 heterodimers or the CXCL4-derived peptide fully prevented CXCL12-CXCR4 induced tumor cell migration ( $p < 0.05$ ).

#### **4.4.3 Comparing the obligate CXCL4-CXCL12 heterodimer, obligate CXCL12 monomer and homodimer migration activities**

The abilities of the obligate CXCL4-CXCL12 heterodimers, obligate CXCL12 monomers and homodimers to induce MDA-MB 231 breast cancer cell migration were assessed (Figure 4.3). Both the wildtype CXCL12 (100nM) and the obligate CXCL12 monomers (LM, 100nM) induced significant MDA-MB 231 cell migration ( $p < 0.05$ ). Of note, the dimerization-impaired obligate CXCL12 monomers (H25 at the dimerization interface was substituted by R25) induced the migration at concentrations as low as 50nM (data not shown), suggesting that it is more potent in stimulating the migration compared to the wildtype CXCL12. In contrast, obligate CXCL12 homodimers (LD, 100nM) did not induce cell migration. Similarly to the obligate CXCL12 homodimers, the obligate CXCL4-CXCL12 heterodimers (100nM) did not stimulate cell migration regardless of the concentrations tested, i.e., 50 and 200nM (data not shown). The data support an inhibitory effect of the CXCL4-CXCL12 chemokine obligate heterodimer on the migration of MDA-MB 231 cells.

#### **4.4.4 Calcium mobilization**

To further assess the obligate CXCL4-CXCL12 heterodimer biological activity, we measured the calcium mobilization in response to increasing doses of the obligate heterodimers (Figure 4.4 A-B). The calcium mobilization assay measured the free intra-cytoplasmic  $\text{Ca}^{2+}$  second messenger produced through activation of the G-protein-coupled receptors, including CXCR4 [99]. The CXCL4-CXCL12 chemokine obligate heterodimer (0-100nM) dose-dependently (0-10nM) stimulated calcium mobilization in MDA-MB-231 cells (Figure 4.4 B). The free cytoplasmic  $\text{Ca}^{2+}$  was maximal for obligate CXCL4-CXCL12 heterodimer concentrations between 10 and 100nM (Figure 4.4 B). Interestingly, higher concentrations (e.g.,

250nM) of the obligate CXCL4-CXCL12 heterodimers led to a decrease in  $\text{Ca}^{2+}$  flux (data not shown). Moreover, calcium mobilization was inhibited when MDA-MB 231 cells were pre-treated with the CXCR4 antagonist AMD3100, suggesting that the obligate CXCL4-CXCL12 heterodimers are binding to the CXCR4 G-protein-coupled receptor and triggering  $\text{Ca}^{2+}$  secondary messenger (Figure 4.4 C). In contrast, in the presence of the CXCR3 antagonist AMG487, the obligate CXCL4-CXCL12 heterodimers retained their ability to induce calcium flux, suggesting that the calcium flux mediated by the obligate CXCL4-CXCL12 heterodimers is not associated with CXCR3 signaling (Figure 4.4 D).

#### **4.5 Discussion**

The CXCL12/CXCR4 signaling axis plays a key role in multiple aspects of breast cancer progression including tumor growth, migration, and distant metastasis to specific organs associated with high secretion of CXCL12 [97, 103, 128]. Through CXCR4 activation, CXCL12 induces intracellular signaling cascades leading to cellular migration – a key step in breast cancer metastasis [128]. Furthering previous studies that focused on CXCR4 antagonism [109, 207-210], we demonstrated that CXCL4-CXCL12 chemokine heterodimerization could be an effective strategy to block the CXCL12-dependent migration in breast cancer. Since CXCL12 existed as a monomer-dimer equilibrium [27], here we assessed the biological potential of CXCL4-CXCL12 heterodimers along with the other disulfide-locked CXCL12 monomers and dimers on tumor cell migration. Our data show that treatments with CXCL4-CXCL12 heterodimers reduce the CXCL12/CXCR4 axis induced migration of MDA-MB 231 breast cancer cells, mainly through the competitive modulation of the CXCR4 signaling as shown by the release of  $\text{Ca}^{2+}$  second messenger. Together, these results highlight that the presence of

chemokine heterodimerization promotes a marked difference in cell migration and extend our knowledge on chemokine heterodimerization in breast cancer.

The promotion of cell migration by CXCL12 chemokine signaling at nano-molar range has been reported in MDA-MB 231 and other cancer cell lines [211-213]. Notably, the effects of cell migration were lost when high CXCL12 doses, i.e., 1000nM, were used, raising the possibility that the wildtype CXCL12 equilibrium shifted toward the formation of homodimers at higher concentrations [81].

Our data show that incubation with the obligate CXCL4-CXCL12 heterodimers inhibited the migration of MDA-MB 231 cells (Figure 4.1A). Importantly, when combining with the wildtype CXCL12, the obligate CXCL4-CXCL12 heterodimers present higher efficacy in inhibiting CXCL12-driven cancer cell migration. Obligate CXCL4-CXCL12 heterodimers mediate signaling via CXCR4 as shown by the release of intracellular calcium upon stimulation and the loss of calcium flux in the presence of CXCR4 antagonist (Figure 4.4 B-C). Taken together, the data indicate that while the obligate CXCL4-CXCL12 heterodimers activate CXCR4 to release calcium flux, they failed to induce cell migration. Critically, obligate CXCL4-CXCL12 heterodimers competed with the wildtype CXCL12 for receptor binding and activation and led to reduced CXCL12-driven migration (Figure 4.2 A). The migration inhibition induced by the obligate CXCL4-CXCL12 heterodimers may result from a distinct signaling mechanism differentially activating the CXCR4 receptor. A fuller understanding of the concomitant  $\text{Ca}^{2+}$  flux and absence of activation of CXCR4 associated with cell migration requires further investigation.

Mechanistically, receptor oligomerization may also participate in the signaling pathway. Indeed, receptor oligomerization is associated with altered signaling and the biological relevance

as observed for some chemokine heterodimers [15]. However, whether the heterodimers trigger receptor CXCR4 oligomerization, i.e., CXCR4 homodimers [214], CXCR3-CXCR4 heterodimers [215], or CXCR4-CXCR7 heterodimers [216] remains unclear. Nevertheless, as exemplified by the CCR2-CCR5 receptor heterodimer, receptor heterodimerization could produce negative binding cooperativity that is the binding of the first ligand to its receptor preventing the subsequent interaction of the other ligand [217]. Therefore, further studies regarding receptor oligomerization in response to chemokine CXCL4-CXCL12 heterodimers should aim to improve our knowledge of the alterations and their biological relevance triggered by the binding of obligate CXCL4-CXCL12 heterodimers to CXCR4.

In comparing the biological activities of the obligate CXCL4-CXCL12 heterodimers with that of other CXCL12 variants, we found that similarly to the obligate CXCL12 homodimers, the obligate CXCL4-CXCL12 heterodimers were unable to stimulate migration, whereas the obligate CXCL12 monomers effectively induced cellular migration. We also demonstrated that the obligate CXCL12 monomers induced cell migration more potently compared to the wildtype CXCL12. Our findings are in agreement with previous studies showing that while both CXCL12 monomers and dimers were functionally active via CXCR4 activation, only CXCL12 monomers induced chemotaxis [59, 81]. The differences in function were the result of altered  $\beta$ -arrestin recruitment and the associated downstream effector proteins in this pathway; thus, leading to changes in cell behavior [81]. Thus, we suggest that aberrant receptor trafficking via alternations in the  $\beta$ -arrestin-mediated pathway could be associated with the down-regulated migration by the obligate CXCL4-CXCL12 heterodimers. Future studies are needed to validate the involvement of  $\beta$ -arrestin signaling upon chemokine heterodimer stimulation.

Altogether, our data highlight a new cancer-related activity of for the new generated and purified obligate CXCL4-CXCL12 heterodimer. Inhibition of CXCL12-mediated tumor migration through chemokine heterodimerization could open a new avenue for chemokine-targeted approaches to prevent breast cancer progression.

## 4.6 Figures

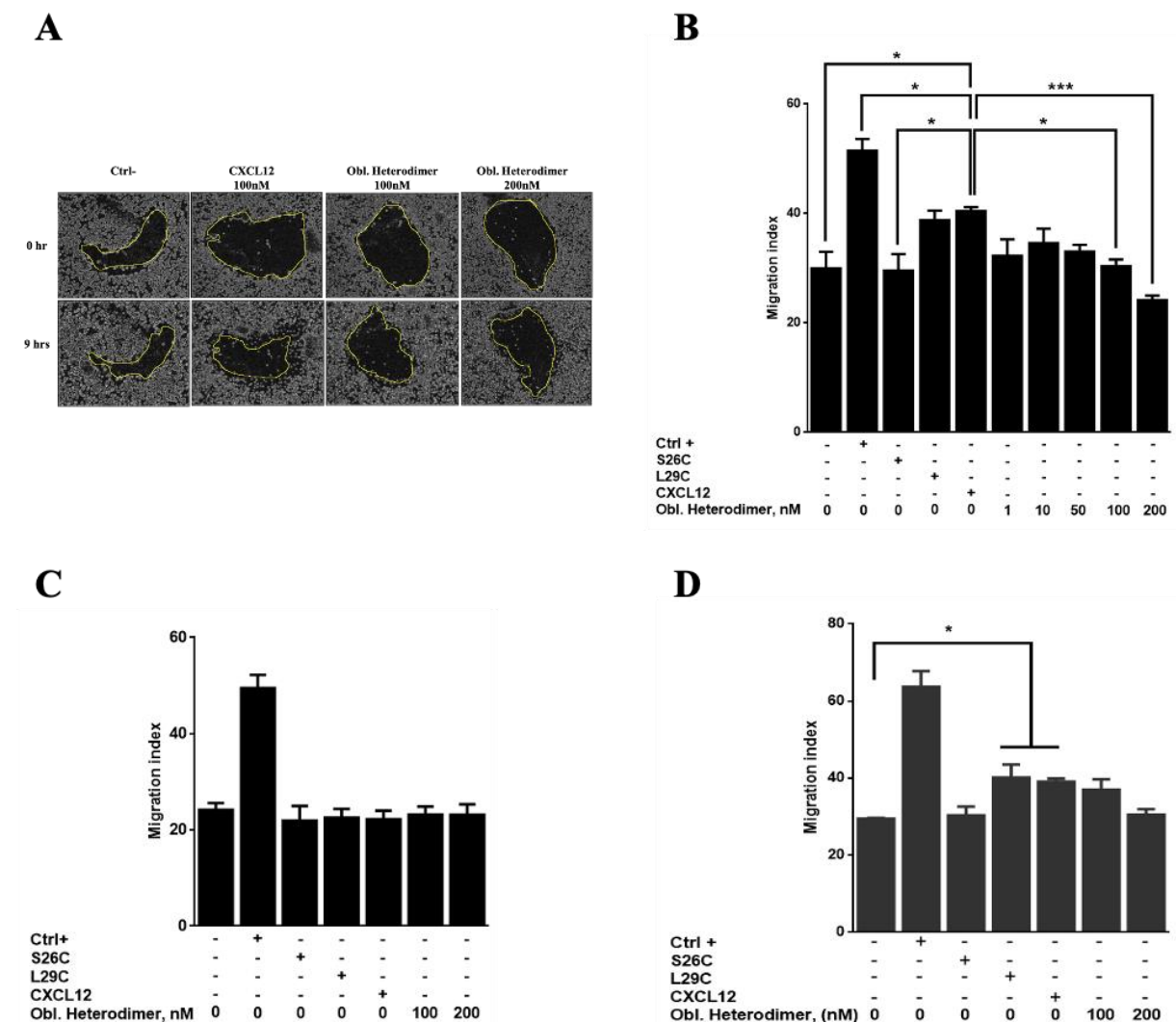


**Figure 4.1: MDA-MB 231 breast cancer cell migration following chemokine treatments including the obligate CXCL4-CXCL12 heterodimers.** (A) Representative microphotographs of the migration of MDA-MB 231 cells pre- (0h; top) and post-treatments (9hrs, bottom) without or with the obligate CXCL4-CXCL12 heterodimers. Briefly, cells stained with the vital dye Hoechst were starved in serum-free media for 6hrs. Cell monolayer wounds were made prior to chemokine treatments. Microphotographs (all microphotographs were taken under the same conditions and at the same magnification) of the wound were taken at time 0 (right after chemokine treatment) and after a 9-hour incubation. (B) High concentration of obligate CXCL4-CXCL12 heterodimers (100 and 200nM) led to a significantly lower migration of MDA-MB 231cancer cells ( $p > 0.05$ ). Migration of cells in the presence of 20nM CXCR4 inhibitor (C) and 5nM CXCR3 inhibitor (D). Migration indexes ( $X\% - \text{neg}/(\text{pos}-\text{neg})$ , where X is the percentage of migration) were calculated to determine the closure of the scratch area achieved after 9 hours of treatment. Data were presented as mean  $\pm$  SEM ( $N \geq 3$ ); ns = not significant,  $*p < 0.05$ ;  $**p < 0.01$ .

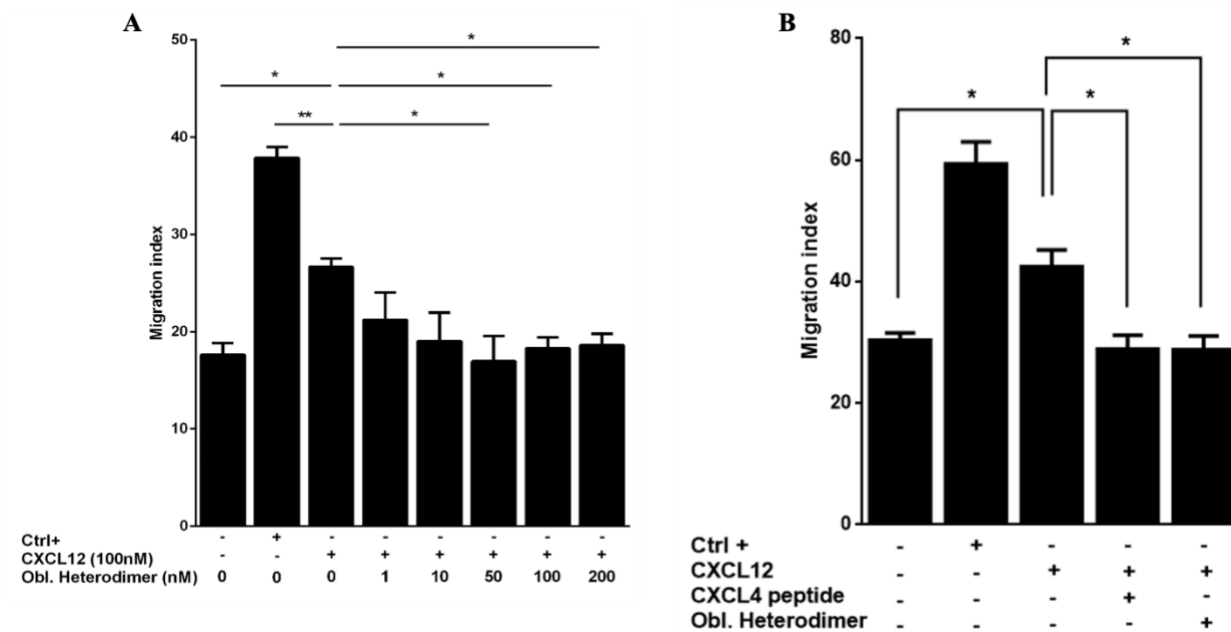


**Figure 4.2: Obligate CXCL4-CXCL12 heterodimers competitively inhibit CXCL12-driven migration in MDA-MB 231 cells.** (A) Tumor cells treated with combinations of the wildtype CXCL12 (100nM) and obligate CXCL4-CXCL12 heterodimers (0-200nM). (B) Both obligate CXCL4-CXCL12 heterodimers (50nM) and the CXCL4-derived peptide (50nM) effectively inhibited migration when combined with 50nM of the wildtype CXCL12. The migration was measured between time 0 hour and 9 hours post-treatment. Data are presented as mean  $\pm$  SEM from three independent experiments. \*\* $p < 0.01$ , \* $p < 0.05$  as analyzed by one-way ANOVA followed by Dunnet's multiple comparisons test.

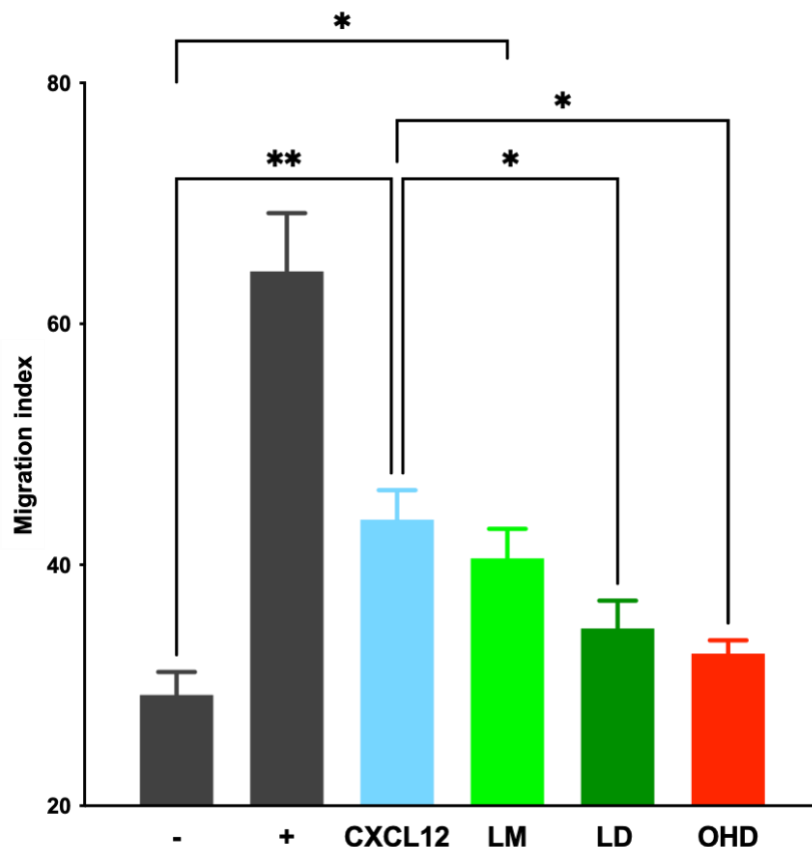


**Figure 4.3: Contrasting with wildtype CXCL12 and obligate CXCL12 monomers, obligate CXCL12 homodimer and CXCL4-CXCL12 heterodimer did not promote MDA-MB 231 cell migration.** Wound healing of MDA-MB 231 cells *in vitro* was significantly improved following incubation with both the wildtype CXCL12 (100nM, blue) and obligate CXCL12 monomers (LM, 100nM, light green) [81] although not as markedly as in the presence of 10% FBS (+, black) compared to the media only (-, black). In contrast, neither obligate CXCL12 homodimers (LD, 100nM, dark green) [81] nor the CXCL4-CXCL12 chemokine obligate heterodimers (OHD, 100nM, red) induced the migration of MDA-MB 231 cells. Of note, high dose (i.e., 1000nM) of wildtype CXCL12 had no effect on MDA-MB 231 cell migration (data not shown). Data are presented as mean  $\pm$  SEM, N=3 in triplicate. ns = not significant; \*p<0.05, \*\*p<0.01.

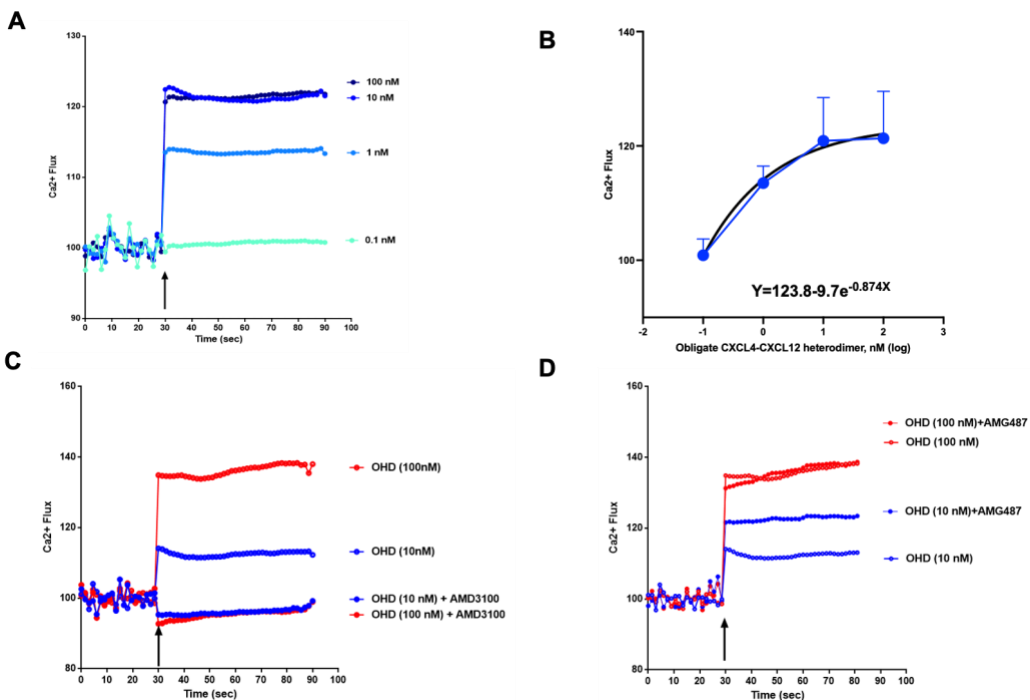


**Figure 4.4: Obligate CXCL4-CXCL12 heterodimers induced dose-dependent calcium flux through CXCR4 receptors in MDA-MB 231 breast cancer cells.** (A-B) Incubation with increasing concentrations of the obligate CXCL4-CXCL12 heterodimers (OHD) induced an increased release of intracellular calcium ( $Ca^{2+}$  flux) that reached a plateau above 10nM. (B) Calcium flux following incubation with increasing obligate CXCL4-CXCL12 heterodimer (OHD) concentrations followed an exponential plateau response. Model curve (black) and equation are provided. (C) Pre-incubation of MDA-MB-231 cells with the CXCR4 antagonist AMD3100 (20nM) fully inhibited the obligate CXCL4-CXCL12 heterodimers (OHD, 10 or 100nM) calcium mobilization. (D) In contrast, pre-incubation of MDA-MB-231 cells with the CXCR3 antagonist AMG487 (5nM) had no effect on the obligate CXCL4-CXCL12 heterodimers (OHD, 10 or 100nM) calcium mobilization. Calcium flux ( $Ca^{2+}$  flux) was measured as the ratio of fluorescent signal at 340/510nm and 380/510nm determined in every 1.5s for 60s. Values were normalized to the baseline (background fluorescence was measured for 30s prior to the obligate CXCL4-CXCL12 heterodimer injection). Data (mean  $\pm$  SEM) are presented as the percentage compared to the negative control from  $N \geq 3$  independent experiments performed in duplicate.

## CHAPTER 5: SUMMARY, DISCUSSION AND FUTURE DIRECTIONS

### 5.1 Summary

According to the Cancer Global Statistics 2020, breast cancer is the most common type of cancer in women and the 5<sup>th</sup> leading cause of cancer-related death worldwide [218]. For patients diagnosed with the metastatic breast cancer (about 6-10%) [219], the five-year survival rate is only 26% [220]. Breast cancer metastasis is characterized by the spread of tumor cells to distant organs. Despite advancements in early cancer detection and treatments, metastatic breast cancer is still an incurable disease. Current treatment options extend the lives of metastatic breast cancer patients by delaying the disease progression [221]. Thus, new treatment approaches are needed to fight metastatic breast cancer.

Chemokines are essential mediators of the metastasis of breast cancer cells. Chemokines support cancer metastasis by directing the migration of tumor cells to specific organs [222]. Tumor cells express specific chemokine receptors, and the overexpression of certain chemokine receptors is an indicator for cancer aggressiveness and poor clinical outcomes [223]. Through receptor activation, chemokines can induce diverse downstream signaling cascades leading to cell migration [103]. The emergence of chemokine signaling as a significant factor of cancer metastasis supports the need for a new treatment approach to prevent breast cancer metastasis.

In particular, the CXCL12/CXCR4 signaling axis has been associated with the breast cancer progression. Breast tumor cells overexpressing CXCR4 preferentially metastasize to distant organs associated with high secretion of the ligand CXCL12, such as bone marrows, lungs, liver, and brain [97, 128]. In patients with triple negative breast cancer, overexpression of CXCR4 is significantly associated with distant metastasis and poor prognosis [137, 224]. Due to its detrimental role in facilitating breast cancer progression, CXCL12/CXCR4 signaling axis has

emerged as a potential therapeutic target to prevent tumor metastasis. [154, 209]. While several strategies aiming to block CXCR4 yielded promising results, the clinical efficacy of using CXCR4 antagonists is limited and is shown to depend on the breast cancer subtype. Two CXCR4 antagonists, i.e., AMD3100 and TN14003, were shown to have therapeutic potential against tumor growth and metastasis in HER2 but failed to impact on the survival of triple-negative breast cancer patients [225]. Thus, further studies for alternative approaches will benefit patients suffering from this devastating disease.

Targeting CXCL12 via chemokine heterophilic interactions is a novel strategy. The advantage of this strategy over the conventional receptor blockage is that it does not block the entire CXCR4 signaling pathways associated with the normal immune cell trafficking. CXCL12 was found to heterodimerize with other CXC- and CC- chemokines [15, 21, 22, 87]. Furthermore, CXCL12 heterodimerization exhibited synergy in the attraction of T cells, monocytes, and malignant B cells [15, 87]. Our knowledge of how chemokine heterodimerization contribute to breast cancer migration – a key step in cancer metastasis, remains limited. Thus, the aim of this dissertation was to assess the role of CXCL12-CXCL4 chemokine heterodimerization in modulating breast cancer cell migration.

Chapter 2 investigates the biological effect of chemokine CXCL4-CXCL12 heterodimerization in CXCL12-driven migration in MDA-MB-231 human breast cancer cells. Overall, CXCL12 is mainly produced by stromal fibroblasts in the breast microenvironment [42, 226], whereas CXCL4 is largely released from activated platelets at high micromolar concentrations [227, 228]. Their co-localization at high local concentrations supports the formation of CXCL4-CXCL12 hetero-complexes [22]. This study demonstrated that CXCL4-CXCL12 heterodimerization could prevent cancer migration mediated by CXCL12-CXCR4

signaling (Figure 2.2 A). Furthermore, by NMR analyses, a putative region of CXCL4 interacting with CXCL12 was identified. A CXCL4-derived peptide mimicking the binding sequence with CXCL12 was designed and further determined to inhibit breast cancer migration. Indeed, a few chemokine-derived peptides mimicking heterophilic interactions have been shown to possess beneficial effects *in vivo* [15, 18, 229, 230]. Future studies will determine the therapeutic potential of the peptide *in vivo*.

The coexistence of different species in the chemokine mixture hinders a direct assessment of heterodimers. Chapter 3 details a disulfide-trapping strategy and generation of an obligate CXCL4-CXCL12 heterodimers. The disulfide-trapped heterodimers may serve as a novel tool for researchers in the chemokine field to unambiguously investigate the biological relevance and signaling associated with chemokine heterophilic interactions. Since  $\text{Ca}^{2+}$  plays a crucial role in G protein coupled receptor signaling, calcium mobilization was assessed to determine whether the obligate CXCL4-CXCL12 heterodimers bind and activate the G-coupled protein receptor CXCR4. Our findings revealed that the obligate CXCL4-CXCL12 heterodimers induced spikes in  $\text{Ca}^{2+}$  intracellular concentrations via CXCR4 receptor activation. However, the obligate CXCL4-CXCL12 heterodimers failed to induce MDA-MB 231 breast cancer cell migration, suggesting the obligate CXCL4-CXCL12 heterodimers bind to CXCR4 but trigger a distinct activation that does not lead to cell migration. Critically, the obligate CXCL4-CXCL12 heterodimers competitively and dose-dependently antagonize CXCL12 binding to CXCR4; thereby, preventing a critical step in tumor progression: cancer cell migration. *In vivo* investigations using pre-clinical immunocompetent breast cancer models are required to validate the therapeutic potential of obligate CXCL4-CXCL12 heterodimers to prevent breast cancer progression.

In summary, we have identified a new cancer-related activity of CXCL4-CXCL12 chemokine heterodimers. Findings from this research warrants future studies especially regarding the development of anti-cancer drugs targeting CXCL12-CXCR4 signaling pathway. Especially, the use of the obligate CXCL4-CXCL12 heterodimers and designing inhibitory peptide that mimic the interactions of heterodimers may be a promising therapeutic approach to block the CXCL12-CXCR4 axis and prevent breast cancer progression.

## 5.2 Discussion

Despite of the dramatic progress in identifying chemokine heterophilic interactions over the past decade [15, 21-23], our understanding of their roles in cancer biology remains limited. Indeed, the biological relevance of chemokine heterodimers has been mainly investigated in inflammatory conditions [15, 18, 229, 230] and the presence of physical interactions with GAGs [23, 90]. Currently, only the effects of the chemokine CXCL9-CXCL12 hetero-complex in tumor has been reported [87]. Actually, among more than 200 chemokine heterophilic interactions identified, none of them has been investigated in breast cancer. Our study reported for the first time that the heterophilic interactions of CXCL4 and CXCL12 could prevent breast cancer cell migration [138]. Findings from our investigations not only advance the current understanding of chemokine heterodimers but also lay the groundwork for the future development of effective therapies targeting chemokine heterophilic interactions in breast cancer.

Our study, along with others [231-235], provide evidence that CXCL12-targeted approach could benefit metastatic breast cancer patients. In Chapter 2, using NMR methodology, we identified the putative binding interface with CXCL12; and functionally determined that a CXCL4-derived peptide led to cancer cell migration inhibition. A major advantage of NMR over other molecular techniques is that NMR can characterize intermolecular interactions at atomic

level, providing insightful structure information for the development of therapeutic drugs [236]. Several targeting CXCL12 peptides have been successfully discovered from the structure-guided information and experimentally validated both in *in vitro* and *in vivo* [232, 237-239]. For example, specific CXCL12-derived peptides were effective in blocking CXCL12-dependent migration via competitive interactions with CXCR4 [231], or *in vivo* reduced tumor size and distant metastasis when combined with other therapies [235]. Moreover, the concept of using peptides mimicking the chemokine heterophilic interactions have been also validated and shown to be beneficial in *in vivo* studies [15, 18, 229, 230]. Thus, our findings of the CXCL4-derived peptide targeting the CXCL4-CXCL12 binding site along with the functional assessments in breast cancer migration support the development of new chemokine inhibitors targeting CXCL4-CXCL12 interface for the use in breast cancer treatments alone or in combination with other therapies.

We also generated an obligate CXCL4-CXCL12 heterodimer to unambiguously assess its functional roles of in signaling and breast cancer migration. Functional assessments of chemokine heterodimers in biological assays are difficult because of the concomitant presence of multiple chemokine oligomeric species at equilibria [25-28]. Consequently, mixture of different oligomeric species results in mixed biological responses. Growing evidence shows that different oligomeric variants of a given chemokine differentially interact with GAGs and receptors, leading to distinct cellular signaling and biological functions [30, 81, 83, 240]. Moreover, multiple chemokines are abundantly and concomitantly expressed in *in vivo* normal tissues [241] or the tumor microenvironment [242], supporting the formation heterodimers and a critical need to develop an approach to determine chemokine heterodimer activity in the *in vivo* condition. Thus, we generated CXCL4-CXCL12 obligate heterodimer to avoid the competition of different

species in equilibria. This strategy has been successfully applied to other pairs of chemokine heterodimers, i.e., CCL5-CXCL4 [15], CCL5-CCL17 [15], or CXCL1-CXCL7 [23], and yielded insightful information regarding the functional activity of heterodimers.

The role of the CXCL12-CXCR4 signaling in breast cancer migration has been demonstrated [97, 128, 143, 243]. Recently, obligate monomers and homodimers of CXCL12 were shown to differentially regulate the chemotaxis of colon carcinoma [81] and monocytic leukemia cells [59]. Whereas CXCL12 obligate monomers induced calcium mobilization, stimulated actin polymerization and cell migration, CXCL12 obligate dimers activated G-protein-dependent calcium flux but did not stimulate actin polymerization or cell migration [59, 81]. Chemokine CXCL4-CXCL12 heterodimers add another layer to this complexity in regulating cell response. Our investigations demonstrated that the CXCL4-CXCL12 obligate heterodimers significantly inhibited the migration in breast cancer cells. Importantly, the inhibitory effects of the CXCL4-CXCL12 obligate heterodimers were observed in the presence of CXCL12, suggesting the inhibition of CXCL12-CXCR4 activation and signaling by the CXCL4-CXCL12 obligate heterodimers. Our finding is consistent with the previous demonstration that CXCL4-CXCL12 heterophilic interactions synergistically inhibited T cell chemotaxis [15]. The heterodimerization-induced inhibitory effects could likely result from receptor oligomerization leading to (1) cross-inhibition of the ligand over the other binding partner in the heterodimeric complex [244, 245], or (2) activation of alternative signaling pathways leading to altered cellular behaviors [89, 246, 247]. Yet, the exact mechanisms by which the obligate CXCL4-CXCL12 heterodimers exhibit inhibitory effects from our study and the other remains to be investigated.

In summary, our investigations indicate that CXCL4-CXCL12 chemokine heterodimerization inhibits CXCL12-induced migration in breast cancer cells. Our findings obtained *in vitro* using a well-defined triple negative breast cancer cell line should be confirmed in *in vivo* breast cancer models to further evaluate the role of chemokine heterodimerization in cancer metastasis. Overall, our data provides a new understanding of chemokine heterophilic interactions in cancer migration and suggest a potential treatment strategy for breast cancer patients.

### 5.3 Future directions

First, receptor stoichiometry should be considered in addition to the complexity of signaling associated with chemokine heterodimerization. Whether the functional effects observed in CXCL4-CXCL12 heterodimers are mediated by receptor oligomerization remains unclear. Homo- or hetero-oligomerization of many chemokine receptors can influence the intracellular signaling, causing distinct cellular responses even with the same ligand [248]. Although the 1:1 binding model of chemokine and chemokine receptor suggests that monomeric CXCL12 is functionally active on monomeric CXCR4, the homodimer CXCL12 was found to interact with CXCR4 to produce differential signaling transductions [81], suggesting that the binding model of 2:1 chemokine:receptor may be relevant. It remains unclear whether dimeric CXCL12 interacts with monomeric or homodimeric CXCR4. Given that CXCR4 also presents as homodimers [214, 249], the model of 2:2 could be biologically relevant [248]. Together, if CXCL4-CXCL12 heterodimers interact with CXCR4, future investigations focusing on CXCR4 dimerization should be considered to explain the observed alternations in cellular responses. Given that CXCR3 and CXCR4 heterodimerized with one another [215], the concept of receptor hetero-oligomerization upon chemokine heterodimer stimulation should also be assessed.

Second, as suggested by our data, although CXCL4-CXCL12 heterodimers only act through CXCR4 receptors, whether the heterodimers can also promote receptor CXCR3-CXCR4 hetero-oligomerization should be clarified. Particularly, receptor heterodimerization could induce negative binding cooperativity in MDA-MB 231 cells that is the binding of CXCL12 to CXCR4 allosterically inhibits the CXCL4-CXCR3 interaction. Notably, the negative binding cooperativity as the consequence of receptor hetero-oligomerization has been reported for CCR2-CXCR4 [244] and CCR2-CCR5 [217] receptor heterodimers. Further investigations are

needed to validate the concept of receptor stoichiometry in response to CXCL4-CXCL12 chemokine heterodimerization.

Third, chemokine heterodimers could activate distinct signaling pathways; thus, future studies on the signaling transductions are needed to address the underlying mechanism for the inhibition of CXCL4-CXCL12 heterodimerization. Chemokine heterodimers induced differential signaling may be correlated with the receptor oligomerization as discussed above. The synergy induced by chemokine heterodimerization resulted from receptor oligomerization was previously reported with CCL5-CCL17, CCL5-CXCL4 chemokine heterodimers [15]. How CXCL4-CXCL12 chemokine heterodimers elicit signaling inhibition remains unclear.

Chemokine heterodimerization induces signaling bias resulting in a unique cellular response compared the wildtype chemokines. For example, compared to the monomeric chemokines, homodimeric CXCL12 and/or CXCL8 activated differential signaling transductions, i.e., changes in level of ERK1/2 phosphorylation and  $\beta$ -arrestin recruitment [81, 83]. Through receptor activation, the heterodimers could mediate  $\beta$ -arrestin signaling leading to receptor desensitization [250]. In addition to GCPR termination,  $\beta$ -arrestin also acts as a scaffold protein by forming complexes with other intracellular effector proteins in p38 MAPK pathways, leading to alternations in cellular chemotaxis [251]. Thus, future studies focusing on the G-protein and  $\beta$ -arrestin mediated pathways may further explain the observed inhibitory effects by CXCL4-CXCL12 heterodimers.

Lastly, whether the chemokine heterodimers and/or CXCL4-derived peptide prevent breast cancer progression in *in vivo* pre-clinical models should also be considered. The concept of using chemokine-derived peptides that specifically target chemokine heterophilic interactions has been experimentally validated *in vivo* and yielded promising therapeutic benefits. So far, this

peptide-based strategy has been derived from CCL5 heterodimerization with other chemokine CXCL4 [18, 229, 230], CCL17 [15], or CXCL12 [15]. Indeed, two CCL5-derived peptides CKEY and MKEK disrupted the pro-inflammatory CCL5-CXCL4 heterodimer *in vivo* atherosclerosis [18], stroke-induced brain injury [230], and abdominal aortic aneurysm [229]. Additionally, the CCL5-derived peptide VREY mimicked the inhibitory effects of CCL5 on CXCL12-driven platelet aggregation in human blood [15]. These data support a novel paradigm of using peptides derived from the chemokine heterodimerization in breast cancer progression.

## REFERENCES

1. Veldkamp, C.T., et al., *Monomeric structure of the cardioprotective chemokine SDF-1/CXCL12*. *Protein Sci*, 2009. **18**(7): p. 1359-69.
2. Clore, G.M., et al., *Three-dimensional structure of interleukin 8 in solution*. *Biochemistry*, 1990. **29**(7): p. 1689-96.
3. Handel, T.M. and P.J. Domaille, *Heteronuclear (1H, 13C, 15N) NMR assignments and solution structure of the monocyte chemoattractant protein-1 (MCP-1) dimer*. *Biochemistry*, 1996. **35**(21): p. 6569-84.
4. Zhang, X., et al., *Crystal structure of recombinant human platelet factor 4*. *Biochemistry*, 1994. **33**(27): p. 8361-6.
5. Hembruff, S.L. and N. Cheng, *Chemokine signaling in cancer: Implications on the tumor microenvironment and therapeutic targeting*. *Cancer Ther*, 2009. **7**(A): p. 254-267.
6. Vindrieux, D., P. Escobar, and G. Lazennec, *Emerging roles of chemokines in prostate cancer*. *Endocr Relat Cancer*, 2009. **16**(3): p. 663-73.
7. Rossi, D. and A. Zlotnik, *The biology of chemokines and their receptors*. *Annu Rev Immunol*, 2000. **18**: p. 217-42.
8. Zlotnik, A. and O. Yoshie, *The chemokine superfamily revisited*. *Immunity*, 2012. **36**(5): p. 705-16.
9. Lazennec, G. and A. Richmond, *Chemokines and chemokine receptors: new insights into cancer-related inflammation*. *Trends Mol Med*, 2010. **16**(3): p. 133-44.
10. de Munnik, S.M., et al., *Modulation of cellular signaling by herpesvirus-encoded G protein-coupled receptors*. *Front Pharmacol*, 2015. **6**: p. 40.
11. Clore, G.M. and A.M. Gronenborn, *Three-dimensional structures of alpha and beta chemokines*. *Faseb j*, 1995. **9**(1): p. 57-62.
12. Miller, M.C. and K.H. Mayo, *Chemokines from a Structural Perspective*. *Int J Mol Sci*, 2017. **18**(10).
13. Mayo, K.H., et al., *NMR solution structure of the 32-kDa platelet factor 4 ELR-motif N-terminal chimera: a symmetric tetramer*. *Biochemistry*, 1995. **34**(36): p. 11399-409.
14. Clark-Lewis, I., et al., *Structure-activity relationships of chemokines*. *J Leukoc Biol*, 1995. **57**(5): p. 703-11.
15. von Hundelshausen, P., et al., *Chemokine interactome mapping enables tailored intervention in acute and chronic inflammation*. *Sci Transl Med*, 2017. **9**(384).
16. von Hundelshausen, P., et al., *Heterophilic interactions of platelet factor 4 and RANTES promote monocyte arrest on endothelium*. *Blood*, 2005. **105**(3): p. 924-30.
17. Dudek, A.Z., et al., *Platelet factor 4 promotes adhesion of hematopoietic progenitor cells and binds IL-8: novel mechanisms for modulation of hematopoiesis*. *Blood*, 2003. **101**(12): p. 4687-94.
18. Koenen, R.R., et al., *Disrupting functional interactions between platelet chemokines inhibits atherosclerosis in hyperlipidemic mice*. *Nat Med*, 2009. **15**(1): p. 97-103.
19. Nesmelova, I.V., et al., *Platelet factor 4 and interleukin-8 CXC chemokine heterodimer formation modulates function at the quaternary structural level*. *J Biol Chem*, 2005. **280**(6): p. 4948-58.

20. Paoletti, S., et al., *A rich chemokine environment strongly enhances leukocyte migration and activities*. Blood, 2005. **105**(9): p. 3405-12.
21. Nesmelova, I.V., et al., *CXC and CC chemokines form mixed heterodimers: association free energies from molecular dynamics simulations and experimental correlations*. J Biol Chem, 2008. **283**(35): p. 24155-66.
22. Carlson, J., et al., *The heterodimerization of platelet-derived chemokines*. Biochim Biophys Acta, 2013. **1834**(1): p. 158-68.
23. Brown, A.J., et al., *Chemokine CXCL7 Heterodimers: Structural Insights, CXCR2 Receptor Function, and Glycosaminoglycan Interactions*. Int J Mol Sci, 2017. **18**(4).
24. Yang, Y., et al., *Subunit association and structural analysis of platelet basic protein and related proteins investigated by 1H NMR spectroscopy and circular dichroism*. J Biol Chem, 1994. **269**(31): p. 20110-8.
25. Wang, X., et al., *Oligomeric structure of the chemokine CCL5/RANTES from NMR, MS, and SAXS data*. Structure, 2011. **19**(8): p. 1138-48.
26. Jansma, A.L., et al., *NMR analysis of the structure, dynamics, and unique oligomerization properties of the chemokine CCL27*. J Biol Chem, 2010. **285**(19): p. 14424-37.
27. Veldkamp, C.T., et al., *The monomer-dimer equilibrium of stromal cell-derived factor-1 (CXCL 12) is altered by pH, phosphate, sulfate, and heparin*. Protein Sci, 2005. **14**(4): p. 1071-81.
28. Chen, M.J. and K.H. Mayo, *Human platelet factor 4 subunit association/dissociation thermodynamics and kinetics*. Biochemistry, 1991. **30**(26): p. 6402-11.
29. Herring, C.A., et al., *Dynamics and thermodynamic properties of CXCL7 chemokine*. Proteins, 2015. **83**(11): p. 1987-2007.
30. Brown, A.J., et al., *Platelet-Derived Chemokine CXCL7 Dimer Preferentially Exists in the Glycosaminoglycan-Bound Form: Implications for Neutrophil-Platelet Crosstalk*. Front Immunol, 2017. **8**: p. 1248.
31. Zlotnik, A., A.M. Burkhardt, and B. Homey, *Homeostatic chemokine receptors and organ-specific metastasis*. Nat Rev Immunol, 2011. **11**(9): p. 597-606.
32. Bonocchi, R., et al., *Chemokines and chemokine receptors: an overview*. Front Biosci (Landmark Ed), 2009. **14**: p. 540-51.
33. Li, A., et al., *IL-8 directly enhanced endothelial cell survival, proliferation, and matrix metalloproteinases production and regulated angiogenesis*. J Immunol, 2003. **170**(6): p. 3369-76.
34. Varney, M.L., S.L. Johansson, and R.K. Singh, *Distinct expression of CXCL8 and its receptors CXCR1 and CXCR2 and their association with vessel density and aggressiveness in malignant melanoma*. Am J Clin Pathol, 2006. **125**(2): p. 209-16.
35. Mestas, J., et al., *The role of CXCR2/CXCR2 ligand biological axis in renal cell carcinoma*. J Immunol, 2005. **175**(8): p. 5351-7.
36. Wenthe, M.N., et al., *Blockade of the chemokine receptor CXCR2 inhibits pancreatic cancer cell-induced angiogenesis*. Cancer Lett, 2006. **241**(2): p. 221-7.
37. Gijssbers, K., et al., *GCP-2/CXCL6 synergizes with other endothelial cell-derived chemokines in neutrophil mobilization and is associated with angiogenesis in gastrointestinal tumors*. Exp Cell Res, 2005. **303**(2): p. 331-42.

38. Singh, J.K., et al., *Targeting CXCR1/2 significantly reduces breast cancer stem cell activity and increases the efficacy of inhibiting HER2 via HER2-dependent and -independent mechanisms*. Clin Cancer Res, 2013. **19**(3): p. 643-56.
39. Wang, R.X., et al., *Value of CXCL8-CXCR1/2 axis in neoadjuvant chemotherapy for triple-negative breast cancer patients: a retrospective pilot study*. Breast Cancer Res Treat, 2020. **181**(3): p. 561-570.
40. Kiefer, F. and A.F. Siekmann, *The role of chemokines and their receptors in angiogenesis*. Cell Mol Life Sci, 2011. **68**(17): p. 2811-30.
41. Lasagni, L., et al., *An alternatively spliced variant of CXCR3 mediates the inhibition of endothelial cell growth induced by IP-10, Mig, and I-TAC, and acts as functional receptor for platelet factor 4*. J Exp Med, 2003. **197**(11): p. 1537-49.
42. Orimo, A., et al., *Stromal fibroblasts present in invasive human breast carcinomas promote tumor growth and angiogenesis through elevated SDF-1/CXCL12 secretion*. Cell, 2005. **121**(3): p. 335-48.
43. Guleng, B., et al., *Blockade of the stromal cell-derived factor-1/CXCR4 axis attenuates in vivo tumor growth by inhibiting angiogenesis in a vascular endothelial growth factor-independent manner*. Cancer Res, 2005. **65**(13): p. 5864-71.
44. Cui, K., et al., *The CXCR4-CXCL12 pathway facilitates the progression of pancreatic cancer via induction of angiogenesis and lymphangiogenesis*. J Surg Res, 2011. **171**(1): p. 143-50.
45. Kryczek, I., et al., *CXCL12 and vascular endothelial growth factor synergistically induce neoangiogenesis in human ovarian cancers*. Cancer Res, 2005. **65**(2): p. 465-72.
46. Wang, Z. and H. Huang, *Platelet factor-4 (CXCL4/PF-4): an angiostatic chemokine for cancer therapy*. Cancer Lett, 2013. **331**(2): p. 147-53.
47. Van Raemdonck, K., et al., *Angiostatic, tumor inflammatory and anti-tumor effects of CXCL4(47-70) and CXCL4L1(47-70) in an EGF-dependent breast cancer model*. Oncotarget, 2014. **5**(21): p. 10916-33.
48. Petrai, I., et al., *Activation of p38(MAPK) mediates the angiostatic effect of the chemokine receptor CXCR3-B*. Int J Biochem Cell Biol, 2008. **40**(9): p. 1764-74.
49. Billottet, C., C. Quemener, and A. Bikfalvi, *CXCR3, a double-edged sword in tumor progression and angiogenesis*. Biochim Biophys Acta, 2013. **1836**(2): p. 287-95.
50. Baghban, R., et al., *Tumor microenvironment complexity and therapeutic implications at a glance*. Cell Commun Signal, 2020. **18**(1): p. 59.
51. Jin, M.Z. and W.L. Jin, *The updated landscape of tumor microenvironment and drug repurposing*. Signal Transduct Target Ther, 2020. **5**(1): p. 166.
52. Vilgelm, A.E. and A. Richmond, *Chemokines Modulate Immune Surveillance in Tumorigenesis, Metastasis, and Response to Immunotherapy*. Front Immunol, 2019. **10**: p. 333.
53. D'Agostino, G., V. Cecchinato, and M. Ugucioni, *Chemokine Heterocomplexes and Cancer: A Novel Chapter to Be Written in Tumor Immunity*. Front Immunol, 2018. **9**: p. 2185.
54. Chow, M.T. and A.D. Luster, *Chemokines in cancer*. Cancer Immunol Res, 2014. **2**(12): p. 1125-31.

55. Nagarsheth, N., M.S. Wicha, and W. Zou, *Chemokines in the cancer microenvironment and their relevance in cancer immunotherapy*. *Nat Rev Immunol*, 2017. **17**(9): p. 559-572.
56. Oliveira-Neto, H.H., et al., *The expression of chemokines CCL19, CCL21 and their receptor CCR7 in oral squamous cell carcinoma and its relevance to cervical lymph node metastasis*. *Tumour Biol*, 2013. **34**(1): p. 65-70.
57. Amersi, F.F., et al., *Activation of CCR9/CCL25 in cutaneous melanoma mediates preferential metastasis to the small intestine*. *Clin Cancer Res*, 2008. **14**(3): p. 638-45.
58. Letsch, A., et al., *Functional CCR9 expression is associated with small intestinal metastasis*. *J Invest Dermatol*, 2004. **122**(3): p. 685-90.
59. Veldkamp, C.T., et al., *Structural basis of CXCR4 sulfotyrosine recognition by the chemokine SDF-1/CXCL12*. *Sci Signal*, 2008. **1**(37): p. ra4.
60. Zielińska, K.A. and V.L. Katanaev, *The Signaling Duo CXCL12 and CXCR4: Chemokine Fuel for Breast Cancer Tumorigenesis*. *Cancers (Basel)*, 2020. **12**(10).
61. Okuyama Kishima, M., et al., *Immunohistochemical expression of CXCR4 on breast cancer and its clinical significance*. *Anal Cell Pathol (Amst)*, 2015. **2015**: p. 891020.
62. Thelen, M., *Dancing to the tune of chemokines*. *Nat Immunol*, 2001. **2**(2): p. 129-34.
63. DeWire, S.M., et al., *Beta-arrestins and cell signaling*. *Annu Rev Physiol*, 2007. **69**: p. 483-510.
64. Hughes, C.E. and R.J.B. Nibbs, *A guide to chemokines and their receptors*. *Febs j*, 2018. **285**(16): p. 2944-2971.
65. Sun, X., et al., *CXCL12 / CXCR4 / CXCR7 chemokine axis and cancer progression*. *Cancer Metastasis Rev*, 2010. **29**(4): p. 709-22.
66. Proudfoot, A.E., *Chemokine receptors: multifaceted therapeutic targets*. *Nat Rev Immunol*, 2002. **2**(2): p. 106-15.
67. Teicher, B.A. and S.P. Fricker, *CXCL12 (SDF-1)/CXCR4 pathway in cancer*. *Clin Cancer Res*, 2010. **16**(11): p. 2927-31.
68. Richmond, A., *Nf-kappa B, chemokine gene transcription and tumour growth*. *Nat Rev Immunol*, 2002. **2**(9): p. 664-74.
69. Troeger, A., et al., *RhoH is critical for cell-microenvironment interactions in chronic lymphocytic leukemia in mice and humans*. *Blood*, 2012. **119**(20): p. 4708-18.
70. Dixit, N. and S.I. Simon, *Chemokines, selectins and intracellular calcium flux: temporal and spatial cues for leukocyte arrest*. *Front Immunol*, 2012. **3**: p. 188.
71. Smith, J.S., et al., *C-X-C Motif Chemokine Receptor 3 Splice Variants Differentially Activate Beta-Arrestins to Regulate Downstream Signaling Pathways*. *Mol Pharmacol*, 2017. **92**(2): p. 136-150.
72. Freitas, C., et al., *The relevance of the chemokine receptor ACKR3/CXCR7 on CXCL12-mediated effects in cancers with a focus on virus-related cancers*. *Cytokine Growth Factor Rev*, 2014. **25**(3): p. 307-16.
73. McDonald, P.H., et al., *Beta-arrestin 2: a receptor-regulated MAPK scaffold for the activation of JNK3*. *Science*, 2000. **290**(5496): p. 1574-7.
74. Gong, K., et al., *A novel protein kinase A-independent, beta-arrestin-1-dependent signaling pathway for p38 mitogen-activated protein kinase activation by beta2-adrenergic receptors*. *J Biol Chem*, 2008. **283**(43): p. 29028-36.

75. Kumar, R., et al., *CXCR7 mediated G $\alpha$  independent activation of ERK and Akt promotes cell survival and chemotaxis in T cells*. Cell Immunol, 2012. **272**(2): p. 230-41.
76. Proudfoot, A.E., et al., *Glycosaminoglycan binding and oligomerization are essential for the in vivo activity of certain chemokines*. Proc Natl Acad Sci U S A, 2003. **100**(4): p. 1885-90.
77. Roscic-Mrkic, B., et al., *RANTES (CCL5) uses the proteoglycan CD44 as an auxiliary receptor to mediate cellular activation signals and HIV-1 enhancement*. Blood, 2003. **102**(4): p. 1169-77.
78. Handel, T.M., et al., *Regulation of protein function by glycosaminoglycans--as exemplified by chemokines*. Annu Rev Biochem, 2005. **74**: p. 385-410.
79. Wang, L., et al., *Endothelial heparan sulfate deficiency impairs L-selectin- and chemokine-mediated neutrophil trafficking during inflammatory responses*. Nat Immunol, 2005. **6**(9): p. 902-10.
80. Sadir, R., et al., *Characterization of the stromal cell-derived factor-1 $\alpha$ -heparin complex*. J Biol Chem, 2001. **276**(11): p. 8288-96.
81. Drury, L.J., et al., *Monomeric and dimeric CXCL12 inhibit metastasis through distinct CXCR4 interactions and signaling pathways*. Proc Natl Acad Sci U S A, 2011. **108**(43): p. 17655-60.
82. Takekoshi, T., et al., *A locked, dimeric CXCL12 variant effectively inhibits pulmonary metastasis of CXCR4-expressing melanoma cells due to enhanced serum stability*. Mol Cancer Ther, 2012. **11**(11): p. 2516-25.
83. Nasser, M.W., et al., *Differential activation and regulation of CXCR1 and CXCR2 by CXCL8 monomer and dimer*. J Immunol, 2009. **183**(5): p. 3425-32.
84. Campanella, G.S., et al., *Oligomerization of CXCL10 is necessary for endothelial cell presentation and in vivo activity*. J Immunol, 2006. **177**(10): p. 6991-8.
85. Das, S.T., et al., *Monomeric and dimeric CXCL8 are both essential for in vivo neutrophil recruitment*. PLoS One, 2010. **5**(7): p. e11754.
86. Nesmelova IV, S.Y., Gao J, Mayo KH, *Energy profile of CXC and CC chemokines quaternary structure from molecular dynamics simulations: chemokine can form heterodimers*. J. Biol. Chem., 2008. **283**(35): p. 24155-66.
87. Venetz, D., et al., *Perivascular expression of CXCL9 and CXCL12 in primary central nervous system lymphoma: T-cell infiltration and positioning of malignant B cells*. Int J Cancer, 2010. **127**(10): p. 2300-12.
88. Sebastiani, S., et al., *CCL22-induced responses are powerfully enhanced by synergy inducing chemokines via CCR4: evidence for the involvement of first beta-strand of chemokine*. Eur J Immunol, 2005. **35**(3): p. 746-56.
89. Mellado, M., et al., *Chemokine receptor homo- or heterodimerization activates distinct signaling pathways*. Embo j, 2001. **20**(10): p. 2497-507.
90. Crown, S.E., et al., *Heterodimerization of CCR2 chemokines and regulation by glycosaminoglycan binding*. J Biol Chem, 2006. **281**(35): p. 25438-46.
91. Guan, E., J. Wang, and M.A. Norcross, *Identification of human macrophage inflammatory proteins 1 $\alpha$  and 1 $\beta$  as a native secreted heterodimer*. J Biol Chem, 2001. **276**(15): p. 12404-9.

92. Zwijnenburg, P.J., et al., *CXC-chemokines KC and macrophage inflammatory protein-2 (MIP-2) synergistically induce leukocyte recruitment to the central nervous system in rats*. Immunol Lett, 2003. **85**(1): p. 1-4.
93. CDC. [Website].
94. Palacios-Arreola, M.I., et al., *The role of chemokines in breast cancer pathology and its possible use as therapeutic targets*. J Immunol Res, 2014. **2014**: p. 849720.
95. Liang, Z., et al., *Development of a unique small molecule modulator of CXCR4*. PLoS One, 2012. **7**(4): p. e34038.
96. Li, C.H., et al., *Current treatment landscape for patients with locally recurrent inoperable or metastatic triple-negative breast cancer: a systematic literature review*. Breast Cancer Res, 2019. **21**(1): p. 143.
97. Muller, A., et al., *Involvement of chemokine receptors in breast cancer metastasis*. Nature, 2001. **410**(6824): p. 50-6.
98. Kang, Y., et al., *A multigenic program mediating breast cancer metastasis to bone*. Cancer Cell, 2003. **3**(6): p. 537-49.
99. Agle, K.A., R.A. Vongsa, and M.B. Dwinell, *Calcium mobilization triggered by the chemokine CXCL12 regulates migration in wounded intestinal epithelial monolayers*. J Biol Chem, 2010. **285**(21): p. 16066-75.
100. Balkwill, F., *The significance of cancer cell expression of the chemokine receptor CXCR4*. Semin Cancer Biol, 2004. **14**(3): p. 171-9.
101. Darash-Yahana, M., et al., *Role of high expression levels of CXCR4 in tumor growth, vascularization, and metastasis*. Faseb j, 2004. **18**(11): p. 1240-2.
102. Vandercappellen, J., J. Van Damme, and S. Struyf, *The role of CXC chemokines and their receptors in cancer*. Cancer Lett, 2008. **267**(2): p. 226-44.
103. Zlotnik, A., *New insights on the role of CXCR4 in cancer metastasis*. J Pathol, 2008. **215**(3): p. 211-3.
104. Marchesi, F., et al., *Increased survival, proliferation, and migration in metastatic human pancreatic tumor cells expressing functional CXCR4*. Cancer Res, 2004. **64**(22): p. 8420-7.
105. Zhou, Y., et al., *CXCR4 is a major chemokine receptor on glioma cells and mediates their survival*. J Biol Chem, 2002. **277**(51): p. 49481-7.
106. Nishio, M., et al., *Nurselike cells express BAFF and APRIL, which can promote survival of chronic lymphocytic leukemia cells via a paracrine pathway distinct from that of SDF-1alpha*. Blood, 2005. **106**(3): p. 1012-20.
107. Smith, M.C., et al., *CXCR4 regulates growth of both primary and metastatic breast cancer*. Cancer Res, 2004. **64**(23): p. 8604-12.
108. Redjal, N., et al., *CXCR4 inhibition synergizes with cytotoxic chemotherapy in gliomas*. Clin Cancer Res, 2006. **12**(22): p. 6765-71.
109. Lee, C.H., et al., *Sensitization of B16 tumor cells with a CXCR4 antagonist increases the efficacy of immunotherapy for established lung metastases*. Mol Cancer Ther, 2006. **5**(10): p. 2592-9.
110. Maione, T.E., et al., *Inhibition of angiogenesis by recombinant human platelet factor-4 and related peptides*. Science, 1990. **247**(4938): p. 77-9.
111. Sharpe, R.J., et al., *Growth inhibition of murine melanoma and human colon carcinoma by recombinant human platelet factor 4*. J Natl Cancer Inst, 1990. **82**(10): p. 848-53.

112. Kolber, D.L., T.L. Knisely, and T.E. Maione, *Inhibition of development of murine melanoma lung metastases by systemic administration of recombinant platelet factor 4*. J Natl Cancer Inst, 1995. **87**(4): p. 304-9.
113. Perollet, C., et al., *Platelet factor 4 modulates fibroblast growth factor 2 (FGF-2) activity and inhibits FGF-2 dimerization*. Blood, 1998. **91**(9): p. 3289-99.
114. Gengrinovitch, S., et al., *Platelet factor-4 inhibits the mitogenic activity of VEGF121 and VEGF165 using several concurrent mechanisms*. J Biol Chem, 1995. **270**(25): p. 15059-65.
115. Javerzat, S., P. Auguste, and A. Bikfalvi, *The role of fibroblast growth factors in vascular development*. Trends Mol Med, 2002. **8**(10): p. 483-9.
116. Ehlert, J.E., et al., *Identification and partial characterization of a variant of human CXCR3 generated by posttranscriptional exon skipping*. J Immunol, 2004. **173**(10): p. 6234-40.
117. Ma, B., A. Khazali, and A. Wells, *CXCR3 in carcinoma progression*. Histol Histopathol, 2015. **30**(7): p. 781-92.
118. Reynders, N., et al., *The Distinct Roles of CXCR3 Variants and Their Ligands in the Tumor Microenvironment*. Cells, 2019. **8**(6).
119. Balan, M. and S. Pal, *A novel CXCR3-B chemokine receptor-induced growth-inhibitory signal in cancer cells is mediated through the regulation of Bach-1 protein and Nrf2 protein nuclear translocation*. J Biol Chem, 2014. **289**(6): p. 3126-37.
120. Datta, D., et al., *Ras-induced modulation of CXCL10 and its receptor splice variant CXCR3-B in MDA-MB-435 and MCF-7 cells: relevance for the development of human breast cancer*. Cancer Res, 2006. **66**(19): p. 9509-18.
121. Romagnani, P., et al., *CXCR3-mediated opposite effects of CXCL10 and CXCL4 on TH1 or TH2 cytokine production*. J Allergy Clin Immunol, 2005. **116**(6): p. 1372-9.
122. Kouroumalis, A., et al., *The chemokines CXCL9, CXCL10, and CXCL11 differentially stimulate G alpha i-independent signaling and actin responses in human intestinal myofibroblasts*. J Immunol, 2005. **175**(8): p. 5403-11.
123. Wu, Q., R. Dhir, and A. Wells, *Altered CXCR3 isoform expression regulates prostate cancer cell migration and invasion*. Mol Cancer, 2012. **11**: p. 3.
124. Ji, R., et al., *Human type II pneumocyte chemotactic responses to CXCR3 activation are mediated by splice variant A*. Am J Physiol Lung Cell Mol Physiol, 2008. **294**(6): p. L1187-96.
125. Datta, D., et al., *Calcineurin inhibitors modulate CXCR3 splice variant expression and mediate renal cancer progression*. J Am Soc Nephrol, 2008. **19**(12): p. 2437-46.
126. Datta, D., et al., *CXCR3-B can mediate growth-inhibitory signals in human renal cancer cells by down-regulating the expression of heme oxygenase-1*. J Biol Chem, 2010. **285**(47): p. 36842-8.
127. Gacci, M., et al., *CXCR3-B expression correlates with tumor necrosis extension in renal cell carcinoma*. J Urol, 2009. **181**(2): p. 843-8.
128. Boimel, P.J., et al., *Contribution of CXCL12 secretion to invasion of breast cancer cells*. Breast Cancer Res, 2012. **14**(1): p. R23.
129. Fridrichova, I., et al., *CXCL12 and ADAM23 hypermethylation are associated with advanced breast cancers*. Transl Res, 2015. **165**(6): p. 717-30.
130. Bouyssou, J.M., I.M. Ghobrial, and A.M. Roccaro, *Targeting SDF-1 in multiple myeloma tumor microenvironment*. Cancer Lett, 2016. **380**(1): p. 315-8.

131. Chinni, S.R., et al., *CXCL12/CXCR4 signaling activates Akt-1 and MMP-9 expression in prostate cancer cells: the role of bone microenvironment-associated CXCL12*. *Prostate*, 2006. **66**(1): p. 32-48.
132. Gros, S.J., et al., *CXCR4/SDF-1alpha-mediated chemotaxis in an in vivo model of metastatic esophageal carcinoma*. *In Vivo*, 2012. **26**(4): p. 711-8.
133. Meng, W., S. Xue, and Y. Chen, *The role of CXCL12 in tumor microenvironment*. *Gene*, 2018. **641**: p. 105-110.
134. Xu, Q., et al., *Stromal-derived factor-1alpha/CXCL12-CXCR4 chemotactic pathway promotes perineural invasion in pancreatic cancer*. *Oncotarget*, 2015. **6**(7): p. 4717-32.
135. Wu, P.F., et al., *Role of CXCL12/CXCR4 signaling axis in pancreatic cancer*. *Chin Med J (Engl)*, 2013. **126**(17): p. 3371-4.
136. Wang, J., R. Loberg, and R.S. Taichman, *The pivotal role of CXCL12 (SDF-1)/CXCR4 axis in bone metastasis*. *Cancer Metastasis Rev*, 2006. **25**(4): p. 573-87.
137. Yu, S., et al., *High level of CXCR4 in triple-negative breast cancer specimens associated with a poor clinical outcome*. *Acta Med Okayama*, 2013. **67**(6): p. 369-75.
138. Nguyen, K.T.P., et al., *CXCL12-CXCL4 heterodimerization prevents CXCL12-driven breast cancer cell migration*. *Cell Signal*, 2020. **66**: p. 109488.
139. Zhang, M., et al., *CCL7 recruits cDC1 to promote antitumor immunity and facilitate checkpoint immunotherapy to non-small cell lung cancer*. *Nat Commun*, 2020. **11**(1): p. 6119.
140. Ramos, C.D., et al., *MIP-1alpha[CCL3] acting on the CCR1 receptor mediates neutrophil migration in immune inflammation via sequential release of TNF-alpha and LTB4*. *J Leukoc Biol*, 2005. **78**(1): p. 167-77.
141. Ramakrishnan, R., et al., *CXCR4 Signaling Has a CXCL12-Independent Essential Role in Murine MLL-AF9-Driven Acute Myeloid Leukemia*. *Cell Rep*, 2020. **31**(8): p. 107684.
142. Weber, C. and R.R. Koenen, *Fine-tuning leukocyte responses: towards a chemokine 'interactome'*. *Trends Immunol*, 2006. **27**(6): p. 268-73.
143. Guembarovski, A.L., et al., *CXCL12 chemokine and CXCR4 receptor: association with susceptibility and prognostic markers in triple negative breast cancer*. *Mol Biol Rep*, 2018. **45**(5): p. 741-750.
144. Dayer, R., et al., *Upregulation of CXC chemokine receptor 4-CXC chemokine ligand 12 axis in invasive breast carcinoma: A potent biomarker predicting lymph node metastasis*. *J Cancer Res Ther*, 2018. **14**(2): p. 345-350.
145. Mukherjee, S., et al., *Non-migratory tumorigenic intrinsic cancer stem cells ensure breast cancer metastasis by generation of CXCR4(+) migrating cancer stem cells*. *Oncogene*, 2016. **35**(37): p. 4937-48.
146. Wu, W., et al., *Prognostic significance of CXCL12, CXCR4, and CXCR7 in patients with breast cancer*. *Int J Clin Exp Pathol*, 2015. **8**(10): p. 13217-24.
147. Jamaludin, S.Y.N., et al., *Assessment of CXC ligand 12-mediated calcium signalling and its regulators in basal-like breast cancer cells*. *Oncol Lett*, 2018. **15**(4): p. 4289-4295.
148. Sun, Y., et al., *CXCL12-CXCR4 axis promotes the natural selection of breast cancer cell metastasis*. *Tumour Biol*, 2014. **35**(8): p. 7765-73.

149. Norton, K.A., A.S. Popel, and N.B. Pandey, *Heterogeneity of chemokine cell-surface receptor expression in triple-negative breast cancer*. *Am J Cancer Res*, 2015. **5**(4): p. 1295-307.
150. Zhou, K.X., et al., *CXCR4 antagonist AMD3100 enhances the response of MDA-MB-231 triple-negative breast cancer cells to ionizing radiation*. *Cancer Lett*, 2018. **418**: p. 196-203.
151. Xu, C., et al., *CXCR4 in breast cancer: oncogenic role and therapeutic targeting*. *Drug Des Devel Ther*, 2015. **9**: p. 4953-64.
152. Chittasupho, C., P. Kewsuwan, and T. Murakami, *CXCR4-targeted Nanoparticles Reduce Cell Viability, Induce Apoptosis and Inhibit SDF-1 $\alpha$  Induced BT-549-Luc Cell Migration In Vitro*. *Curr Drug Deliv*, 2017. **14**(8): p. 1060-1070.
153. Gil, M., et al., *Targeting CXCL12/CXCR4 signaling with oncolytic virotherapy disrupts tumor vasculature and inhibits breast cancer metastases*. *Proc Natl Acad Sci U S A*, 2013. **110**(14): p. E1291-300.
154. Pusic, I. and J.F. DiPersio, *Update on clinical experience with AMD3100, an SDF-1/CXCL12-CXCR4 inhibitor, in mobilization of hematopoietic stem and progenitor cells*. *Curr Opin Hematol*, 2010. **17**(4): p. 319-26.
155. Ramsey, D.M. and S.R. McAlpine, *Halting metastasis through CXCR4 inhibition*. *Bioorg Med Chem Lett*, 2013. **23**(1): p. 20-5.
156. Liu, Q., et al., *CXCR4 antagonist AMD3100 redistributes leukocytes from primary immune organs to secondary immune organs, lung, and blood in mice*. *Eur J Immunol*, 2015. **45**(6): p. 1855-67.
157. Teixidó, J., et al., *The good and bad faces of the CXCR4 chemokine receptor*. *Int J Biochem Cell Biol*, 2018. **95**: p. 121-131.
158. Redondo-Muñoz, J., A. García-Pardo, and J. Teixidó, *Molecular Players in Hematologic Tumor Cell Trafficking*. *Front Immunol*, 2019. **10**: p. 156.
159. Ray, P., et al., *Secreted CXCL12 (SDF-1) forms dimers under physiological conditions*. *Biochem J*, 2012. **442**(2): p. 433-42.
160. Singh, A.K., et al., *Chemokine receptor trio: CXCR3, CXCR4 and CXCR7 crosstalk via CXCL11 and CXCL12*. *Cytokine Growth Factor Rev*, 2013. **24**(1): p. 41-9.
161. Bronger, H., et al., *Induction of cathepsin B by the CXCR3 chemokines CXCL9 and CXCL10 in human breast cancer cells*. *Oncol Lett*, 2017. **13**(6): p. 4224-4230.
162. Agten, S.M., et al., *Probing Functional Heteromeric Chemokine Protein-Protein Interactions through Conformation-Assisted Oxime Ligation*. *Angew Chem Int Ed Engl*, 2016. **55**(48): p. 14963-14966.
163. Belloc, C., et al., *The effect of platelets on invasiveness and protease production of human mammary tumor cells*. *Int J Cancer*, 1995. **60**(3): p. 413-7.
164. Zhu, G., et al., *CXCR3 as a molecular target in breast cancer metastasis: inhibition of tumor cell migration and promotion of host anti-tumor immunity*. *Oncotarget*, 2015. **6**(41): p. 43408-19.
165. Park, K.S., et al., *Biologic and biochemical properties of recombinant platelet factor 4 demonstrate identity with the native protein*. *Blood*, 1990. **75**(6): p. 1290-5.
166. Delaglio, F., et al., *NMRPipe: a multidimensional spectral processing system based on UNIX pipes*. *J Biomol NMR*, 1995. **6**(3): p. 277-93.

167. Johnson, B.A. and R.A. Blevins, *NMR View: A computer program for the visualization and analysis of NMR data*. J Biomol NMR, 1994. **4**(5): p. 603-14.
168. Tamamura, H., et al., *T140 analogs as CXCR4 antagonists identified as anti-metastatic agents in the treatment of breast cancer*. FEBS Lett, 2003. **550**(1-3): p. 79-83.
169. Fernandis, A.Z., et al., *Regulation of CXCR4-mediated chemotaxis and chemoinvasion of breast cancer cells*. Oncogene, 2004. **23**(1): p. 157-67.
170. Ridolfi, E., et al., *Inhibitory effect of HGF on invasiveness of aggressive MDA-MB231 breast carcinoma cells, and role of HDACs*. Br J Cancer, 2008. **99**(10): p. 1623-34.
171. Mayo, K.H. and M.J. Chen, *Human platelet factor 4 monomer-dimer-tetramer equilibria investigated by 1H NMR spectroscopy*. Biochemistry, 1989. **28**(24): p. 9469-78.
172. St Charles, R., D.A. Walz, and B.F. Edwards, *The three-dimensional structure of bovine platelet factor 4 at 3.0-A resolution*. J Biol Chem, 1989. **264**(4): p. 2092-9.
173. Rajarathnam, K., et al., *Probing receptor binding activity of interleukin-8 dimer using a disulfide trap*. Biochemistry, 2006. **45**(25): p. 7882-8.
174. Fernando, H., et al., *Dimer dissociation is essential for interleukin-8 (IL-8) binding to CXCR1 receptor*. J Biol Chem, 2004. **279**(35): p. 36175-8.
175. Yang, C., W. Zheng, and W. Du, *CXCR3A contributes to the invasion and metastasis of gastric cancer cells*. Oncol Rep, 2016. **36**(3): p. 1686-92.
176. Urra, S., et al., *Differential expression profile of CXCR3 splicing variants is associated with thyroid neoplasia. Potential role in papillary thyroid carcinoma oncogenesis?* Oncotarget, 2018. **9**(2): p. 2445-2467.
177. Kufareva, I., et al., *Disulfide Trapping for Modeling and Structure Determination of Receptor: Chemokine Complexes*. Methods Enzymol, 2016. **570**: p. 389-420.
178. Nguyen, L.T. and H.J. Vogel, *Structural perspectives on antimicrobial chemokines*. Front Immunol, 2012. **3**: p. 384.
179. Veldkamp, C.T., et al., *Production of Recombinant Chemokines and Validation of Refolding*. Methods Enzymol, 2016. **570**: p. 539-65.
180. Lortat-Jacob, H., A. Grosdidier, and A. Imberty, *Structural diversity of heparan sulfate binding domains in chemokines*. Proc Natl Acad Sci U S A, 2002. **99**(3): p. 1229-34.
181. Dyer, D.P., et al., *The dependence of chemokine-glycosaminoglycan interactions on chemokine oligomerization*. Glycobiology, 2016. **26**(3): p. 312-26.
182. Gutiérrez-González, M., et al., *Optimization of culture conditions for the expression of three different insoluble proteins in Escherichia coli*. Sci Rep, 2019. **9**(1): p. 16850.
183. Murphy, J.W., et al., *Structural and functional basis of CXCL12 (stromal cell-derived factor-1 alpha) binding to heparin*. J Biol Chem, 2007. **282**(13): p. 10018-10027.
184. Merkley, N., K.R. Barber, and G.S. Shaw, *Ubiquitin manipulation by an E2 conjugating enzyme using a novel covalent intermediate*. J Biol Chem, 2005. **280**(36): p. 31732-8.
185. Schägger, H., *Tricine-SDS-PAGE*. Nat Protoc, 2006. **1**(1): p. 16-22.
186. Konnova, T.A., C.M. Singer, and I.V. Nesmelova, *NMR solution structure of the RED subdomain of the Sleeping Beauty transposase*. Protein Sci, 2017. **26**(6): p. 1171-1181.
187. Rane, A.M., S. Jonnalagadda, and Z. Li, *On-column refolding of bone morphogenetic protein-2 using cation exchange resin*. Protein Expr Purif, 2013. **90**(2): p. 135-40.

188. Kufareva, I., C.L. Salanga, and T.M. Handel, *Chemokine and chemokine receptor structure and interactions: implications for therapeutic strategies*. Immunol Cell Biol, 2015. **93**(4): p. 372-83.
189. Raynal, B., et al., *Quality assessment and optimization of purified protein samples: why and how?* Microb Cell Fact, 2014. **13**: p. 180.
190. Irvine, G.B., *Determination of molecular size by size-exclusion chromatography (gel filtration)*. Curr Protoc Cell Biol, 2001. **Chapter 5**: p. Unit 5.5.
191. Ghosh, R., J.E. Gilda, and A.V. Gomes, *The necessity of and strategies for improving confidence in the accuracy of western blots*. Expert Rev Proteomics, 2014. **11**(5): p. 549-60.
192. Iqbal, H., D.R. Akins, and M.R. Kenedy, *Co-immunoprecipitation for Identifying Protein-Protein Interactions in Borrelia burgdorferi*. Methods Mol Biol, 2018. **1690**: p. 47-55.
193. McLachlin, D.T. and S.D. Dunn, *Disulfide linkage of the b and delta subunits does not affect the function of the Escherichia coli ATP synthase*. Biochemistry, 2000. **39**(12): p. 3486-90.
194. Baggiolini, M., *Chemokines and leukocyte traffic*. Nature, 1998. **392**(6676): p. 565-8.
195. Luster, A.D., *Chemokines--chemotactic cytokines that mediate inflammation*. N Engl J Med, 1998. **338**(7): p. 436-45.
196. Baggiolini, M., *Chemokines in pathology and medicine*. J Intern Med, 2001. **250**(2): p. 91-104.
197. Strieter, R.M., et al., *CXC chemokines in angiogenesis*. Cytokine Growth Factor Rev, 2005. **16**(6): p. 593-609.
198. Mackay, C.R., *Chemokines: immunology's high impact factors*. Nat Immunol, 2001. **2**(2): p. 95-101.
199. Raman, D., T. Sobolik-Delmaire, and A. Richmond, *Chemokines in health and disease*. Exp Cell Res, 2011. **317**(5): p. 575-89.
200. Youn, B.S., C. Mantel, and H.E. Broxmeyer, *Chemokines, chemokine receptors and hematopoiesis*. Immunol Rev, 2000. **177**: p. 150-74.
201. Rajagopalan, L. and K. Rajarathnam, *Structural basis of chemokine receptor function--a model for binding affinity and ligand selectivity*. Biosci Rep, 2006. **26**(5): p. 325-39.
202. Stone, M.J., et al., *Mechanisms of Regulation of the Chemokine-Receptor Network*. Int J Mol Sci, 2017. **18**(2).
203. Johnson, Z., A.E. Proudfoot, and T.M. Handel, *Interaction of chemokines and glycosaminoglycans: a new twist in the regulation of chemokine function with opportunities for therapeutic intervention*. Cytokine Growth Factor Rev, 2005. **16**(6): p. 625-36.
204. Wang, X., et al., *Chemokine oligomerization in cell signaling and migration*. Prog Mol Biol Transl Sci, 2013. **117**: p. 531-78.
205. Ellyard, J.I., et al., *Eotaxin selectively binds heparin. An interaction that protects eotaxin from proteolysis and potentiates chemotactic activity in vivo*. J Biol Chem, 2007. **282**(20): p. 15238-47.
206. Baltus, T., et al., *Oligomerization of RANTES is required for CCR1-mediated arrest but not CCR5-mediated transmigration of leukocytes on inflamed endothelium*. Blood, 2003. **102**(6): p. 1985-8.

207. Pitt, L.A., et al., *CXCL12-Producing Vascular Endothelial Niches Control Acute T Cell Leukemia Maintenance*. *Cancer Cell*, 2015. **27**(6): p. 755-68.
208. Mette M. Rosenkilde, L.-O.G., Janus S. Jakobsen, Renato T. Skerlj, Gary J. Bridger and Thue W. Schwartz, *Molecular Mechanism of AMD3100 Antagonism in the CXCR4 Receptor*. *THE JOURNAL OF BIOLOGICAL CHEMISTRY*, 2004. **279**(4): p. 3033–3041.
209. Hitchinson, B., et al., *Biased antagonism of CXCR4 avoids antagonist tolerance*. *Sci Signal*, 2018. **11**(552).
210. Chatterjee, S., B. Behnam Azad, and S. Nimmagadda, *The intricate role of CXCR4 in cancer*. *Adv Cancer Res*, 2014. **124**: p. 31-82.
211. Alsayed, Y., et al., *Mechanisms of regulation of CXCR4/SDF-1 (CXCL12)-dependent migration and homing in multiple myeloma*. *Blood*, 2007. **109**(7): p. 2708-17.
212. Ieranò, C., et al., *CXCL12 loaded-dermal filler captures CXCR4 expressing melanoma circulating tumor cells*. *Cell Death Dis*, 2019. **10**(8): p. 562.
213. Wendel, C., et al., *CXCR4/CXCL12 participate in extravasation of metastasizing breast cancer cells within the liver in a rat model*. *PLoS One*, 2012. **7**(1): p. e30046.
214. Wang, J., et al., *Dimerization of CXCR4 in living malignant cells: control of cell migration by a synthetic peptide that reduces homologous CXCR4 interactions*. *Mol Cancer Ther*, 2006. **5**(10): p. 2474-83.
215. Watts, A.O., et al., *Identification and profiling of CXCR3-CXCR4 chemokine receptor heteromer complexes*. *Br J Pharmacol*, 2013. **168**(7): p. 1662-74.
216. Xu, D., et al., *Drug Design Targeting the CXCR4/CXCR7/CXCL12 Pathway*. *Curr Top Med Chem*, 2016. **16**(13): p. 1441-51.
217. Springael, J.Y., et al., *Allosteric modulation of binding properties between units of chemokine receptor homo- and hetero-oligomers*. *Mol Pharmacol*, 2006. **69**(5): p. 1652-61.
218. Sung, H., et al., *Global Cancer Statistics 2020: GLOBOCAN Estimates of Incidence and Mortality Worldwide for 36 Cancers in 185 Countries*. *CA Cancer J Clin*, 2021. **71**(3): p. 209-249.
219. [http://www.breastcancer.org/symptoms/understand\\_bc/statistics](http://www.breastcancer.org/symptoms/understand_bc/statistics).
220. Malmgren, J.A., et al., *Metastatic breast cancer survival improvement restricted by regional disparity: Surveillance, Epidemiology, and End Results and institutional analysis: 1990 to 2011*. *Cancer*, 2020. **126**(2): p. 390-399.
221. Peart, O., *Metastatic Breast Cancer*. *Radiol Technol*, 2017. **88**(5): p. 519m-539m.
222. Marcuzzi, E., et al., *Correction: Marcuzzi, E., et al. Chemokines and Chemokine Receptors: Orchestrating Tumor Metastasis*. *Int. J. Mol. Sci.* 2019, 20, 96. *Int J Mol Sci*, 2019. **20**(11).
223. Liu, Y., et al., *Association of chemokine and chemokine receptor expression with the invasion and metastasis of lung carcinoma*. *Oncol Lett*, 2015. **10**(3): p. 1315-1322.
224. Zhang, Z., et al., *Expression of CXCR4 and breast cancer prognosis: a systematic review and meta-analysis*. *BMC Cancer*, 2014. **14**: p. 49.
225. Lefort, S., et al., *CXCR4 inhibitors could benefit to HER2 but not to triple-negative breast cancer patients*. *Oncogene*, 2017. **36**(9): p. 1211-1222.
226. Allinen, M., et al., *Molecular characterization of the tumor microenvironment in breast cancer*. *Cancer Cell*, 2004. **6**(1): p. 17-32.

227. Huo, Y., et al., *Circulating activated platelets exacerbate atherosclerosis in mice deficient in apolipoprotein E*. *Nat Med*, 2003. **9**(1): p. 61-7.
228. von Hundelshausen, P. and M.M. Schmitt, *Platelets and their chemokines in atherosclerosis-clinical applications*. *Front Physiol*, 2014. **5**: p. 294.
229. Iida, Y., et al., *Peptide inhibitor of CXCL4-CCL5 heterodimer formation, MKEY, inhibits experimental aortic aneurysm initiation and progression*. *Arterioscler Thromb Vasc Biol*, 2013. **33**(4): p. 718-26.
230. Fan, Y., et al., *MKEY, a Peptide Inhibitor of CXCL4-CCL5 Heterodimer Formation, Protects Against Stroke in Mice*. *J Am Heart Assoc*, 2016. **5**(9).
231. Portella, L., et al., *Preclinical development of a novel class of CXCR4 antagonist impairing solid tumors growth and metastases*. *PLoS One*, 2013. **8**(9): p. e74548.
232. Di Maro, S., et al., *Exploring the N-Terminal Region of C-X-C Motif Chemokine 12 (CXCL12): Identification of Plasma-Stable Cyclic Peptides As Novel, Potent C-X-C Chemokine Receptor Type 4 (CXCR4) Antagonists*. *J Med Chem*, 2016. **59**(18): p. 8369-80.
233. Di Maro, S., et al., *Structure-Activity Relationships and Biological Characterization of a Novel, Potent, and Serum Stable C-X-C Chemokine Receptor Type 4 (CXCR4) Antagonist*. *J Med Chem*, 2017. **60**(23): p. 9641-9652.
234. Egorova, A., et al., *Chemokine-derived peptides as carriers for gene delivery to CXCR4 expressing cells*. *J Gene Med*, 2009. **11**(9): p. 772-81.
235. Hassan, S., et al., *CXCR4 peptide antagonist inhibits primary breast tumor growth, metastasis and enhances the efficacy of anti-VEGF treatment or docetaxel in a transgenic mouse model*. *Int J Cancer*, 2011. **129**(1): p. 225-32.
236. Ziarek, J.J. and B.F. Volkman, *NMR in the Analysis of Functional Chemokine Interactions and Drug Discovery*. *Drug Discov Today Technol*, 2012. **9**(4): p. e293-e299.
237. Loetscher, P., et al., *N-terminal peptides of stromal cell-derived factor-1 with CXC chemokine receptor 4 agonist and antagonist activities*. *J Biol Chem*, 1998. **273**(35): p. 22279-83.
238. Kim, S.Y., et al., *Inhibition of the CXCR4/CXCL12 chemokine pathway reduces the development of murine pulmonary metastases*. *Clin Exp Metastasis*, 2008. **25**(3): p. 201-11.
239. Faber, A., et al., *The many facets of SDF-1alpha, CXCR4 agonists and antagonists on hematopoietic progenitor cells*. *J Biomed Biotechnol*, 2007. **2007**(3): p. 26065.
240. Salanga, C.L. and T.M. Handel, *Chemokine oligomerization and interactions with receptors and glycosaminoglycans: the role of structural dynamics in function*. *Exp Cell Res*, 2011. **317**(5): p. 590-601.
241. de Haas, A.H., et al., *Neuronal chemokines: versatile messengers in central nervous system cell interaction*. *Mol Neurobiol*, 2007. **36**(2): p. 137-51.
242. Mishra, P., D. Banerjee, and A. Ben-Baruch, *Chemokines at the crossroads of tumor-fibroblast interactions that promote malignancy*. *J Leukoc Biol*, 2011. **89**(1): p. 31-9.
243. Cojoc, M., et al., *Emerging targets in cancer management: role of the CXCL12/CXCR4 axis*. *Onco Targets Ther*, 2013. **6**: p. 1347-61.
244. Sohy, D., M. Parmentier, and J.Y. Springael, *Allosteric transinhibition by specific antagonists in CCR2/CXCR4 heterodimers*. *J Biol Chem*, 2007. **282**(41): p. 30062-9.

245. Han, Y., et al., *Allosteric communication between protomers of dopamine class A GPCR dimers modulates activation*. Nat Chem Biol, 2009. **5**(9): p. 688-95.
246. Contento, R.L., et al., *CXCR4-CCR5: a couple modulating T cell functions*. Proc Natl Acad Sci U S A, 2008. **105**(29): p. 10101-6.
247. Molon, B., et al., *T cell costimulation by chemokine receptors*. Nat Immunol, 2005. **6**(5): p. 465-71.
248. Stephens, B. and T.M. Handel, *Chemokine receptor oligomerization and allostery*. Prog Mol Biol Transl Sci, 2013. **115**: p. 375-420.
249. Babcock, G.J., M. Farzan, and J. Sodroski, *Ligand-independent dimerization of CXCR4, a principal HIV-1 coreceptor*. J Biol Chem, 2003. **278**(5): p. 3378-85.
250. Cheng, Z.J., et al., *beta-arrestin differentially regulates the chemokine receptor CXCR4-mediated signaling and receptor internalization, and this implicates multiple interaction sites between beta-arrestin and CXCR4*. J Biol Chem, 2000. **275**(4): p. 2479-85.
251. Sun, Y., et al., *Beta-arrestin2 is critically involved in CXCR4-mediated chemotaxis, and this is mediated by its enhancement of p38 MAPK activation*. J Biol Chem, 2002. **277**(51): p. 49212-9.

## SUPPLEMENTARY DATA APPENDIX

### 1. Expression and purification of wildtype CXCL4

#### 1.1 Expression protocol

*E. coli* BL21 DE3 competent cells were transformed with pET24d+ plasmid (2.5ng/uL) as follow: The bacteria-plasmid mixture (in TE buffer) was incubated on ice for 30 min, treated with 10 sec heat shock at 42°C, and then placed on ice for 5 min. 100uL of SOC media was added to the competent cell-plasmid mixture and incubated at 37°C with 225rpm shaking for an hour. An aliquot of 100μL cell culture was plated in an LB agar media supplemented with 60μg/mL Kanamycin. Kanamycin-resistant colonies were isolated and cultured in 10ml of the LB medium at 37°C, under shaking (250rpm) for 6 hours. The bacteria pellets were collected by centrifugation (3000rpm, 10 min). Bacteria pellets were resuspended in fresh LB media (100mL) supplemented with 60μg/mL Kanamycin. Bacteria were grown overnight under similar conditions and then diluted in M9 media (1L) and further grown until the bacterial culture optical density at 600nm (OD<sub>600</sub>) reached 0.60. Protein expression was induced by an addition of 0.5mM IPTG and a further 4-hour incubation (37°C with 250rpm shaking). Bacterial pellets were collected by centrifugation (3000rpm, 30 min).

#### 1.2. Purification protocol

##### 1.2.1 Cell lysis and extraction

Lysis buffer: 50mM Tris pH 8.0, 1% Triton X

Extraction buffer: 50mM Tris, 8M Urea, pH 8.0

Cell pellets were suspended in the lysis buffer consisted of 50mM Tris, 1% Triton, pH 8 (4g pellets per 12 mL lysis buffer). 100mM of the protease inhibitor PMSF and 0.1% beta-mercaptoethanol was freshly added to the suspension, followed by sonication by 40% power 2

seconds ON and 0.5 second OFF. After sonication, the cell lysates were centrifuged 20,000rpm for 1 hour at 4°C. Inclusion bodies were settled at the bottom of the centrifuge tubes. The inclusion bodies were dissolved in the extraction buffer, followed by overnight shaking. After the inclusion bodies were completely homogenized in the buffer, the solution was clarified to remove cell debris by ultra-centrifugation at 20,000rpm, 4°C for 1 hour. The supernatant containing soluble proteins was injected to the cation exchange column for purification.

### **1.2.2 Cation exchange chromatography**

Cation exchange column buffer A: 100mM Tris, 8M Urea, pH 8.0

Cation exchange column buffer B: 100mM Tris, 6M Urea, 2M Sodium Chloride, pH 8.0

The clarified supernatant was primarily purified by cation exchange column (20-mL SP/FF sepharose, GE Healthcare) connected with AKTA-FPLC system (GE Healthcare). The purification was programmed in Unicorn software 7.3 (GE Healthcare) and eluates were monitored by UV-L9 cell flow, and automatically fractionated by using the fractionator FL-9. The column was initially equilibrated with the cation exchange binding buffer A for 4CV. Samples were injected at 3 ml/min, followed by 5 column volume (CV) wash with buffer A and 2.5% of the cation exchange elution buffer B. Protein elution was done using a gradient of buffer B for 20CV.

### **1.2.3 Protein refolding**

Refolding buffer: 100mM Tris, 10mM Cysteine, 1mM Cystine, pH 8.0

The eluate fraction from cation exchange chromatography was refolded in the refolding buffer with stirring overnight at room temperature (dropwise dilution 1:50 v/v). After refolding, precipitates were removed by centrifuging at 4000rpm, 1 hour at 4°C. The clarified supernatant containing folded protein of interest was buffered exchanged to 20 mM NaCl, pH 7.3.

#### **1.2.4. Heparin affinity chromatography**

Heparin column binding buffer A: 50mM Tris, pH 7.3

Heparin column elution buffer B: 50mM Tris, 2M Sodium Chloride, pH 7.3

The heparin column (20-mL SF/FF heparin, GE Healthcare) was initially equilibrated by 3 CV of the heparin column buffer A. The above refolded fraction was injected into the column at 3mL/min, followed by 5 CV wash by buffer A containing 2.5% buffer B. Proteins were eluted from the column using NaCl gradient (from 0 to 100% B) and monitored by UV280nm. The wildtype CXCL4 was eluted at 60-70% B. Heparin eluate fractions containing CXCL4 were pooled together and concentrated using 3kDa MW Amicon filter (Millipore Sigma, MA, USA). The protein concentration was determined by BCA assay kit (Thermo Scientific, MA, USA). The wildtype CXCL4 and the mutant S26C were eluted at 60-70% B. Yield of the wildtype CXCL4 and mutant was 2mg/mL.

## **2. Expression and purification of wildtype CXCL12**

### **2.1 Expression protocol:**

The expression protocol of CXCL12 was similar to the wildtype CXCL4, except that cells were induced by 0.25mM IPTG.

### **2.2 Purification protocol:**

Purification steps are similar to the wildtype CXCL4 from cation exchange, refolding, to heparin column. Additionally, the purity of CXCL12 was polished by size exclusion using 50mM sodium phosphate, 150mM NaCl, pH 7.0 with 2 CV of column equilibration and 2CV of elution at the rate of 1.3mL/min. Eluted peak from size exclusion was pooled and concentrated by 3kDa filters. Protein concentration was determined by BCA. Yield of wildtype CXCL12 was 1-1.5 mg/mL.

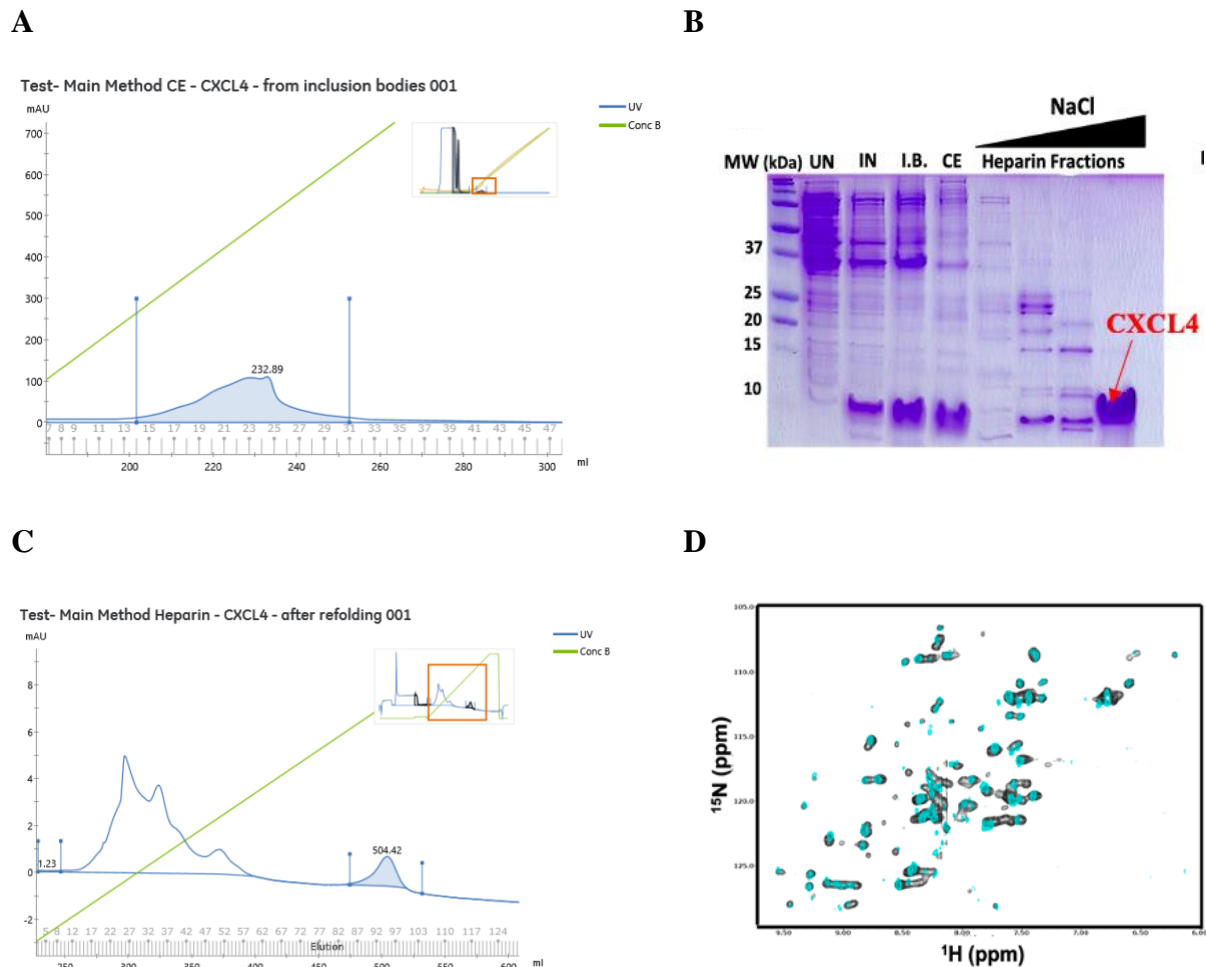


**Figure S.1: Expression, purification, and NMR characterization of  $^{15}\text{N}$ -labeled CXCL4.** (A) Cation exchange chromatogram of purification of CXCL4. Peak was detected at 10-15% buffer B. (B) Heparin chromatogram of purification of CXCL4. The CXCL4 peak (shaded) was eluted at 60-70% buffer B. (C) SDS-PAGE of the wildtype CXCL4. UN – uninduced cells, IN – induced cells, IB – inclusion bodies, CE – eluate from cation exchange chromatography, HP – eluate from heparin affinity chromatography. (D) The HSQC spectrum of  $^{15}\text{N}$ -CXCL4 produced in our lab (black) is similar to the HSQC spectrum of  $^{15}\text{N}$ -CXCL4 in [19]. The spectrum was collected at 40°C using the 950MHz at DMRI. Labeled CXCL4 (~150 $\mu\text{M}$ ) was prepared in 90% H<sub>2</sub>O/10% D<sub>2</sub>O in water pH 5.5.

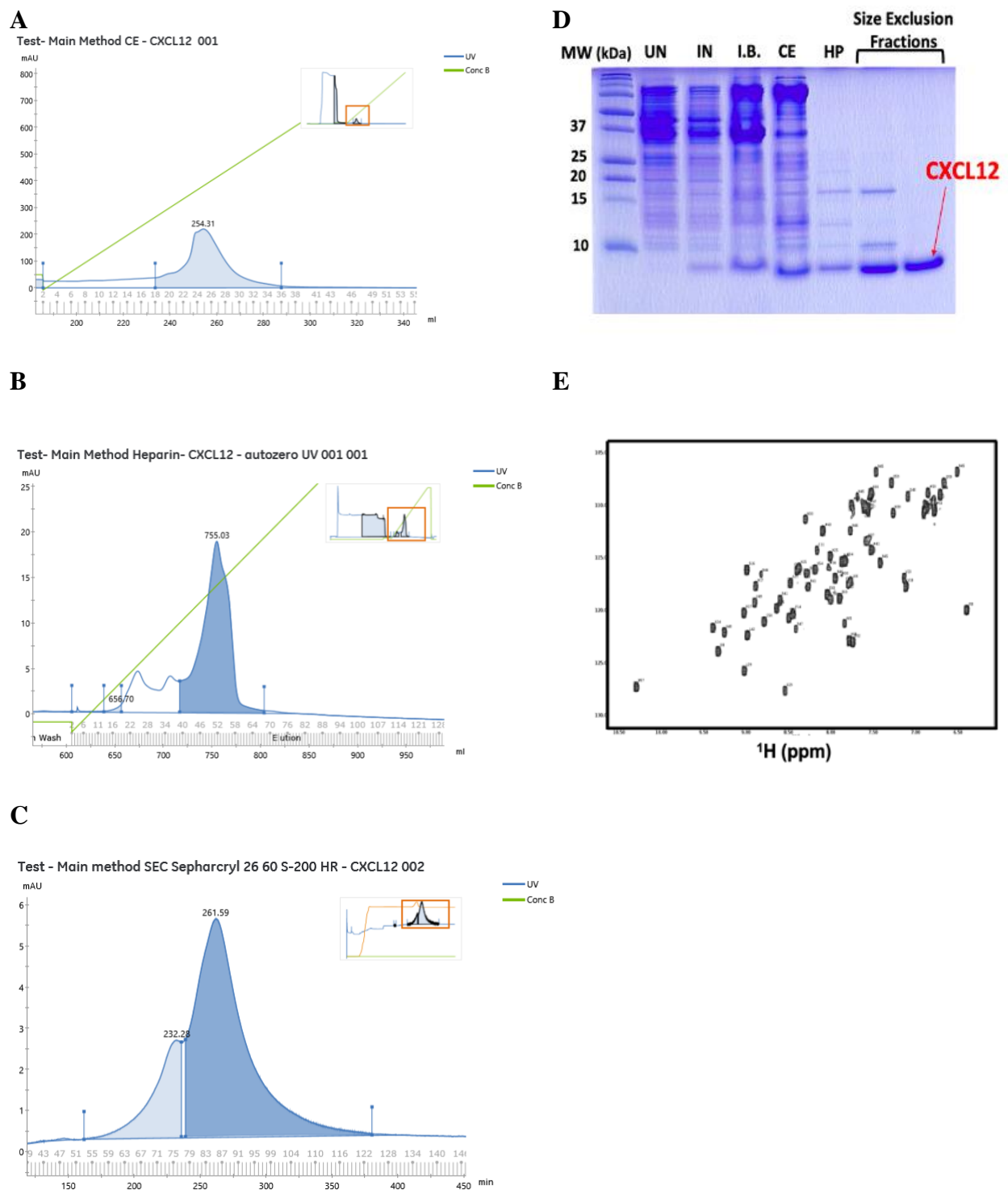


**Figure S.2: Expression, purification, and NMR characterization of  $^{15}\text{N}$ -labeled CXCL12.** (A) Cation exchange chromatogram. CXCL12 peak was eluted at 10-15% buffer B. (B) Heparin chromatogram. CXCL12 peak was eluted at 30-40% buffer B. (C) Size exclusion chromatogram. (D) SDS-PAGE of the wildtype CXCL12. UN – uninduced cells, IN – induced cells, IB – inclusion bodies, CE – eluate from cation exchange chromatography, HP – eluate from heparin

affinity chromatography, size exclusion fractions (3 last lanes). **(E)** The HSQC spectrum of  $^{15}\text{N}$ -CXCL12 collected at 25°C. Labeled CXCL12 (~150 $\mu\text{M}$ ) was prepared in 20mM MES buffer with 10%  $\text{D}_2\text{O}$ , pH 6.8.